GEOCHIMICA ET COSMOCHIMICA ACTA

UNIVERSITY OF HAWAII
SEP 10 '57

JOURNAL OF THE GEOCHEMICAL SOCIETY

EDITORIAL ADVISORY BOARD

T. BARTH-OSLO · A. F. BUDDINGTON-PRINCETON, N.J. · L. CAPDECOMME-TOULOUSE
E. J. CONWAY-DUBLIN · P. ESKOLA-HELSINKI · P. GALLITELLI-MODENA
D. GUIMARÃES-BELO HORIZONTE · A. HADDING-LUND · O. HAHN-GÖTTINGEN
H. W. HARVEY-PLYMOUTH · F. HEIDE-JENA · A. HOLMES-EDINBURGH
G. E. HUTCHINSON-NEW HAVEN, CONN. · W. Q. KENNEDY-LEEDS · PH. H. KUENEN-GRONINGEN · S. LANDERGREN-STOCKHOLM · F. MACHATSCHKI-VIENNA
B. H. MASON-NEW YORK · A. MUIR-HARPENDEN · J. ORCEL-PARIS · E RAGUIN-PARIS · K. RANKAMA-HELSINKI · E. REINHARD-BASLE · TH. G. SAHAMA-HELSINKI
C. E. TILLEY-CAMBRIDGE · T. VOGT-TRONDHEIM · W. WAHL-HELSINKI
T. WATANABE-TOKYO · F. WHIPPLE-CAMBRIDGE, MASS.
R. WILDT-NEW HAVEN, CONN.

EDITORS

L. H. AHRENS, CAPETOWN
C. W. CORRENS, GÖTTINGEN
E. INGERSON, WASHINGTON
S. R. NOCKOLDS, CAMBRIDGE
F. A. PANETH, MAINZ
H. C. UREY, CHICAGO
JOHN VERHOOGEN, BERKELEY, CALIF.
A. P. VINOGRADOV, MOSCOW
L. R. WAGER, OXFORD
F. E. WICKMAN, STOCKHOLM

VOLUME 12 No. 3

1957

QE 351
G 725

PERGAMON PRESS LONDON · NEW YORK · PARIS

Geochim. et Cosmochim. Acta

GEOCHIMICA ET COSMOCHIMICA ACTA

EDITORS

PROF. L. H. AHRENS *Department of Chemistry, University of Capetown, Rondebosch, Cape Province, South Africa*
PROF. C. W. CORRENS *Sedimentpetrographisches Institut der Universitat, Lotzestr.* 13, *Göttingen, Germany*
DR. E. INGERSON *Geochemistry and Petrology Branch, U.S. Geological Survey, Washington* 25, *D.C., U.S.A.*
DR. S. R. NOCKOLDS *Department of Mineralogy and Petrology, The University, Cambridge, England*
PROF. F. A. PANETH, F.R.S. *Max-Planck-Institut für Chemie, Mainz, Saarstrasse* 23, *Germany*
PROF. H. C. UREY, For. Mem. R.S. *The Enrico Fermi Institute for Nuclear Studies, University of Chicago, Illinois, U.S.A.*
DR. JOHN VERHOOGEN *Department of Geology, University of California, Berkeley, California, U.S.A.*
PROF. A. P. VINOGRADOV *The Academy of Sciences of the U.S.S.R., Moscow, U.S.S.R.*
PROF. L. R. WAGER, F.R.S. *Department of Geology and Mineralogy, The University, Oxford, England*
PROF. F. E. WICKMAN *Naturhistoriska Riksmuseets, Mineralogiska Avdelning, Stockholm* 50, *Sweden*

VOLUME 12, No. 3 1957

CONTENTS

PAGE

JOHN H. REYNOLDS: Comparative study of argon content and argon diffusion in mica and feldspar 177

K. I. MAYNE: Natural variations in the nitrogen isotope abundance ratio in igneous rocks 185

J. R. BUTLER: Rare earths in yttrotungstite 190

P. G. HARRIS: Zone refining and the origin of potassic basalts 195

H. R. CORNWALL and H. J. ROSE JR: Minor elements in Keweenawan lavas, Michigan . 209

ROYAL R. MARSHALL: Isotopic composition of common leads and continuous differentiation of the crust of the earth from the mantle 225

JOHN F. LOVERING: Differentiation in the iron-nickel core of a parent meteorite body . 238

JOHN F. LOVERING: Pressures and temperatures within a typical parent meteorite body 253

HIROSHI ONISHI and E. B. SANDELL: Meteoritic and terrestrial abundance of tin . . 262

Geochemical note:

SOL BERMAN: Determination of yttrium, lanthanum, cerium, neodymium, and ytterbium in test samples granite G–1 and diabase W–1 by a combined chemical-spectrochemical technique 271

Abstracts from current literature

S. P. VINOGRADOV, A. B. RONOV, and V. M. RATYNSKII: Variation in the chemical composition of carbonate rocks of Russian platform 273

Publishing Offices: Pergamon Press Ltd., 4 & 5 Fitzroy Square, London W.1. (EUS 4455)

Subscription *per annum* (including postage) (A) £16. 10s. (U.S.A. $46.50); (B) For individual subscribers who certify that the Journal is for their private use, £10. 10s. (U.S.A. $30.00). Members of the Geochemical Society, or non members who occasionally publish papers in the Journal, £3. 10s. (U.S.A. $10.00) *per annum.*

Back numbers, £7 (U.S.A. $19.60) per volume

Distributors: I. R. Maxwell & Co., Ltd., 4 & 5 Fitzroy Square, London W.1
and Pergamon Press, Inc., 22 East 55th Street, New York 22, N.Y.

PERGAMON PRESS

4 & 5 FITZROY SQUARE, LONDON W.1 122 EAST 55TH STREET, NEW YORK 22, N.Y.

24 RUE DES ÉCOLES, PARIS Ve

PRINTED IN NORTHERN IRELAND AT THE UNIVERSITIES PRESS, BELFAST

Geochimica et Cosmochimica Acta, 1957, Vol. 12, pp. 177 to 184. Pergamon Press Ltd., London

Comparative study of argon content and argon diffusion in mica and feldspar*

JOHN H. REYNOLDS†
Department of Physics, University of California, Berkeley, California

(*Received* 1 *February*, 1957)

Abstract—The A^{40}/K^{40} ratios for coarse and fine-mesh samples of 100-m.y.-old feldspar (perthitic orthoclase-microline) were compared with those for coarse- and fine-mesh samples of lepidolite from the same pegmatite and found to be in agreement, although there was some evidence for migration of argon from the potash feldspar phase to the soda feldspar phase of the perthite. Fine samples of both minerals were then heated to various temperatures for 48 hours and the radiogenic and atmospheric argon released was measured. At all temperatures below that at which mica is disrupted, leakage from the feldspar was greater. The temperature-dependence of the leakage from the two minerals was found to be quite different. That for the mica suggests that there are two components of argon in the mineral: a minor component which is loosely bound, and a major component tightly bound. The leakage curve for feldspar is quite regular, suggesting that there is only a single argon component. If this is assumed to be so, an extrapolation of the curve provides a lower limit of 10^{-19} cm²/sec for D, the diffusion coefficient. This value of D is high enough to account for about 35 per cent argon loss in 1-cm grains of 2000-m.y.-old potash feldspar. Atmospheric argon in the minerals appears to be more loosely bound than the radiogenic argon. The A^{40}/K^{40} ratio for samples from the Pala District, California, pegmatite is $0{\cdot}00525 \pm 0{\cdot}00016$, corresponding to an age of $92{\cdot}0 \pm 2{\cdot}5$ m.y.

INTRODUCTION

ONE of the difficulties which has been encountered in the potassium-argon method of dating is the discrepancy between the argon content of micas and feldspars—a discrepancy which has been established beyond any doubt by several groups of workers (WETHERILL, ALDRICH, and DAVIS, 1955; FOLINSBEE, LIPSON, and REYNOLDS, 1956; WASSERBURG, HAYDEN, and JENSEN, 1956; JEFFERY, 1956). In an attempt to gain information about this discrepancy and its possible cause, a series of systematic experiments was carried out at Berkeley on samples from the Pala District, California. A programme of measurements was completed during the summer of 1956 without the data being analysed. This has now been done and although there are very obvious gaps in the work which need to be filled, a fairly coherent experimental picture has emerged. This report is prepared in the belief that an early account will be useful, even if incomplete.

SAMPLES

Large hand specimens of pegmatitic lepidolite and potash feldspar were collected in August 1955 from open pits near the Stewart Mine, Pala District, California. In late February 1956 the specimens were sawed into $\frac{3}{4}$ in. cubes with a diamond saw, all surface material and (to the greatest extent feasible) all badly altered material being rejected. Within a day the cubes were crushed and ground in clean equipment. Sieve fractions 16–28 (hereafter called coarse) and 100–150-mesh (fine) were selected for the experiments to follow and were split into convenient sample lots with a sample splitter. Smaller splits were ground without loss, using diamond and agate mortars, to minus–100-mesh for alkali

* Work supported by the U.S. Atomic Energy Commission.
† Presently on leave at the Department of Physics, University of Bristol, England.

analysis. A dozen or so cubes of each mineral were crushed separately and then ground without loss to minus–100-mesh so as to provide additional samples for alkali analysis which should be representative of the hand specimens as a whole.

The lepidolite is a pure, hard, rose-coloured material which exhibits no alteration. In thin section it is seen to be densely composed of grains which on the average can be circumscribed by a square 0·28 mm on edge. The alkali analyses of the three fractions of lepidolite (coarse, fine, and hand specimen-representative) are all identical within experimental error.

The potash feldspar is a much more complex material. We are indebted to Professor G. H. CURTIS of the Department of Geology, who examined it and provided the following description:

"The alkali feldspar used in this work is part of a large single crystal of cream coloured perthitic orthoclase-microcline. Subparallel blebs and veinlets of albite (An_3) up to $\pm$0·5 mm in thickness, with very irregular margins, traverse the crystal more or less parallel with 100, and compose about 25% of the feldspar. Virtually all of the albite shows the same crystallographic orientation as the potash feldspar, suggesting an exsolution origin for it. The albite twinning of the albite is fine (320 + twins per mm, about 0·8 mm in average length) and omnipresent, whereas albite-pericline twinning in the microcline is largely confined to areas adjacent to the albite, probably indicative of more complete removal of sodium from these margins (CHAYES, 1952).

"Quartz is sparingly present in the feldspar in equant grains up to approximately 5 mm in diameter, the larger grains being slightly graphic in shape. White mica occurs in trace amounts. A dark mineral, tentatively identified as manganocolumbite from optical properties, hardness and specific gravity (5·45), is present in minor amounts in tabular grains up to 3 mm in length and 1 mm in thickness. Clay minerals compose about 5% of the specimen. They occur in reticulating veinlets and small patches which are confined to the potash feldspar. Limonite staining of the clay suggests that the clay is of supergene origin; however, the distribution of the clay is clearly not cleavage-controlled, and, since the feldspar crystal came from an intermediate zone in the pegmatite, the clay may be of both hypogene and supergene origin (JAHNS and WRIGHT, 1951)."

The alkali analyses of the three fractions are of some interest. Those for the hand specimen are consistent with 27·6% soda feldspar, 67·8% potash feldspar, and 4·6% nonalkali-bearing material. The fine fraction analyses are consistent with 33·6% soda feldspar, 63·8 potash feldspar, and 2·6 extraneous matter. Note the purification accomplished (presumably by sifting out of the finest material) and the enrichment of this fraction in soda feldspar. The coarse-fraction analyses are consistent with 22·3% soda feldspar, 76·5% potash feldspar, and 1·2% contamination. This fraction is the purest feldspar of the three, and is enriched in potash feldspar with respect to the hand specimen.

METHODS

The methods used at Berkeley for the determination of the radiogenic argon and atmospheric argon in minerals have been previously described by FOLINSBEE, REYNOLDS, and LIPSON (1956), by LIPSON (1956), and by REYNOLDS (1956). It suffices here to note that the measurements are

by isotope dilution, using an A^{38} dilutant or "spike," of the gases released from the mineral by 12–20-hour fluxing of the sample with molten NaOH. The samples were outgassed beforehand for 20 ± 4 hours at 270° in an attempt to remove adsorbed atmospheric gases. All steps in the process were carried out in compact, highly outgassed vacuum systems. The attack on the mineral was never begun until the pressure in the reaction vessel had been brought below 10^{-8}mm Hg. Blank runs in the equipment yielded a total of about 10^{-6} c.c. STP argon of atmospheric composition.

In order to study the diffusion of argon from the minerals, the samples (again preliminarily outgassed at 270°) were kept for 48 hours at the desired temperature in the presence of a "spike." The same nickel reaction vessel was used for this heating as was used in the total extraction runs, except that now no NaOH was employed, and the temperature was regulated very closely by a servomechanism. At the conclusion of the 48-hour period, the mixture of evolved gases was purified as usual.

The alkali measurements were all made by flame photometry, using a lithium internal standard. Since the Pala minerals contain lithium, the lithium content was also determined and used to calculate the resulting small correction to the sodium and potassium percentages.

Calculations

To calculate diffusion coefficients, D, the simplest possible model was employed, namely isotropic, volume-diffusion from a sphere with zero argon concentration at the surface. The equivalent spherical radius of the coarse particles was determined by weighing a counted number of grains of feldspar and assuming a density of 2·55. The equivalent spherical radius of the fine particles was determined from that of the coarse by assuming that this quantity remains in fixed proportion to the average sieve opening. The radius deduced for the 100–150-mesh particles by this method was 54 μ.

If the fraction of argon released, $f = (Q_0 - Q)/Q_0$, exceeds 0·3, the simplest method of computing D is to read it off a graph of the exact function

$$f = 1 - \frac{6}{\pi^2} \sum_{n=1}^{\infty} \exp\left[(-n^2\pi^2 \,.\, Dt/a^2)/n^2\right],$$

which can be constructed without difficulty. If f is less than about 0·3, the slow convergence of the series presents a difficulty, and an approximation for f, valid when the time of diffusion is short (Carslaw and Jaeger, 1947), is to be preferred. Here

$$f = \frac{6}{\pi^{1/2}} \left(\frac{Dt}{a^2}\right)^{1/2} - 3\,\frac{Dt}{a^2}$$

It will be noted that, in calculating diffusion coefficients in this way, we have neglected diffusion of the released argon back into the mineral. In principle this effect could be taken into account without difficulty, since the problem is mathematically identical with the problem of heat-flow from a sphere into a well-stirred calorimeter (Carslaw and Jaeger, 1947). However, fixing the constant which couples the crystalline and gaseous phases in our application requires a knowledge of what is essentially the lifetime of absorbed atoms before evaporation from the surface of the heated mineral, and there are no data available for these lifetimes at the temperatures of interest. However, even if a significant fraction of the mineral becomes coated with an absorbed layer of argon under the conditions of the experiments, any error arising from this circumstance is very largely cancelled

by a diffusion of the spike argon into the mineral to an extent which depends on the same coupling constant and introduces an error of opposite sign.

RESULTS

Total argon content

The data on the total argon contents appear in Table 1. The striking fact is that within the probable errors quoted there are no significant differences among the four values of the A^{40}/K^{40} ratio. In particular, the average feldspar value (0·00528) and the average mica value (0·00522) are almost identical, so that in this instance *there is no mica-feldspar discrepancy.*

Table 1. Results of total argon determinations for Pala District, California, minerals. All samples were preheated in vacuum for 20 ± 4 hours at 270°C.

Sample No.	Description	Weight (g)	Per cent K	Per cent Na	Radiogenic A^{40} (c.c. STP/g × 10^6)	Atmospheric argon (c.c. STP/g × 10^6)	A^{40}/K^{40}
KA82-5	Feldspar fine	8·20	8·96 ± 0·09	2·95 ± 0·03	33·2	1·8	0·00544 ± 0·00018
KA83-1A	Feldspar coarse	6·89	10·76 ± 0·11	1·96 ± 0·02	37·5	1·4	0·00511 ± 0·00017
KA84	Feldspar hand specimen	—	9·54 ± 0·10	2·44 ± 0·02	—	Feldspar average: —	0·00528 ± 0·00017 —
KA87-3	Lepidolite fine	6·31	8·50 ± 0·08	0·33 ± 0·01	31·0	4·2	0·00534 ± 0·00017
KA86-1	Lepidolite coarse	9·43	8·56 ± 0·09	0·38 ± 0·01	29·8	1·3	0·00511 ± 0·00017
KA88	Lepidolite hand specimen	—	8·55 ± 0·09	0·37 ± 0·01	—	Lepidolite average: —	0·00522 ± 0·00017 —

The largest difference in the A^{40}/K^{40} ratio occurs between that for the fine feldspar and that for the coarse feldspar, the former being greater by 6·5%. This difference is hardly significant in view of the errors involved, but additional evidence for such a difference was noted in earlier, preliminary measurements with Pala feldspar. If real, this "inverse size effect" implies a diffusion of argon from the potash feldspar into the soda feldspar, the latter being concentrated in the fine sample. A transfer of 12% of the argon into the albite would account for the difference in the present instance. Adopting a much oversimplified model of the perthite, i.e. alternate layers of potash feldspar and albite 1·5 mm and 0·5 mm thick, respectively, this transfer implies a diffusion coefficient for argon in potash feldspar of about 5×10^{-20} cm²/sec. The A^{40}/K^{40} ratio, if corrected for this diffusion, is 0·00535.

The average A^{40}/K^{40} ratio for the four samples, 0·00525 ± 0·00016, provides a reliable age determination for the Pala pegmatite. Using the K^{40} decay constants reported by WETHERILL *et al.* (1956) ($\lambda = 0{\cdot}528 \times 10^{-9}\text{y}^{-1}$ and $R = 0{\cdot}118$) we find the age to be 92·0 ± 2·5 m.y. The probable error arises from a possible 3% systematic error in the argon measurements. Possible errors in the decay constants have been neglected.

The atmospheric argon released is, on the average, 16 times that found in blank runs, so that it must be accepted that atmospheric argon from the minerals is

being observed. Individual values are, however, always suspect in that they can be attributed to a small air-leak. Barring this being responsible, the fine mica appears to be more gassy than the other samples.

Table 2. Results of heating experiments for Pala minerals. All samples were preheated in vacuum for 20 ± 4 hours at 270°C, then heated for 48 hours at the indicated temperature.

Sample No.	Description	Weight (g)	Temperature (°C)	Radiogenic A^{40} released (c.c. STP/g × 10^6)	Fraction of radiogenic argon released	D (cm^2/sec × 10^{12})	Atmospheric argon released (c.c STP/gm × 10^6)	Fraction atmospheric argon released
KA82-6	Feldspar fine	7·46	391	1·42	0·043	0·028	0·8	0·45
KA82-2	,,	7·68	508	4·36	0·131	0·27	1·7	0·96
KA82-3	,,	7·61	602	7·73	0·232	0·96	0·5	0·27
—	,,	—	900*	—	0·976*	56*	—	—
KA87-4	Lepidolite fine	6·18	391	1·09	0·035	0·019	Atmospheric data invalidated by air-leak repaired just prior to run	
KA87-1	,,	6·34	508	1·22	0·039	0·023	2·2	0·52
KA87-2	,,	6·37	602	5·36	0·173	0·49	2·9	0·69
—	Lepidolite coarse	—	900*	—	1·000*	∞*	—	—

* Earlier preliminary work on Pala specimens. Residual argon in mineral was determined after heating.

Argon diffusion

The data from the heating experiments are collected in Table 2 and are plotted in Figs. 1 and 2. It will be noted that the temperature-dependence of argon loss in mica is quite different from that in feldspar. In the feldspar specimen, the points describe a smooth curve of gradually changing slope. In the mica specimen,

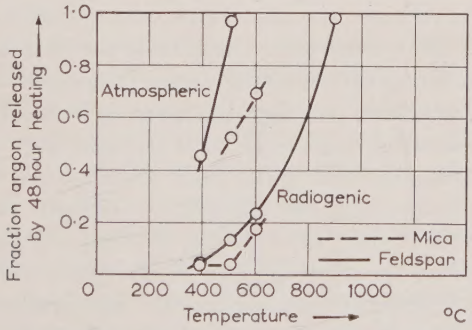

Fig. 1. Fraction of radiogenic and atmospheric argon expelled by 48-hour heating, as a function of temperature in feldspar and mica.

however, any curve passing through the three points must necessarily have an abrupt change in slope somewhere between 500 and 600°C. The appearance of such a curve suggests immediately that there are two argon components involved: one which is easily expelled by heating and is largely driven off at any temperature above 400°C, and another which is tightly bound and thus has a steep temperature-dependence. Another difference arises from the fact that between 600° and 900°C, vacuum-heated lepidolite undergoes a marked change of appearance and suffers a

weight-loss, presumably due to the expulsion of water. Correspondingly, loss of radiogenic argon after 900°C heating is found to be complete.

At all other temperatures, the argon loss from feldspar is greater than that from mica. This fact alone is of little importance to our considerations, however, since the temperatures of cooled rock are far below the temperatures for which we have obtained laboratory data; we are of necessity forced to a gross extrapolation of the curves.

If the rate of a process is entirely simple in that only one energy of activation is involved, a plot of ln D vs. $1/T$ will be a straight line, and extrapolation is entirely feasible. The diffusion process for a rare gas in a solid is, however, almost never a simple process in this sense. Typically, diffusion occurs by migration of the rare-gas atoms through vacancies in the crystal. The diffusion rate depends, then, on at

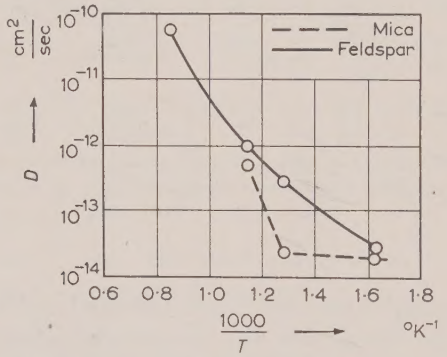

Fig. 2. Coefficient of diffusion of radiogenic argon, as a function of reciprocal absolute temperature in feldspar and mica

least two factors: the rate at which rare-gas atoms advance into adjacent vacancies and the volume density of the vacancies. Both of these factors are temperature-dependent, and a common temperature-dependence includes three distinct regions on a ln D vs. $1/T$ plot. First, there is a high-temperature linear region where both factors are temperature-activated and the slope is governed by a composite energy of activation; second, a transitional region; and third, a low-temperature linear region where the density of vacancies has fallen to a constant value determined by other considerations altogether (such as impurity content or the rate at which the mineral crystallized) and where a lower energy of activation determines the slope. The ln D curve will not be a straight line, then, but—important for our purpose—will be concave upwards. This means that if we extrapolate the diffusion curve to low temperatures at the last observed slope, we shall get a lower limit to the diffusion coefficient at any temperature. Extrapolating the feldspar curve in this way, we conclude that at room temperature (300°K), D is greater than 10^{-19} cm^2/sec in these particular crystals.

It should be stressed that the validity of the foregoing argument leading to a lower limit for D depends on there being only one argon component under observation. If the feldspar curve in Fig. 2 is a composite leakage curve where the low-temperature slope depends, as in the mica case, on the behaviour of a minor but loosely bound argon component, the lower limit we have deduced is of no

applicability to the main bulk of dissolved argon. However, there is nothing in the appearance of the feldspar curves to suggest such a dichotomy.

In Fig. 1 there is also plotted the fraction of atmospheric argon released as a function of temperature. In the absence of any checks for these data they cannot be given any great weight, although they would appear to show that in both mica and feldspar the atmospheric argon is less tightly bound than the radiogenic argon and that in feldspar the atmospheric argon is less tightly bound than in mica. The point for the fraction expelled from feldspar by 600° heating is obviously in error and has not been plotted. This point is in fact quite disturbing, for there appears to be no ready explanation for the low value other than that all other feldspar runs were accompanied by air contamination—which seems highly unlikely in view of experience with blank runs.

Conclusions

One of the disturbing features of the mica-feldspar discrepancy which has been noted (Lipson, 1956) is that, if leakage from feldspar is accepted as the cause, this leakage appears to be fractionally the same for many samples and over a long range of geological time. An example of this is the important work of Wasserburg and Hayden (1955) on feldspars of known age ranging from 200 to 2000 m.y., where all the data were consistent with a single, but as we now know, low-branching ratio. Subsequent feldspar-mica comparisons by Wasserburg, Hayden, and Jensen also exhibit this uniformity of argon leakage. Whereas Wetherill, Aldrich, and Davis reported a considerable spread in mica-to-feldspar ratios, to the extent that the ratios correlated with age, the younger samples showed greater argon loss. But if a diffusion mechanism is responsible for the argon leakage, we should expect, fractionally, very much greater argon loss in ancient specimens than in recent.

In contrast with the work just mentioned, Berkeley data, though limited, would appear to illustrate the diffusion behaviour. We have in the present work data which show little or no argon loss from feldspar of 100 m.y. age, whereas in the work of Folinsbee, Lipson, and Reynolds on 2300-m.y.-old rocks from the Yellowknife District, N.W.T., argon loss from potash feldspar appeared to be about 30%, as deduced from nonseparates.

The present laboratory data suggest a room-temperature diffusion coefficient for argon in the Pala feldspar which exceeds 10^{-19} cm^2/sec. This value is high enough already to account for appreciable diffusion loss in 2000-m.y.-old specimens For example, if this were the value of D, about 35% diffusion loss would be noted in 2000-m.y. potash feldspar spheres of radius 1 cm.

Even in large single crystals of feldspar, this diffusion coefficient can lead to appreciable leakage of the radiogenic argon into the plagioclase phase of a perthitic feldspar. A common sampling technique is to grind the perthite and use a coarse-sieve fraction for analysis. In the present work this coarse fraction was found to be materially enriched in potash feldspar. It is suggested that this effect may have contributed to lower apparent A^{40}/K^{40} ratios in some cases of past work. A method of sampling the original feldspar which does not discriminate against the plagioclase phase is wanted in work on perthite.

More laboratory work is needed. The leakage curves presented here are obviously tentative and need to be plotted much more minutely. The work, unfortunately, is tedious, yet requires the taking of great pains.

Acknowledgements—I am grateful to Professor R. JAHNS and Mr. W. OKE of the Department of Geology, California Institute of Technology, for help in obtaining samples from the Pala District. Mr. D. TILLES did the actual collecting and assisted in preliminary work with the argon-extraction apparatus. I have benefited greatly from discussions with Professor G. H. CURTIS of the Department of Geology at Berkeley. I wish to thank Mr. LAURENCE BEAL for making the precise alkali analyses needed, and Professor C. F. POWELL and members of the cosmic-ray laboratory at the University of Bristol, for their hospitality while this paper was written.

REFERENCES

CARSLAW H. S. and JAEGER J. C. (1947) *Conduction of Heat in Solids*. Oxford.

CHAYES F. (1952) On the association of perthitic microcline with highly undulant or granular quartz in some calcalkaline granites. *Amer. J. Sci.* **250,** 281–296.

FOLINSBEE R. E., LIPSON J., and REYNOLDS J. H. (1956) Potassium argon dating. *Geochim. et Cosmochim. Acta* **10,** 60–68.

JAHNS R. H. and WRIGHT L. A. (1951) Gem-and lithium-bearing pegmatites of the Pala District, San Diego County, California. Spec. Rep. 7-A, State of Calif., Dept. of Natural Resources, Div. of Mines.

JEFFERY P. M. (1956) The radioactive age of four Western Australian pegmatites by the potassium and rubidium methods. *Geochim. et Cosmochim. Acta* **10,** 191.

LIPSON J. I. (1956) Potassium-argon dating of sediments. *Bull. Amer. Geol. Soc.* (in press).

REYNOLDS J. H. (1956) High sensitivity mass spectrometer for noble gas analysis. *Rev. Sci. Instrum.* **27,** 928.

WASSERBURG G. J., and HAYDEN R. J. (1955) A^{40}-K^{40} dating. *Geochim. et Cosmochim. Acta* **7,** 51-60.

WASSERBURG G. J., HAYDEN R. J., and JENSEN K. T. (1956) A^{40}-K^{40} dating of igneous rocks and sediments. *Geochim. et Cosmochim. Acta* **10,** 153-165.

WETHERILL G. W., ALDRICH, L. T., and DAVIS G. L. (1955) A^{40}/K^{40} ratios of feldspars and micas from the same rock. *Geochim. et Cosmochim. Acta* **8,** 171-172.

WETHERILL G. W., WASSERBURG G. J., ALDRICH, L. T., TILTON, G. P., and HAYDEN R. J. (1956) The decay constants of K^{40} as determined by the radiogenic argon content of potassium minerals. *Phys. Rev.* **103,** 987.

Geochimica et Cosmochimica Acta, 1957, Vol. 12, pp. 185 to 189. Pergamon Press Ltd., London

Natural variations in the nitrogen isotope abundance ratio in igneous rocks*

K. I. Mayne
Clarendon Laboratory, Oxford

(*Received* 3 *March* 1957)

Abstract—A brief preliminary survey of the amount and isotopic composition of the nitrogen found in a range of igneous rocks shows that there is a substantial variation (about a factor of 25) in the yield of nitrogen per gram of rock; and that the isotopic composition of the nitrogen varies regularly with the yield within the range of a few per cent.

Introduction

Nitrogen is cosmically one of the more abundant elements; but on the earth it has been depleted (relative to Si) by a factor of approximately $7{\cdot}5 \times 10^{-7}$ (Urey, 1952), because of its ability to form volatile compounds which were probably lost during the formative stage of the planet. A study of the terrestrial occurrence of nitrogen and its isotopic composition would contribute towards understanding the conditions at the time of the formation of the earth and the development of its atmosphere.

There is little reference to be found in the literature to work on nitrogen contained in igneous rocks. In some early work, Lord Rayleigh (1939) found that on heating to redness for 4–5 hr a sample of rock which was ground to a fine powder and mixed with an approximately equal amount of CuO, the yield of nitrogen was constant, within about ± 20 per cent, at 0·04 cm³ s.t.p./g of rock for the wide range of igneous rocks which he investigated. This nitrogen he considered to be in the form of an ammonium compound in the rock. Recently, Hoering (1956) degassed samples of crushed rock at 1400°C for several hours in an induction furnace, and found the nitrogen content to be about one hundred times less than the value given by Rayleigh. The nitrogen from some granites was less than 1‰ enriched in ^{14}N with respect to atmospheric nitrogen. The low nitrogen content found by Hoering has been questioned by workers engaged in extracting argon from igneous rocks.

Nitrogen has also been reported as occurring in chondritic meteorites to the extent of 0·0008 cm³ s.t.p./g (Noddack, 1934), about fifty times less than Rayleigh's value for igneous rocks. No isotopic analysis was made.

Large variations in the isotopic composition of nitrogen from radioactive minerals have been reported by White and Yagoda (1950), but not confirmed by Hoering. The isotopic ratio showed a marked age effect, and it has been suggested that the high level of radioactivity may be the cause. Only rocks of low activity (several p.p.m. of uranium and thorium) are considered here. Biological fractionation of the nitrogen isotopes has been reported by Hoering (1956) and Parwell *et al.* (1957), but is not dealt with here.

* In the autumn of 1951 the author was privileged to spend a term in Prof. H. C. Urey's laboratory at the University of Chicago, and at his suggestion an investigation was begun of the naturally occurring variations in the isotopic ratio of the nitrogen found in igneous rocks. The work was never completed, but in view of recent publications by Hoering (1956) and Parwel *et al.* (1957), the results obtained may be of some interest.

Experimental Details

In the present work the method of degassing the rock sample was in principle similar to that adopted by Rayleigh. Most of the samples obtainable were unfortunately not freshly mined; however, in every case the outside exposed portion of the sample was broken off and discarded and only a piece from the inside was used. This was crushed, and ground to pass 120-mesh,

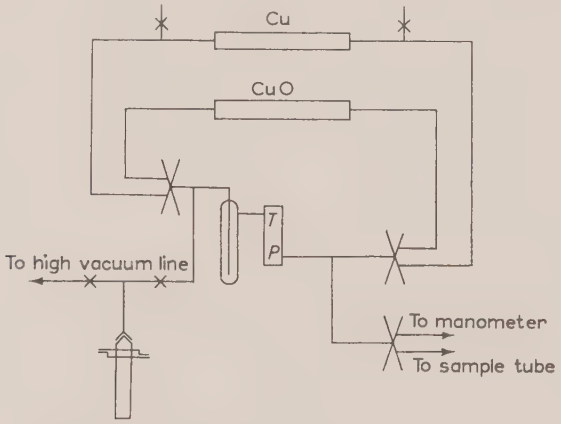

Fig. 1.

Table 1

Sample	Location	Age (approximate)	Yield (cm^3 s.t.p./g)	δ
Rhyolite	Lipari Island	Recent, extrusive	0·049	−15·6
Hornblende-mica-andesite	Hoosac Mt., Eureka County, Nevada.	Tertiary 30 m.y.	0·0187	−11·8
Trachyte	Mauna Hualalai Hawaii.	Recent, highly siliceous.	0·016	−1·2 −1·0
Basalt	Disco Island	Tertiary 40 m.y.	0·015	−0·2
Basalt	Holyoke, Mass.	Triassic 160 m.y.	0·016 0·018	+4·8 +5·2
Olivine	Braunshausen, S.W. Germany.	Permian 200 m.y.	0·017	+6·9
Granite	Zehren, nr. Meissen, Germany.	Carboniferous 250 m.y.	0·0074 0·0069 0·0070	+8·1 +8·0
Olivine basalt	Mauna Loa, Hawaii	Lava from 1942 eruption	0·0025	+9·9
Obsidian	Monolake, Calif.	Recent	0·0022 0·003	+30·9
Dunite*	Jackson County N. Caroline	Pre-Cambrian 500 m.y.	0·0018	+5·5

* See text.

dried in an oven, and about 30 g weighed out. A somewhat greater amount of CuO was weighed out (the CuO was prepared by degassing Merck CuO and then re-oxidizing with nitrogen-free oxygen). Most of this was mixed with the powdered rock and loaded into a silica tube, closed off at one end, which formed a lining for a stainless-steel combustion tube: the remainder of the CuO was added on top of the mixture. The lining was inserted in the combustion tube, which was joined on to the gas-handling system shown in Fig. 1 by means of a greased cone and socket joint. The tube was pumped out very slowly, vacuum-tested, and degassed at about 100°C for several hours while being pumped, to remove adsorbed air. A final test of the vacuum was made by isolating the system overnight.

In order to degas the rock, the temperature of the combustion tube, while closed off from the vacuum system, was raised slowly to 950°C and maintained there for at least 15 hr. It was found by experiment that a few hours only were apparently sufficient to extract all of the nitrogen; at least, continuing the treatment for periods up to 30 hr gave no further yield. The yields from three samples of the same piece of granite subjected to widely varying heat treatment are given in Table 1; they indicate the consistency to be expected in the experiments.

The gaseous products of the combustion were then cleaned, to leave only nitrogen and the rare gases; the amount of these latter represented only a small part of the total gas sample. Firstly, the gas was pumped into the CuO furnace, by means of an electrically operated Toeppler pump, and then, while the CuO furnace was heated to 800°C and allowed to cool, the gas was continually circulated over the CuO, condensibles being removed by the liquid-nitrogen-cooled trap. In this way, H_2, CO, CO_2, SO_2, and hydrocarbons are effectively removed. The gas was then circulated over hot copper maintained at 400°C, in order to remove O_2. Finally, the N_2 and the rare gases remaining were pumped into a constant-volume manometer, and the volume of gas measured by observing the pressure. For isotopic analysis, the gas was compressed into a sample tube and transferred to the gas-handling system of a double-collection mass-spectrometer of the Nier type, previously described by Allen *et al.* (1950). This was designed for the measurement of small differences in isotopic ratios between samples and a standard.

Results

The yield and isotopic composition of the nitrogen obtained from a range of igneous rocks are given in Table 1. The isotopic variation δ shown in the last column is expressed in the usual way as

$$\delta^{15}\mathrm{N}‰ = \frac{(^{15}\mathrm{N}/^{14}\mathrm{N})_{\text{sample}} - (^{15}\mathrm{N}/^{14}\mathrm{N})_{\text{standard}}}{(^{15}\mathrm{N}/^{14}\mathrm{N})_{\text{standard}}} \times 1000$$

The standard for comparison in all this work was atmospheric nitrogen, obtained by cleaning a sample of air in the gas-handling system. Thus, positive values for δ indicate an excess of ^{15}N in the sample, and negative values an excess of ^{14}N, with respect to atmospheric nitrogen. The uncertainty of the measurements of the isotopic composition of the standard was less than 0·2‰. Samples of nitrogen from the same rock prepared at different times were about as good as this, when the amount of gas sample was large. However, where the yield of nitrogen is very small, the precision is adversely affected by background in the mass spectrometer and any CO contamination which may remain in the gas sample. Furthermore, with low yield the effect of incomplete desorption of atmospheric nitrogen, or of a small leak in the vacuum system, is most pronounced. Thus, in the case of the Jackson County Dunite, Hoering found a nitrogen yield of less than 0·0004 cm^3 s.t.p./g of rock. If the higher yield reported here is due to contamination by atmospheric nitrogen, the true value of δ for the nitrogen of the rock is greater than 30‰.

Discussion

From the data in Table 1 it is evident that there is a substantial variation in the yield of nitrogen per gram of rock, and in its isotopic composition. The extent of the isotopic fractionation is, however, less than that reported for hydrogen, carbon, and sulphur, and about the same as the measured fractionation of the oxygen isotopes in nature. The high values of nitrogen content reported here correspond closely to Lord Rayleigh's abundance figures, the lowest ones are in reasonable agreement with Hoering's determinations; and there is a continuous variation from one to the other. Contrary to Rayleigh's findings, the nitrogen content of igneous rocks is not constant. Although the data are insufficient to draw any detailed conclusions, there is a parallelism between the nitrogen content and its isotopic composition, in that the more depleted the rock is in nitrogen, the more enriched this is in ^{15}N. The logarithm of the nitrogen yield is an approximately linear function of δ. There appears to be no well-defined correlation of the age of the rock sample with the isotopic composition or yield of its nitrogen; possibly any age-effect which may exist is obscured in some cases by a re-melting process; considerably more data from well-selected rocks are required on this point.

The measured effect can hardly be produced by an incomplete extraction of nitrogen from the samples; if this were the case, one would expect that the nitrogen which is extracted, if showing any fractionation at all, would be enriched in ^{14}N. It could be produced by preferential loss of ^{14}N during the preliminary desorbing process; but the fact that the German granite samples gave consistent results under widely varying desorbing treatment makes this appear unlikely. One might suppose that the total nitrogen content of the rocks is constant, as Rayleigh finds, but occurs in various chemical compounds, from some of which it can be extracted by the present method, and some of which are exceedingly stable, even in the presence of water, at 950°C; and that ^{14}N is enriched in the more stable form. Since it is most unlikely that all of the rocks of the earth's crust would be leached of nitrogen to exactly the same extent, the constant nitrogen yield found by Rayleigh would suggest that the earth's atmosphere is not derived from the crust, but is in large part primordial. On this basis also, together with the present isotopic analysis, atmospheric nitrogen would be "heavy" with respect to the average of crustal nitrogen.

It seems more likely that the effects governing the distribution of nitrogen and its isotopes, as measured here, represent a process of loss of nitrogen from the crust to the atmosphere, and in such a way that the nitrogen remaining in the rocks is concentrated in ^{15}N.

The evidence from the present work, and from that of Hoering, and of the Noddacks, would suggest that very old rocks contain only small amounts of nitrogen. If the Pre-Cambrian rocks of the earth originally held as much nitrogen as some of the recent ones now contain (i.e. 0·05 cm^3 N/g), then from an estimated $2{\cdot}5 \times 10^{25}$ g of rock in the earth's crust (of which about 90 per cent is Pre-Cambrian) approximately one-half of the 4×10^{21}g of nitrogen in the atmosphere would be derived by leaching and weathering, quite apart from any contribution from the mantle. A substantial nitrogen-containing primitive atmosphere would not be

required for the earth. On this basis also the nitrogen residing in the crust is only a few per cent of that in the atmosphere.

Urey, (1952, p. 123, etc.) has considered in some detail the thermodynamic stability of nitrogen compounds in the presence of cosmic proportions of the elements, over a range of total pressure (in effect the hydrogen pressure) and temperature. In particular, he has shown (in Fig. 13, p. 129) the regions of temperature and pressure in which nitrogen can be retained as nonvolatile NH_4Cl; and in which more than half of the nitrogen will be present as ammonia. If the earth accreted under these conditions of (low) temperature and pressure, then the nitrogen of the rocks would be largely in ammoniacal form, as Rayleigh believed it was. Nitrides of some of the elements may also be present. (At the higher temperatures, $\sim$1200°C, which exist in the earth's crust today, this situation may not hold: and unless the pressure of hydrogen is great enough, the nitrogen may exist largely as gas, dissolved in the melt. As the melt rises and cools, the conditions favour ammonium-salt formation.) As these salts are leached from the rocks, some fractionation of the nitrogen isotopes can be produced (Friedman and Bigeleisen, 1950). It would seem desirable to examine the chemical form in which the nitrogen is present in the rocks. It would also be interesting to have data on the nitrogen of stone meteorites.

Acknowledgements—The author is extremely grateful to Prof. H. C. Urey for making possible his visit to Chicago in 1951. Prof. Urey is always a source of inspiration, and has shown interest in the present work; he has been good enough to read this manuscript. Thanks are also due to Prof. L. R. Wager and Dr. H. D. Holland for reading the manuscript.

References

Allen H. A. *et al.* (1950) *Rev. Sci. Instrum.* **21,** 724.
Friedman L. and Bigeleisen J. (1950) *J. Chem. Phys.* **18,** 1325.
Hoering T. (1956) Nuclear Processes in Geologic Settings, NAS–NRC, Proceedings of Second Conference, p. 39.
Noddack I. and Noddack W. (1934) *Svensk. Kem. Tidskr.* **46,** 173.
Parwel A., Ryhage R., and Wickman F. E. (1957) *Geochim. et Cosmochim. Acta* **11,** 165.
Rayleigh Lord (1939) *Proc. Roy. Soc.* **A170,** 451.
Urey H. C. (1952) *The Planets.* Oxford University Press.
White W. and Yagoda H. (1950) *Science* **111,** 307.

Geochimica et Cosmochimica Acta, 1957, Vol. 12, pp. 190 to 194. Pergamon Press Ltd., London

Rare earths in yttrotungstite

J. R. Butler
Department of Geology, Imperial College of Science, London

(*Received* 20 *February* 1957)

Abstract—The rare earth mineral yttrotungstite accords with Goldschmidt's complete assemblage type in containing sensible amounts of Yt and all the lanthanons except Pm and Eu. The relative abundances of the lanthanons in yttrotungstite and in the cosmos are similar except that the ratio La/Ce is substantially higher in the latter.

Introduction

In the course of a survey of the distribution of rare earths in rare-earth minerals an opportunity arose to examine a sample of yttrotungstite from Kramat Pulai, Perak, Malaya. When originally analysed in 1926 the mineral was reported to contain nearly 70% WO_3 and 16% ThO_2 and was accordingly named thorotungstite (Scrivenor and Shenton, 1927). Recent analysis by Bennett, Chadwick, and Tooke (Bradshaw, 1950) has confirmed the WO_3 content but not the presence of ThO_2, and it is clear that what was reckoned as ThO_2 was largely rare-earth oxides. Hence the name yttrotungstite was proposed (Bradshaw, 1950).

Individual rare earths were determined spectrographically (by a method to be described elsewhere) following a chemical separation of total rare earths. There seems little agreement among chemical textbooks about methods for estimating total rare earths, and the procedure followed is therefore mentioned below. The method leads to a separation of rare earths from all elements except Th, which in yttrotungstite is negligible.

Analytical Procedure

500 mg yttrotungstite were decomposed in a platinum dish by twice evaporating with mixtures of 10 ml concentrated HNO_3 and 20 ml 40% HF. The residue was treated with a few ml of 40% HF, followed by 20 ml 10% HF, and allowed to stand overnight.

The insoluble fluorides were collected on a Whatman No. 40 filter paper and washed ten times with 10% HF. Using a wash bottle with a fine jet the fluorides were water-washed back into the platinum dish and evaporated to dryness on a steam bath. 15 ml 60% $HClO_4$ were added and the mixture was fumed almost to dryness on a hot plate. The filter paper was ashed in a platinum crucible and the small residue also evaporated with $HClO_4$ almost to dryness. The perchlorates from both vessels were taken up in cold water, a few drops of 20-vol H_2O_2 added, and the solutions transferred to a 600-ml Pyrex beaker. The rare earths were precipitated as oxalates by the method of Gordon *et al.* (1949) although after the addition of the 8 gm of oxalic acid and the 30 min stirring

(*loc. cit.*, p. 1325) the solution was allowed to stand overnight. The oxalates were then collected on Whatman No. 40 filter paper, washed with 2% oxalic acid solution adjusted to pH 1·0 with HCl, and subsequently ignited to oxides.

Discussion

From the point of view of cosmic abundance the rare earths may be considered in three groups, the first consisting of the abundant Sc and Yt, the second of the lanthanons with even atomic number, and the third of the lanthanons with odd atomic number. (Pm, $Z = 61$, is sensibly absent in nature.) The abundance figures given recently by Suess and Urey (1956) show that both the Z-even and the Z-odd lanthanons tend to become rarer with increasing atomic number; however, a Z-even lanthanon is always more and sometimes substantially more abundant than those (Z-odd) lanthanons of adjacent atomic numbers.

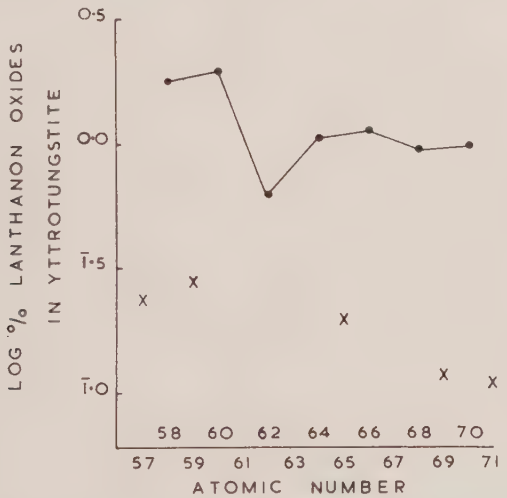

Fig. 1. Distribution of the lanthanons in yttrotungstite from Kramat Pulai, Perak, Malaya. Points representing the Z-even lanthanons are joined.

Under geochemical influences it is to be expected that the relative abundances of the rare earths will be modified in comparison with their cosmic abundances (although it is to be remembered that the cosmic abundance estimates are based partly on data of abundances in the lithosphere). Nevertheless, certain of the rare earths form geochemically coherent groups and the closeness of their association can be regarded partly as a result of the similarities in size of their trivalent ions together with the tendency of a few of the rare earths to form quadrivalent or divalent ions. The ionic sizes of the trivalent lanthanon ions decrease regularly from 1·14 Å for La^{+3} to 0·85 Å for Lu^{+3}. Yt^{+3} and Sc^{+3} have radii of 0·92 Å and 0·81 Å respectively. Eu is readily reduced to Eu^{+2} (1·24 Å) and it is possible that Sm^{+2} (1·25 Å approx.) and Yb^{+2} (1·06 Å) exist in minerals (Goldschmidt, 1954). Ce^{+4} (0·94 Å) is thought to be present in freyalite and may well occur in other minerals formed under highly oxidizing conditions but it need not lose its association with other rare earths on this account, as it could easily be incorporated by capture in, for example, Yt-rich minerals. To a less extent Yb^{+2}

might be incorporated by admittance in rare-earth minerals, but Eu^{+2} and Sm^{+2} are too large to be closely associated with La^{+3} etc. as shown by their occurrence (together with Yb) in Ca, Sr, and Pb minerals. On the other hand, Sc^{+3} is too small to concentrate appreciably in rare-earth minerals unless they are Lu-rich, and much Sc^{+3} is captured in common ferromagnesian minerals.

Table 1

	1	σ	2	3
Sc_2O_3	*	—	—	—
Yt_2O_3	45·5	5	58·9	50·6
La_2O_3	1·25	7	1·12	11·3
CeO_2	9·55	5	8·11	12·8
Pr_6O_{11}	1·49	7	1·28	2·27
Nd_2O_3	10·3	5	8·94	8·16
Sm_2O_3	3·37	5	2·82	3·75
Eu_2O_3	*	—	—	—
Gd_2O_3	5·62	$6\frac{1}{2}$	4·54	3·88
Tb_4O_7	1·05	6	0·82	0·54
Dy_2O_3	6·10	5	4·78	3·16
Ho_2O_3	—	—	—	—
Er_2O_3	5·07	13	3·89	1·80
Tm_2O_3	0·62	7	0·47	0·18
Yb_2O_3	5·24	5	3·89	1·25
Lu_2O_3	0·59	28	0·43	0·28
	95·75		(99·99)	(99·97)

1 Percentage composition of rare earths separated from yttrotungstite, Kramat Pulai, Malaya. Sc_2O_3 and Eu_2O_3 below sensitivity limit of 0·1%. No data for Ho_2O_3.
σ Percentage standard deviation of estimates of individual rare earths from duplicated spectrograms.
2 Atomic percentage composition of rare earths except Ho from yttrotungstite (calculated to 100%).
3 Atomic percentage composition of rare earths excluding Sc, Pm, Eu, and Ho in the cosmos derived from data selected by Suess and Urey (1956).

The close association of Yt and the lanthanons is preserved in yttrotungstite (Table 1, col. 1) which contained 18·96% total rare earths (Analyst: Miss Rosemary Hall). Sc and Eu are lacking, Yt is easily the most abundant rare earth and the *Z*-even lanthanons preponderate over the *Z*-odd lanthanons. Moreover, the most common *Z*-even lanthanon (Nd) is only 3·2 times more abundant than the rarest *Z*-even lanthanon (Sm) and, similarly, the variation in concentration of the *Z*-odd lanthanons is, excluding Pm, Eu, and Ho, most moderate. Thus, in a plot of lanthanon concentration against atomic number (Fig. 1), the peak occurring above $Z = 58$ and $Z = 60$ is not a sharp one and the mineral accordingly resembles yttrofluorite and gadolinite in belonging to Goldschmidt's complete assemblage type (Goldschmidt and Thomassen, 1924). The evident tolerance of the yttrotungstite lattice in accepting rare earths of differing ionic size might suggest that the environment in which the mineral was formed had relative concentrations of rare earths not too dissimilar from those now

found in the yttrotungstite; if this is so, then it is of interest to compare the cosmic abundances of the rare earths excluding Sc, Eu, and Ho with those found in the mineral (Table 1 col. 3). The agreement is striking for all elements except La, Er, and Yb. In particular, the Nd : Sm : Gd ratios are similar and it is unnecessary to suppose that much Sm has been divorced from either Nd or Gd due to reduction to Sm^{+2} prior to the formation of the yttrotungstite. Fleugge (1946) has drawn attention to the peculiar isotopic distribution of Sm which shows Sm^{148} and Sm^{152} each substantially in excess of Sm^{150} and helps to explain why the cosmic abundance of Sm is nearer that of Gd rather than midway between that of Nd and Gd. (Sm^{148} is radioactive, but the half-life period of $1{\cdot}4 \times 10^{11}$ years is too great to account for much reduction in the cosmic concentration during geological time.) The heavier lanthanons are relatively concentrated in the yttrotungstite and as the values for Gd, Dy, Er, and Yb are so close and without sensible trend it may be supposed that the concentration ratio heavier/lighter lanthanons in the solutions giving rise to the yttrotungstite was higher than that obtained from the data taken to represent cosmic abundance.

It will be of great interest if other rare-earth minerals are found associated with the yttrotungstite. The ratio Ce/La is very high in the yttrotungstite (7·2) compared with the cosmic ratio (1·1) but it compares more favourably with Ce/La ratios in other Yt-rich rare-earth minerals (Goldschmidt and Thomassen, 1924, and unpublished results from this laboratory on gadolinites and a variety of Nb-Ta rare earth minerals). Even the most abundant rare-earth mineral, monazite, does not have Ce/La less than about 1·5 (Sahama and Vähätalo, 1939; Wylie, 1950; Murata *et al.*, 1953) and rare-earth minerals with La exceeding Ce cannot be common. It is possible that trace amounts of La may be concentrated relative to Ce in K-feldspars (Goldschmidt, 1954, and Sandell, 1952), and Ce/La ratios near and below unity have been reported in granites and syenites from Lapland (Sahama, 1945). Nevertheless, in sea-water, Ce, which is at the low concentration of 4×10^{-4} g/ton, exceeds La (Goldschmidt, 1937) and in the hydrolysate group of sediments (which must extract much of the La and Ce brought to the oceans by rock weathering) likewise Ce/La exceeds unity; Minami (1935) found Ce/La varying from about 2 to nearly 4 in composite samples of European and Japanese shales. It is suggested that the cosmic value selected for Ce/La by Suess and Urey (1956) may be rather high.

Acknowledgements—I am grateful to Mr. E. Bradshaw of the Malaya Geological Survey for the specimen of yttrotungstite; Miss Rosemary Hall for carrying out chemical analyses; and to Sir William Ogg and Dr. Alex Muir of Rothamsted Experimental Station for permission to use the Mannkopff Spectrograph there.

References

Bradshaw E. H. (1950) *Colon. Geol. Min. Resour.* **1,** 50–51.

Fleugge S. (1946) *Nuclear Physics; Tables and an Introduction to Nuclear Physics*, Interscience Publishers, N.Y.

Goldschmidt V. M. (1937) *J. Chem Soc.* **1937,** 644–673.

Goldschmidt V. M. (1954) *Geochemistry* pp. 306–318, Oxford.

Goldschmidt, V. M. and Thomassen, L., 1924. *Vidensk. Skr. I, Math-nat. Kl.* **5.**

Gordon L., Vanselow C. H. and Willard, Hobart H. (1949) *Analyt. Chem.* **21,** 1323–5.
Minami E. (1935) *Nachr. Ges Wiss,* Göttingen, IV, N.F. 1, **14,** 155–170.
Murata K. J., Rose H. J. Jr., and Carron M. K. (1953) *Geochim. et Cosmochim. Acta* **4,** 292–300.
Sahama Th. G. (1945) *Bull. Comm. Géol. Finlande* **135.**
Sahama Th. G. and Vähätalo V. (1939) *Bull. Comm. Géol. Finlande* **126.**
Sandell E. B. (1952) *Geochim. et Cosmochim. Acta* **2,** 211–216.
Scrivenor J. B. and Shenton J. C. (1927) *Amer. J. Sci.* **13,** 487–490.
Suess H. E. and Urey H. C. (1956) *Rev. Mod. Physics* **28,** 53–74.
Wylie A. W. (1950) *Aust. J. Appl. Sci.* **1,** 164–171.

Geochimica et Cosmochimica Acta, 1957, Vol. 12, pp. 195 to 208. Pergamon Press Ltd., London

Zone refining and the origin of potassic basalts

P. G. Harris
Department of Geology, University of Leeds

(*Received* 25 *February* 1957)

Abstract—The process of "zone refining" or "zone melting" is described. By an analogous process, magma formed at great depth within the mantle and ascending by solution and crystallization, could become enriched in those elements unable to substitute in the mineral phases of the mantle. The geological possibility of the process and its application to potassic basalts are discussed. Some sodic basalts are attributed to fractional crystallization modified by reaction with mantle material.

Introduction

In a process called "zone melting" or "zone refining" (Pfann, 1952; Goodman, 1954), recently developed for the purification of metals and organic compounds, impurities are removed by passage of a molten zone along a bar or tube of the solid material. It is suggested that the existence of such a process on a geological scale within the mantle could explain the origin of potassic basalts.

The Process of Zone Refining

A simple account of the process is that of Goodman (1956). In one variant of it, a tube filled with the material to be purified, has one end of its contents melted by a heating coil. If the tube is then moved slowly through the heating coil, the material will melt as it passes into the heated region and solidify as it emerges, so that in effect a molten zone moves along the length of the tube. Impurities that are more soluble in the liquid material than in its crystalline phase will be largely retained when they enter the liquid zone and will be swept along in the zone to the end of the tube.

This removal of impurities will be limited, being defined by the distance through which the molten zone moves and by the distribution or partition coefficient k of the impurity between the solid and liquid phases of the host material.

I.e. $$k = \frac{\text{concentration of impurity in solid phase}}{\text{concentration of impurity in liquid phase}},$$

the solid phase in chemical equilibrium with the liquid being that crystallizing behind the molten zone.

In a tube of solid material containing x p.p.m. of an impurity A, the initial molten zone will contain x p.p.m. of A also, but crystals deposited behind the moving molten zone may be impoverished in A. E.g. if $k = \frac{1}{2}$, the initial crystals deposited will contain $\frac{1}{2}x$ p.p.m. of A, while if $k = 1/100$, the crystals will contain $1/100x$ p.p.m. of A. Continued melting of the original solid in front of the liquid zone and crystallization of the purified material behind it will cause an increase in concentration of the impurity A in the liquid, accompanied by a proportional increase in the newly deposited solid. This increase in concentration of A in the liquid zone will have a maximum, attained in the above cases at concentrations

of $2x$ p.p.m. and $100x$ p.p.m. of A respectively. At this stage, the solid material deposited behind the molten zone will have the same concentration of x p.p.m. of A as the original solid, melting in front of the zone.

Following Pfann (1952), equations can be given for the concentration of the impurity at any stage in the passage of the moving molten zone.

$$\frac{\text{Concentration in deposited material}}{\text{Concentration in original material}} = 1 - (1 - k)e^{-kl}$$

and since $$\frac{\text{concentration in deposited material}}{\text{concentration in liquid phase}} = k$$

$$\therefore \quad \frac{\text{concentration in liquid phase}}{\text{concentration in original material}} = \frac{1}{k} - \left(\frac{1}{k} - 1\right)e^{\ kl}$$

In the equations, l is the number of zone lengths traversed by the molten zone, i.e. the total distance of travel divided by the length of the zone itself, while e is the exponential function. The assumption is made that the liquid within the zone is kept uniform by convection and diffusion.

These relationships are shown graphically in Fig. 1, the impurity being enriched in the liquid zone from an original concentration of unity to a value dependent on the distribution coefficient and the distance traversed. As indicated by the figure, enrichment of an impurity in the final liquid can be very great if the distribution

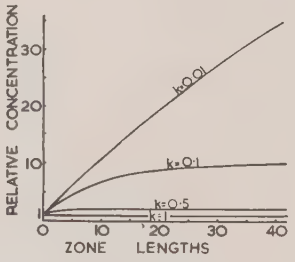

Fig. 1. The effect of zone refining on the concentration of an impurity in the liquid, for various values of k, the distribution coefficient. The progress of the zone refining is shown in zone lengths, i.e.

$$\frac{\text{total distance traversed}}{\text{length of a single zone}}.$$

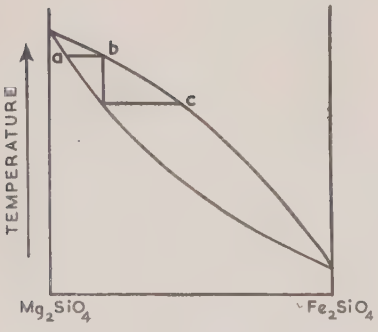

Fig. 2. The system Mg_2SiO_4–Fe_2SiO_4.

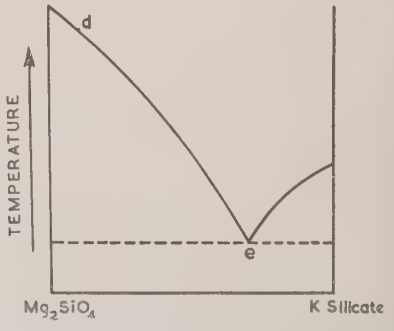

Fig. 3. A possible equilibrium diagram of a system forsterite–potassium silicate.

factor or ease of substitution in the solid phase is sufficiently small. Since the equations are exponential, increase in concentration of an impurity in the liquid will tend towards a maximum of $1/k$ times the original concentration. This maximum is never attained, but is approached to within 1% when the product of k and l reaches a value of about 5, i.e. when $k = \frac{1}{2}, l = 10$; when $k = 1/100, l = 500$.

The zone-refining process can be discussed equally readily in terms of silicates and phase diagrams. A tube filled with a fayalite-forsterite mixture of composition b, on complete fusion at one end of the tube will form a liquid of the same composition. If the fused zone is moved along the tube, olivine of composition a will begin to crystallize behind the zone, where the temperature falls low enough (Fig. 2). Continued incorporation of olivine b into the zone and crystallization of olivine a behind the zone will cause the liquid to become enriched in Fe_2SiO_4, its composition moving down the liquidus, accompanied by a corresponding increase in Fe_2SiO_4 content in the deposited solid, as shown by the liquidus-solidus relationship. This enrichment of fayalite in the liquid will cease at c, however, when the deposited olivine has a composition b the same as that of the original olivine melting in front of the zone.

A long tube of olivine of composition b through which a single molten zone has passed, will show three stages of Fe_2SiO_4 concentration—an initial few zone lengths in which the composition changes exponentially from a to b, the balance of the tube of uniform composition b, and a final zone length of average composition c.

A tube of Mg_2SiO_4 containing a small concentration d, of potassium silicate, subjected to the same process of zone refining, will behave in conformity with the appropriate phase diagram, probably of the nature of Fig. 3. Assuming the degree of substitution by potassium in olivine to be negligible under ideal conditions, the olivine deposited behind the liquid zone will contain no potassium, the latter being completely retained in the liquid and becoming increasingly concentrated there. The liquid composition will move down the liquidus until either the eutectic e is reached, or the zone refining ceases. In actual practice, ideality will not be attained and there will be a small amount of liquid trapped between the deposited crystals and some very slight retention of potassium in the olivine crystals, so that the potassium silicate will have an effective distribution coefficient slightly greater than zero. If, for example, k was 1/100, enrichment of potassium in the liquid zone would have a maximum at 100 times its original concentration, reaching 99% of this after about 500 zone lengths The concentration of potassium in a very long tube of olivine would show three stages—an initial 500 zone lengths in which potassium increased exponentially from $1/100d$ almost to d, an intermediate stage of nearly uniform composition d the same as that of the original material, and a final stage of one zone length with an average potassium concentration of $100d$.

In each case, although the final zone length will have an average concentration of impurity determined by the values of k and l, the actual distribution of the impurity within it will be a result of the cooling history of the final zone length itself. If quenched, it will have a uniform composition, but if cooling has extended gradually to the very end of the tube, the result within the final zone length will be that of fractional crystallization. The impurity distribution will then be similar

to that shown for various values of k, by Neumann, Mead, and Vitaliano (1954) in Fig. 3 of their paper. A last, very small fraction of the final zone could have a very high concentration of impurity.

The general effect of a zone-refining process on a very long tube of material can be summarized from the three stages of concentration of the impurity in the deposited solid. If the impurity is really soluble in the host crystal, i.e. if there is some degree of substitution or diadochy, the initial stage of slightly lower concentration than the original will be short. If there is no degree of substitution or solubility in the host material, the initial stage will be long and of very much lower concentration than the original. In the middle stage, the crystals will be of the same concentration as the original material in each case. A single final zone length will have a slightly higher concentration in the case of the diadochic impurity, and a very much higher concentration of the nondiadochic impurity.

If the tube contains two materials in eutectic proportions, the process will effect no separation between them. If the two are not in eutectic proportions they will again show three stages of composition. In the initial stage, the component in excess will be deposited. In the middle stage, the liquid will have attained the eutectic composition, and to maintain this will require to deposit material of the same composition as that dissolving in front of it. The final zone length will consist of the eutectic mixture. Several impurities in a mixture of several independently crystalline substances will behave as predicted from their solubilities or ease of substitution (i.e. their distribution coefficients) in each or all of the crystalline substances deposited behind the moving liquid zone.

The Application of the Process to Geology

It is generally recognized that magma formed by a limited degree of partial fusion of mantle material will be primary basalt of tholeiitic type, approximately saturated in silica with only minor normative olivine or normative quartz. Presumably, this magma represents the minimum melting-point mixture or eutectic for the major minerals of the mantle, olivine, pyroxene, spinel, and perhaps plagioclase, under the conditions prevailing at the place of formation. Of the major constituents, calcium and aluminium are likely to be the most critical in the eutectic relationship. Assuming a mantle composition somewhere between average L-chondrite (Urey and Craig, 1953) and average peridotite (Nockolds, 1954), CaO will have a concentration between 2·2% and 3·5%, and Al_2O_3 between 3·0% and 4·0%. Even with complete melting of these constituents, a primary basalt, e.g. normal tholeiitic basalt of Nockolds (1945), with 10% CaO and 14% Al_2O_3, cannot result from fusion of more than 20–30% of the original mantle. (The value of 40% calculated by Bowen (1928) is based on a different mantle composition.) A greater degree of fusion would give a magma undersaturated in plagioclase, and require a higher temperature. A lesser degree of fusion would give the same minimum melting-point mixture of the major components, with slight adjustment of the diadochic ratios. However, this minimum melting-point mixture is not strictly an eutectic but rather a cotectic, since other minor ions occur, which are not diadochic with the major ions, and with which the liquid is

unsaturated. These minor constituents will enter the liquid phase almost completely so that their concentrations in the liquid will be inversely proportional to the degree of partial fusion.

If at any stage in its history the mantle was molten, then on solidification the temperature gradient at depth would have been very close to the minimum melting-point gradient. Subsequent heat-losses by conduction would have been very small at depths greater than 500 km, so that at such depths the temperature must be very close still to the minimum melting-point (VERHOOGEN, 1956), though, as VERHOOGEN points out, possible increases in thermal conductivity at very great depth may cause greater cooling than expected. In any case, present estimates of radioactive heat-generation based on the composition of stony meteorites are more than adequate to balance heat-losses in the deep mantle; so much so as to require special explanation (UREY, 1955). The thermal models of JACOBS and ALLAN (1956) indicate that while at depths of less than 100 km the earth has cooled, at depths greater than 500–1000 km the temperature will have risen during geological time.

In view of this, partial fusion of the mantle to form magma cannot be considered to be restricted to the top of the mantle alone, but is possible also at greater depths, even down to the core boundary. Factors which might invalidate this, are the possibility of differentiation in the deep mantle so that the minimum melting-point of its constituents is much higher than the temperature of the original liquid from which they formed, or the possibility that, due to convection currents, the temperature gradient at depth approaches the adiabatic gradient rather than the melting-point gradient (TURNER and VERHOOGEN, 1951). However, if the deep mantle is undifferentiated and if convection currents have not been operative within the solid mantle, the minimum melting-point gradient must be close enough to the temperature gradient for partial fusion to be feasible.

Magma formed within the mantle, being lighter than its surroundings, will have a tendency to move upward. Movement could be by flow along channels resulting from tensional faulting or deformation of the country rock, or by a process of solution and stoping. Since fusion at the top of the mantle may be initiated often by tensional faulting and consequent pressure-release (YODER, 1952), magma escape from here is likely to be along tensional channels. The magma itself will be almost unaltered, since any differentiation or other changes must be subsequent to its escape from its original environment, or due to changes in the environment. Within the deep mantle below the zone of fracture, tensional channels are unlikely and movement of the magma will be by the deformation of the country rock or by solution or stoping. In a gravitational pressure gradient, crystals will be more soluble at the top of a liquid body than at the bottom where the pressure is higher. Provided that the liquid is kept uniform by convection, solution of roof material and crystallization of an equivalent amount at the bottom will occur spontaneously —what might be termed solution stoping. There will be no heat-loss or diminution in liquid volume if the mantle is already at its minimum melting-point, since the heat of solution of crystals at the top of the body will be balanced by the heat of crystallization of material deposited at the bottom. Recent work shows that the speed of crystallization, and presumably also of solution, increases very markedly

with pressure and the attendant increased fusion temperature (Abelson, 1955), so in the deep mantle, magma ascent by this solution mechanism might be relatively rapid. This mechanism is likely to be more effective than deformation of the country rock in permitting the ascent of the magma body. An argument that might be raised against this solution mechanism is the possibility that since the compressibility of liquids is greater than that of solids, at very high pressures (i.e. at very great depth) liquids may be as dense as solid phases of the same composition. If this occurred, melting-point, or in this case solubility, would be a function of pressure no longer, and the mechanism could not operate even though the minimum melting-point liquid in which were concentrated the lighter constituents would still be less dense than the solid mantle. However, there seems no evidence for this supposition.

The process of solution in front of and crystallization behind an ascending magma body would have an effect very much akin to zone refining. The molten zone of the same composition as the solid moving along a tube would be replaced by a liquid body of minimum melting composition moving outward through the mantle. The product of most interest, no longer would be the solid from which the impurities had been removed, but the liquid zone itself in which the impurities had been concentrated. Also, the material involved, no longer would be a single element or compound with only minor impurities, but a mixture of all the elements. However, the effect on impurities not soluble in the deposited crystal phases would be that expected in zone refining and could be calculated from the same equations so long as the distribution factor for each element remained constant. The term "distribution factor" rather than "distribution coefficient" is used for magma-mineral relationships, as suggested by Neumann, Mead, and Vitaliano (1954).

The magma if not already saturated with the major mineral species, olivine, pyroxene, spinel, and perhaps plagioclase, would rapidly reach saturation—a quaternary cotectic. Thereafter the minerals would be deposited below the magma at the same rate as they dissolved above it. At the same time, the liquid would become adjusted rapidly for the diadochic ions of each mineral phase e.g. (Mg, Fe^{2+}, Mn^{2+}, Ni, Co, Sc); (Ca, Na); (Fe^{3+}, Cr^{3+}), etc. After this, each mineral deposited would have the same diadochic composition as its counterpart dissolved above. Those elements too large or too small, or differing too much in valency and bond type to replace the ions in the minerals being deposited, and not sufficiently abundant for their own mineral phases to crystallize, would be retained almost entirely in the liquid. Probably these elements are present in the original mantle material not so much in the crystals of the major minerals as in minute grains of accessory minerals along the crystal boundaries, the relics of the final interstitial liquid, in the same manner as radioactive elements have been shown to occur in granite. If this is true, their selective concentration does not even require complete dissolution of the mantle material by the magma. Stoping of fragments of single-crystal size would permit solution of the intergranular material.

The elements expected to be concentrated in this way would be K, Rb, Cs, Ba, Pb, Zr, Th, U, Nb, Ta, P, C, H, Cl, etc. All these should have extremely low distribution factors under these conditions, and would be greatly enriched in the

ascending magma body. For convenience, subsequent discussion will refer mainly to potassium, though these other elements would have the same behaviour.

Upward ascent of the magma would cease when the temperature gradient fell sufficiently below the solidification temperature of the magma. From this region the magma could escape only along tensional channels or by mechanical rupture of the rocks above.

Near the top of the mantle, magma ascended from depth would have much in common with magma locally formed. Both would contain the major phases of the mantle in their minimum melting proportions, and both would be in adjustment with the mantle minerals at that point so that they would contain similar proportions of the diadochic ions entering those minerals, e.g. Mg : Fe^{2+} and Ca : Na, etc. In contrast, those elements unable to enter the mantle minerals would have been greatly concentrated in the magma from the deep mantle. Depending on the number of zone lengths through which the magma had passed and the relevant distribution factors, enrichment by a factor as much as 50 or 100, compared with original mantle, could be expected for elements such as potassium. The only enrichment for such elements in the locally-derived tholeiite, however, would be that due to the partial fusion process. For example, potassium with a mantle concentration of 0·08% (K_2O), could have a maximum concentration of 0·4% (K_2O) in a magma resulting from 20% fusion, and of 8% (K_2O) in a magma in which impurities from 100 times as much mantle material were concentrated by zone refining. These values are for a distribution factor of zero for potassium, and since the factor could never be as low as this, the maximum concentrations would never be attained in practice.

The zone-refining process differs essentially from any of the conventional mechanisms of magmatic differentiation. In differentiation, the elements are derived from the original liquid body itself, and while additions can be made by assimilation. these are regarded usually as merely modifying the concentrations—not being their prime cause. Zone refining is not assimilation in the strict sense, since the total addition to the magma is small. It could be considered as a process of prolonged reaction with mantle material, rejection of minerals higher in the discontinuous reaction series, and retention of those ions of low concentration that do not enter the minerals of the continuous reaction series but form minerals low in the discontinuous series (i.e. K, OH, etc.).

Before discussing in more detail the specific application of the process to potassic basalts, attention should be drawn to two variants of the process.

Fusion of a small proportion (e.g. 1%) of mantle material would give a liquid in adjustment with the main mantle phases and hence with the expected ratios for Mg/Fe and Ca/Na, while at the same time nearly all the nondiadochic minor elements would be selectively concentrated by the melting. A magma formed by fusion of 1% of mantle material would be very similar to one that had reacted with or zone-refined 100 times its amount of mantle material. It is possible even that fusion would not be required and that the mantle has never cooled enough to lose a very small proportion of a low melting-point residual liquid, held in intergranular spaces and not abundant enough to affect the physical properties of the solid mantle. It is highly unlikely that 1% of liquid could be pressed out of the mantle,

but the liquid could be collected by a magma body ascending by a solution process as in zone refining. The process would be analogous to zone refining except that in one case the magma body of constant minor-element concentration would grow in volume as it ascended and incorporated the 1% of liquid, while in the other case the magma body of constant volume would increase in minor-element concentration as it selectively removed the traces from the solid mantle.

The same result might be achieved also by fractional crystallization within the mantle of a body of magma, itself formed no doubt by partial fusion further down. The fractional crystallization alone would cause increases in potassium concentration and in the ratios Fe/Mg and Na/Ca. However, if crystallization was accompanied by sufficient reaction with the mantle material, the Mg/Fe and Ca/Na ratios could be maintained at their original values, and the major change in the residual liquid would be its enrichment in potassium. If the final liquid represented 1% of the original mantle material in which fusion occurred, the nondiadochic impurities would have the same concentrations as in the alternative processes. This second alternative mechanism of fractional crystallization accompanied by reaction with the mantle may seem impossible from a thermal aspect. However, as Bowen (1928) has pointed out, although a magma cannot dissolve and retain in solution, phases with which it is already saturated, it can react with them. In the case of members of continuous reaction series, the reaction will tend to restore or maintain those diadochic ratios indicated by the appropriate liquidus-solidus equilibria between the magma and the solid mantle. Whether the high degree of fractionation necessary to give a great enrichment of the nondiadochic constituents is likely to be accompanied by the high degree of reaction with the mantle necessary to maintain the diadochic ratios, seems unlikely. What appears much more probable, a moderate degree of fractionation accompanied by a limited degree of mantle reaction does offer an explanation of the geochemical features of some sodic basalts, and will be discussed in more detail as an appendix.

The zone-refining process and its variants have a common feature. Those elements unable to enter the mineral phases of the mantle are concentrated from a large volume of solid mantle material in a very much smaller volume of magma. Since the magma remains in adjustment with the mantle, those elements able to enter the mineral phases will be in the concentrations and proportions expected for primary basaltic magma.

The Application of the Process to Potassic Basalts

Much of the information about the petrology and geochemistry of potassic basalts is due to Holmes (1950) and, most recently, to Higazy (1954). The various theories of origin have been reviewed by them and by Turner and Verhoogen (1951).

The origin preferred by Turner and Verhoogen (1951) is one of "assimilative reaction between normal olivine-basalt magma or nepheline-basalt magma and the granitic rocks of continental basements." Holmes (1950) suggests a mechanism of reaction between magmatic carbonatite and granitic material. The presence of ubiquitous xenoliths of olivine, biotite, and pyroxene ("O.B.P." material) and of mica peridotite in potassic basalts are explained as part of the reaction products.

The explanation is supported by Higazy (1954). Very recently, potassic basalts have been considered to be due to the partial fusion of biotite peridotite (Waters, 1955), the biotite peridotite itself being the result of uralitization of "sweated out" tectogene roots. From this hypothesis, the biotite peridotite xenoliths in potassic basalts, like the ultrabasic nodules in other basalts, may represent the original material from which the magma was formed by partial fusion.

In all these theories it is implied that once a primary undersaturated basalt with a high content of potassium and certain trace elements has been formed, the great variety of unusual rocks typical of the association can be derived by normal processes of fractionation and differentiation. Such an assumption is made also in this paper.

From Higazy's (1954) values for the trace-element distribution in African examples, the following essential and conflicting feature of potassic basalts require explanation.

(a) They contain elements such as Si, Mg, Fe, Ca, Na, Li, Ni, and Cr in concentrations characteristic of the earliest stages of basaltic differentiation, and show no effect of crystal fractionation in their high

$$\frac{MgO}{MgO + FeO} \text{ and } \frac{CaO}{CaO + Na_2O} \text{ ratios.}$$

(b) Other elements such as K, Rb, Sr, Ba, and Zr are present in concentrations characteristic of the last stages of differentiation.

The ions occurring with similar concentrations to those of early basalt are those capable of entering the crystal phases of peridotites and basalts, (Si) and (Mg, Fe, Ni, Co, Li) in olivines and pyroxenes, (Cr) in spinels and pyroxenes, and (Ca, Na) in plagioclase. On the other hand, those ions whose abnormal concentration gives the suite its distinctive geochemical character are those unable to take part in ionic substitution in these minerals, and which by default undergo residual concentration. In short, there has been differentiation of those elements incapable of early basaltic crystallization, and not of those taking part in this early crystallization.

This is the effect that would be expected from a zone-refining process or its variants within the mantle, as already discussed. Such a process could explain many of the features of potassic basalts.

(1) The product would have concentrations of Si, Mg, Fe, Ni, Mn, Cr, Ca, and Na of the order found in primary basalts. The mechanism does not suppose or require a homogeneous mantle, since the liquid in its ascent would adjust its composition to that of its surroundings, and on escape to the surface would reflect the composition of the top only of the mantle, in this respect being comparable with primary basaltic magmas.

(2) K, Rb, Ba, Zr etc., would be concentrated until
   (a) rise of the magma by melting or solution ceased, or
   (b) new mineral phases containing these elements formed, or
   (c) maximum concentration as determined by the distribution factor was attained.

(3) The low Li content which contrasts greatly with the high Rb content

would be due to the ionic replacement of Mg by Li in pyroxenes so that Li would be little concentrated by zone refining.

(4) Water and carbon dioxide are thought to occur also in the mantle and would be concentrated equally with potassium. High contents of these volatiles would account for the unusually explosive and gaseous nature of potassic basalts, and their tendency to occur as pyroclastic rocks rather than lavas. In the presence of a high potassium and a high water content in the magma, biotite could crystallize along with the other ferromagnesian minerals. The xenoliths of mica peridotite and of biotite in potassic basalts would be representative of the accumulative phase at the floor of the magma chamber, either during the zone-refining ascent, or more probably in a later stage of crystallization. The low content of Al in African potassic basalts could be ascribed to the effects of the crystallization of biotite. Biotite peridotite formed as an accumulative phase at the floor of an ascending magma, or by solidification of a cooling magma, no doubt could yield potassic basalt again on subsequent partial refusion.

If potassic basalts are formed by zone refining, other features dependent on the process should occur also and could be predicted.

(1) All the elements incapable of entering the mineral phases of the mantle should be concentrated—not only K, Ba, Zr, Rb, H, and C, but also Cs, B, U, Th, Nb, Ta, As, Sb, Bi, Cl, Br, I, etc. The enrichment of these relative to normal basalts has not been demonstrated as yet.

(2) The process is independent of the presence of a sialic crust, so that potassic basalts should have the same areal frequency in ocean basins as on continents. Potassic basalts are sufficiently rare and the products of oceanic volcanism so seldom visible, that any assessment of this point is prevented.

(3) From the earlier discussion, the zone-refining process would not seem to be dependent on any particular tectonic environment. The connection between Rift Valley seismicity, which is shallow depth only (Gutenberg and Richter, 1954) and the African potassic basalts remains obscure.

(4) As mentioned, zone refining would give a very considerable enrichment of volatiles. Still greater enrichment would occur after the zone refining ceased, to be replaced by fractional crystallization. Even after the appearance of biotite among the deposited phases, the residual water concentration would still increase. E.g. 25% of biotite would give an average water content over all the mineral phases of only 1%. In a magma with only 5% water, the combined distribution factor would be only 1/5, so that the residual enrichment of water would continue rapidly (see Fig. 2 of Neumann, Mead, and Vitaliano, 1954). Ultimately, water might become sufficiently concentrated to cause its separation from the silicate magma as an immiscible phase. In magmatic solution, the specific volume of water is probably less than unity. Separation of a water phase at about 1000°C, unless accompanied by an increase in volume, would develop enormous pressure. Even with 50% increase in volume, i.e. at a specific volume of 1·5, water at 1000°C would have a pressure of about 60,000 bars (by extrapolation from the data of Kennedy, 1950). At smaller specific volume, the pressure would be of a very much greater order. In an undeformable environment in which the necessary expansion could not occur, the water and carbon dioxide pressure developed

might cause crystallization of eclogite minerals as well as those of mica peridotite (i.e. kimberlite). The gas pressures could also explain the occurrence of kimberlite as explosion breccias filling explosion vents.

(5) Carbon dioxide, enriched by the zone-refining process at the same time as potassium and water, might reach sufficient concentration to permit the precipitation of magmatic calcite. The genetic relationship between carbonatite and potassic basalt could be the reverse of that postulated by Holmes and Higazy, with carbonatite a descendant, not an ancestor, of potassic basalt. However, an actual mode of formation of the carbonatite magma from potassic basalt is not apparent unless there is immiscibility between carbonate and silicate liquids.

(6) If the thermal model of the earth of Jacobs and Allan (1956) is correct, the temperature at depth is increasing with time, so that the possibility of the initiation of the zone-refining process will increase with time. On this basis, potassic basalts and perhaps carbonatites and kimberlites, if these are related, should become increasingly common from ancient rocks to the present, whereas normal basalts formed near the surface in a zone that may be cooling with time should become increasingly rare. There appears to be insufficient data to comment on either of these possibilities.

Some geophysical features that could possibly invalidate the whole hypothesis have already been discussed. The chief geochemical feature at variance with the hypothesis is the abundance of strontium in potassic basalts. Calcium can be replaced in its minerals by strontium, so that zone refining should not give much Sr/Ca enrichment. Sr would be expected to remain at the same low concentration as in other basalts, while Ba which cannot replace Ca should be concentrated. The ratio of the concentrations of Ca, Sr, and Ba in stony meteorites (perhaps comparable with the mantle), tholeiitic magmas, and potassic basalts, are

	Ca	Sr	Ba
Stony meteorites (Rankama and Sahama, 1950)	1×10^3	1·5	0·5
*Parental tholeiitic magmas (Nockolds and Allen, 1956)	1×10^3	3·0	1·2
Potassic basalts (average katungite, Higazy, 1954)	1×10^3	58	29

In potassic basalts, Ba has been enriched as expected, but Sr has been enriched to almost the same degree. The only explanations that can be offered are:

(a) That there seems to be no data for the relative distribution factors of Ca and Sr, and the ease of replacement of Ca by Sr may be less than generally thought.

(b) That trace-element data for occurrences of potassic basalts other than those described by Higazy may be more favourable.

(c) That Herzog and Pinson (1955) have shown that Sr contents, as determined by different laboratories, may vary by as much as a factor of 4. Probably, Sr and Ba values found by Higazy (Mitchell's laboratory) and by Nockolds and Allen are not directly comparable (Ahrens, 1954; Herzog and Pinson, 1955).

In conclusion, whether the zone-refining mechanism is accepted or not, the

* The values for tholeiitic magmas are averages of analyses 1–5, Table 32, of Nockolds and Allen.

geochemistry of potassic basalts does indicate that these have been formed by concentration of potassium and other elements from mantle material, the magma still remaining in adjustment with the mantle and preserving the major element features of primary basalts. Accepting this, mica peridotites, kimberlites, and carbonatites, if genetically related to potassic basalts, must be descended from them and not ancestral to them.

APPENDIX

The Formation of Undersaturated Sodic Basalts by Crystal Fractionation with Mantle Reaction

The possibility of the effects of crystal fractionation of a magma within the mantle being modified by reaction with the solid mantle material is mentioned on an earlier page.

At the top of the mantle, particularly beneath oceans and nonorogenic continental areas, a magma body probably would be in an environment of the same or a slightly lower temperature than its own. Cooling of the magma body by conduction would be slow or nonexistent, but if the body was directly connected to an open vent or lava lake with transport of heat to the surface by convection, cooling would be much more rapid and would be hastened by recurring engulfment of solidified lava and perilith material. With cooling and consequent crystallization, the magma would be expected to show signs of crystal fractionation, especially in increases in the ratios $\frac{FeO}{MgO + FeO}$ and $\frac{Na_2O}{CaO + Na_2O}$ in the residual magma (Wager and Deer, 1939; Walker and Poldervaart, 1949). At the same time, since the environmental temperature was so near that of the magma and conductive losses so small, there would be no chilled margin and the magma would be in contact with the mantle material. There would be a considerable amount of reaction with the roof and wall material and especially with smaller stoped fragments, the reaction tending to restore the ratios of the diadochic ions in the liquid to those in equilibrium with the mantle phases. Assuming the mantle to have a composition intermediate between average L-chondrite (Urey and Craig, 1953) and average peridotite (Nockolds, 1954), and the original magma to correspond to the average "normal tholeiitic basalt" of Nockolds, the mantle will contain 44–46% (MgO + FeO) and 3·5–4·0% ($CaO + Na_2O$), and the magma $15\frac{1}{2}$% (MgO + FeO), and $12\frac{1}{2}$% ($CaO + Na_2O$). From these values it can be seen that readjustment of diadochic ratios in the liquid by reaction with the mantle could be ten times as effective for magnesium and iron as for calcium and sodium. During differentiation, reaction with a limited amount of mantle material could maintain in the magma a high Mg/Fe ratio while the Ca/Na ratio decreased as expected for normal crystal fractionation. At the same time, continued reaction with olivine would prevent any tendency to silica enrichment in the residuum. With sufficient sodium concentration, and in the continued presence of olivine from the mantle, equilibrium in the reaction

$$\text{olivine} + \text{albite} \rightleftarrows \text{pyroxene} + \text{nepheline}$$

could be displaced sufficiently to the right for nepheline to appear.

This mechanism can be applied to the best-known occurrences of nepheline-basalts, those of Hawaii, particularly in the light of Macdonald's (1949) and Powers' (1955) reviews of Hawaiian petrogenesis. The following features described especially by Powers, seem significant to this discussion.

(1) The bulk of Hawaiian lavas are basalts more or less saturated with silica.

(2) Crystal fractionation does not seem to have been operative in the period of eruption of these saturated basalts from each centre.

(3) Silica-deficient sodic basalts (nepheline basalts, etc.) occur only as subordinate phases, and then only in a late decadent and declining stage in the volcanic history of each centre.

(4) Eruptions of sodic basalts appear to be separated by greater time-intervals than were those of the primitive-stage basalts.

(5) The sodic basalts are generally lower in silica and higher in alkali content than primitive-stage lavas of comparable magnesia content The sodic basalts do not show the normal effects of differentiation in a decreased Mg/Fe ratio. Indeed, the average nepheline basalt (Macdonald, 1949) has almost twice as high an MgO content and Mg/Fe ratio as average basalt or olivine basalt.

(6) A pronounced feature of late-stage sodic lavas are the abundant ultrabasic nodules contained in them. Such nodules are rare in primitive-stage basalts.

(7) Seismic data indicate that the lavas are erupted from depths of 30–40 miles. Whether this is the place of formation (by partial fusion) or of storage (the magma reservoir) is uncertain, but the uniformity of successive flows of primitive basalt from the same centre indicate the latter.

These features indicate an initial history of continued formation and frequent eruption of primary magma with no opportunity for differentiation. After construction of the lava pile, generation of magma will cease because the excess heat has been used up, or for hydrostatic reasons (Daly, 1944, p. 1375), the weight of the magma column becoming as great as that of a column of ocean water, crust and mantle to a depth of 30–40 miles. From then on, eruptions will be infrequent and less voluminous, and the magma presumably will be derived from a magma reservoir in which some form of differentiation is occurring, the erupted lava no longer being a primitive-stage, silica-saturated basalt.

If the magma chamber is within the mantle, i.e. deeper than 10 km, there will be a considerable degree of stoping and reaction of the magma with the solid-mantle material. As discussed earlier, the normal results of basaltic fractionation shown by increases in the ratios $\frac{FeO}{MgO + FeO}$ and $\frac{Na_2O}{CaO + NaO}$ (Wager and Deer, 1939; Walker and Poldervaart, 1949) will be modified by reaction and readjustment with mantle material. The ratio Mg/Fe will be maintained near its original high value much more than the ratio Ca/Na, so that a product of high magnesia as well as high soda content could be formed. Stoped fragments of mantle would form those ultrabasic nodules whose compositions have been so thoroughly investigated by Ross, Foster, and Myers (1954). The fact that the differentiation process has changed the Ca/Na ratio but had little effect on the Mg/Fe ratio is shown for the Hawaiian Alkaline magma series by Wager (1956) in a diagram (Fig. 3), in which are contrasted behaviour in the two continuous reaction series—Ca-Na plagioclase and Mg-Fe silicate.

This mechanism has much in common with that of Macdonald (1949) for nepheline-bearing rocks. However, Macdonald attributes the high magnesium content to assimilation or reaction with early-formed olivine from higher in the magma, with subsequent fractionation. It is suggested here that reaction with original olivine (and other minerals) in the mantle, contemporaneous with fractionation, could be the operative mechanism.

References

Abelson P. H. (1955) Carnegie Institution of Washington Year Book No. 54, 95–152.

Ahrens L. H. (1954) *Quantitative Spectrochemical Analysis of Silicates.* Pergamon Press, London.

Bowen N. L. (1928) *The Evolution of the Igneous Rocks.* Princeton University Press, Princeton.

Daly R. A. (1944) *Bull. Geol. Soc. Amer.* **55,** 1363–1400.

Eitel W. (1954) *The Physical Chemistry of Silicates.* University of Chicago Press, Chicago.

Goodman C. H. L. (1954) *Research* **7,** 168–177.

Goodman C. H. L. (1956) *Science News* **39,** 26–41.

Gutenberg B. and Richter C. F. (1954) *Seismicity of the Earth and Associated Phenomena.* Princeton University Press, Princeton.

Herzog L. F. and Pinson W. H. (1955) *Geochim. et Cosmochim. Acta* **8,** 295–298.

Higazy R. A. (1954) *Bull. Geol. Soc. Amer.* **65,** 39–70.

Holmes A. (1950) *Amer. Mineral.* **35,** 772–792.

Jacobs J. A. and Allan D. W. (1956) *Nature* **177,** 155–157.

Kennedy G. C. (1950) *Amer. J. Sci.* **248,** 540–564.

Macdonald G. P. (1949) *Bull. Geol. Soc. Amer.* **60,** 1541–1596.

Neumann H., Mead J., and Vitaliano C. J. (1954) *Geochim. et Cosmochim. Acta* **6,** 90–99.

Nockolds S. R. (1954) *Bull. Geol. Soc. Amer.* **65,** 1007–1032.
Nockolds S. R. and Allen R. (1956) *Geochim. et Cosmochim. Acta* **9,** 34–37.
Pfann W. Q. (1952) *J. Metals* **4,** 747–753.
Powers H. A. (1955) *Geochim. et Cosmochim. Acta* **7,** 77–107.
Rankama K. and Sahama Th. G. (1950) *Geochemistry.* University of Chicago Press, Chicago.
Ross C. S., Foster M. D., and Myers A. T. (1954) *Amer. Mineral.* **39,** 693–737.
Turner F. J. and Verhoogen J. (1951) *Igneous and Metamorphic Petrology.* McGraw-Hill Book Company. Inc., New York.
Urey H. C. (1955) *Proc. Nat. Acad. Sci.* **41,** 127–144.
Urey H. C. and Craig H. (1953) *Geochim. et Cosmochim. Acta* **4,** 36–82.
Verhoogen J. (1956) in *Physics and Chemistry of the Earth,* Vol. 1. Pergamon Press, London.
Wager R. L. (1956) *Geochim. et Cosmochim. Acta* **9,** 217–248.
Wager R. L. and Deer W. A. (1939) *Medd. om Grønland* **105,** (No. 4), 1–352.
Walker F. and Poldervaart A. (1949) *Bull Geol. Soc. Amer.* **60,** 591–706.
Waters A. C. (1955) in Crust of the Earth, *Geol. Soc. Amer.* Special Paper **62,** 703–722.
Yoder H. S. (1952) *J. Geol.* **60,** 364–374.

Geochimica et Cosmochimica Acta, 1957, Vol. 12, pp. 209 to 224. Pergamon Press Ltd., London

Minor elements in Keweenawan lavas, Michigan*

H. R. Cornwall and H. J. Rose jr.
U.S. Geological Survey

(*Received* 8 *January* 1957)

CONTENTS LIST

	Page
Abstract	209
Introduction	209
Methods of spectrographic determination	211
Standards	211
Samples	211
Apparatus and working conditions	211
Distribution of minor elements	212
Minor elements in flows	212
Minor elements in minerals of the Greenstone flow	214
Phosphorus	216
Beryllium	216
Gallium	217
Chromium	217
Titanium	217
Nickel	217
Cobalt	218
Copper	218
Vanadium	220
Niobium	220
Zirconium	220
Manganese	221
Scandium	221
Lanthanum and yttrium	221
Strontium	221
Barium	221
Minor elements in lodes	221
References	223

Abstract—The distribution of minor elements in three basaltic flows of the Keweenawan series, of Michigan, is related to differentiation in the flows. Thus, nickel is most abundant in the early differentiates; nickel, chromium, and barium are generally deficient in the pegmatites, which formed late; whereas copper, vanadium, yttrium, and other minor elements are concentrated in the pegmatites.

The minor-element content of individual minerals in the Greenstone flow varies markedly from one mineral to another and seems to depend primarily on the presence or absence in the minerals of major elements for which the minor elements can substitute. Minor elements have substituted most readily for those major elements with similar ionic radii. Valence and electronegativity also seem to influence the ease of substitution.

The distribution of other minor elements in copper-bearing lodes of the Michigan copper district shows no apparent relation to copper mineralization.

Introduction

This paper describes a study of the distribution of minor elements in mafic Keweenawan lava-flows of the Michigan copper district, on the south shore of Lake

* Publication authorized by the Director, U.S. Geological Survey.

Superior. Spectrographic analyses for minor elements were made of the following types of samples: (1) rock samples representing all of the units in three flows; (2) mineral separates from seven units in one flow; (3) eight copper-bearing and barren conglomerates and amygdaloidal flow-tops.

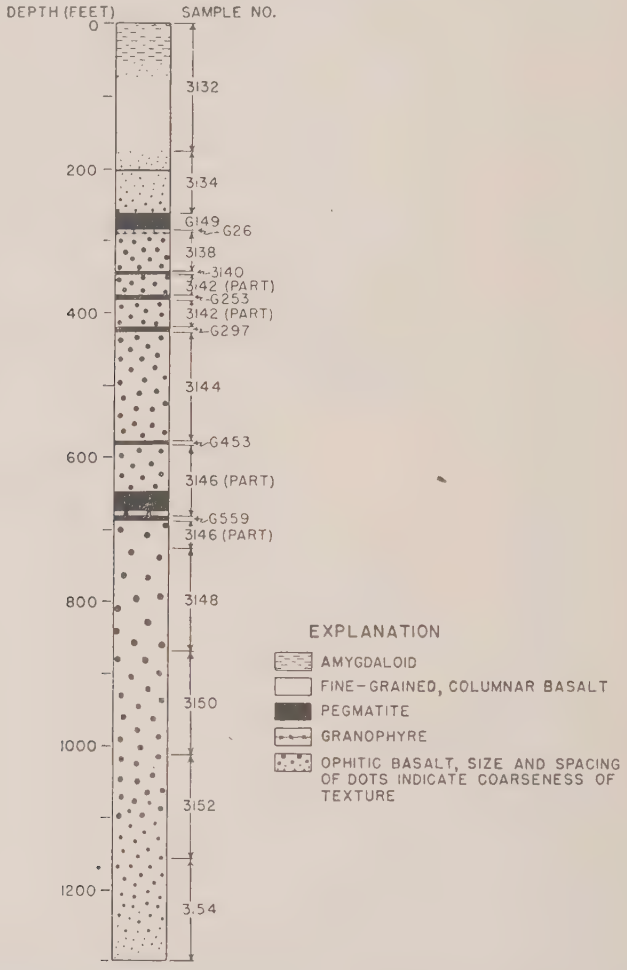

Fig. 1. Columnar section of the Greenstone flow as exposed in three overlapping diamond-drill holes at Delaware, Michigan. Granophyre was not found in the diamond-drill core but was projected into the section on the basis of field data. Sample numbers indicate positions of analyses listed in Table 1.

A total of 104 samples was analysed. Thirty-two rock analyses have been made in recent years (Broderick, 1935; Cornwall, 1951a) of units in the Kearsarge, Greenstone, and Copper City (Big trap) flows. In the present work, minor elements were determined spectrographically on the same samples that Broderick (1935) and Cornwall (1951a) had previously submitted for determination of the major constituents. Mineral separations were made of individual samples of seven units in the Greenstone flow, and a total of forty-five mineral samples were analysed.

In addition, twenty-seven samples of six amygdaloidal flow-tops and two conglomerates, thirteen containing commercial copper ore, and fourteen barren, were analysed for minor elements.

The petrology of the Greenstone and Kearsarge flows has been described in detail by Broderick (1935); one of the present writers (Cornwall, 1951a,b,c) has also investigated the Greenstone flow, and, in addition, the Copper City flow. At the place where it was sampled for the present study, the Greenstone flow is 1300 ft thick (see Fig. 1); the Copper City (Big trap) flow is 400 ft thick; and the Kearsarge flow is 165 ft thick. All the flows are coarse-grained ophitic basalts with thick amygdaloidal upper chill zones and thin slightly amygdular basal chill zones. The Greenstone and Copper City flows contain pegmatitic layers and lenses that parallel the flow-planes in their middle and upper parts, and these flows also contain small amounts of granophyre associated with the pegmatitic facies in crosscutting dikes, and as interstitial intergrowths.

Methods of Spectrographic Determination

Standards. Standards were prepared by adding known amounts of the various elements investigated to a matrix of pegmatite base (60 quartz, 40 feldspar, 1 ferric oxide). A series of standards was prepared by further dilution of the initial standard with pegmatite base. No internal standard was used in the method because of the large number of elements determined.

Samples. All samples were ground in agate mortars to pass 150-mesh silk bolting cloth. The samples were then ground in agate mortars with an equal weight of a mixture of 10 parts Na_2CO_3 + 90 parts quartz in order to overcome the effects of varying types of matrix in the samples analysed, and to cause the quality of the burning of the samples to approach that of the pegmatite standards. Any further dilutions that were required to bring elements into a better range for analysis were done with pegmatite base.

The finely-crystalline nature of the basalts precluded any extensive hand-picking in separating the individual minerals. Marie L. Lindberg and Jewell J. Glass devoted much effort and thought to the problem of preparing pure mineral separates. Heavy-liquid separations were made on the finely ground samples, using bromoform, methylene iodide, and clerici solution. The gravity separates were then passed repeatedly through the Frantz isodynamic magnetic separator at appropriate settings. The purity of the various separated minerals was checked both optically and by means of X-ray diffraction patterns.

Apparatus and working conditions. In this study a set of standards was exposed on each plate along with duplicate exposures of the samples. The apparatus and working conditions were as follows:

Spectrograph:	Grating spectrograph with Wadsworth mounting, dispersion 5·0 Å/mm.
Cathode:	Graphite rod, 3-mm-diameter.
Anode:	Graphite, 6-mm diameter, cavity 4 mm deep, wall thickness 0·5 mm.
Samples and standards:	25 mg.

Analytical gap:	3 mm, maintained throughout excitation period.
Excitation source:	250-V ballasted d.c. arc, 16 A.
Length of exposure:	Sample arced to completion.
Emulsion:	Eastman-type III-O, developed at 21°C in DK-50 for 5 min. with continuous agitation.
Wavelength region:	2300–4700 Å.
Microphotometer:	Projection comparator-microphotometer using a scanning slit at the plate.
Emulsion calibration:	Iron-line group method of Dieke and Crosswhite (1943).

Distribution of Minor Elements

The distribution of minor elements is discussed below, first as to their occurrence in various differentiates of three flows, second as to their relative abundance in individual minerals in the Greenstone flow, and third as to their relationship to copper mineralization in lodes of the Michigan copper district. The three lava flows occur near the middle of the Keweenawan lava sequence in the Michigan copper district. The Copper City flow is the oldest; the Kearsarge flow lies 4000 ft higher in the section; and the Greenstone flow is 8000 ft above the Copper City flow.

Minor elements in flows. Spectrographic analyses of units in the Kearsarge, Greenstone, and Copper City flows are given in Table 1. The analyses were not complete. The elements looked for were: Cr, Ni, Co, Cu, V, Zr, Mn, Ag, Y, Sr, Ba. As mentioned above, the samples used for these analyses are the same as those used for the determination of the major constituents (Broderick, 1935, p. 513, 523; Cornwall, 1951a, p. 185, 188). Copper, nickel, and cobalt were also determined chemically in the Kearsarge and Greenstone flows by Sandell and Goldich (1943, p. 103). The agreement is good between those analyses and the spectrographic determinations presented in this paper.

The amounts of minor elements in the Michigan lavas are in general comparable to those found in rocks of similar composition elsewhere. Wager and Mitchell (1951, p. 199, Table 15) have assembled the estimates of several investigators on the general distribution of minor elements for comparison with the Skaergaard intrusive rocks of east Greenland. Minor elements in the Michigan lava-flows are generally present in amounts comparable to these estimates.

Considering the distribution of minor elements within single flows, several features are evident. The marked concentration of nickel in the mafic, lower olivine-rich zone of the Greenstone flow (samples 3152, 3154, Table 1, and Fig. 1) is striking. Its deficiency in the pegmatitic and other late differentiates is also noticeable. Cr and Ba likewise are generally relatively low in the pegmatites, whereas the remaining elements are concentrated there, particularly Cu, V, and Y. The granophyre, a residual differentiate of the Greenstone flow, is low in many minor elements, including the base and ferrous metals, but it contains marked concentrations of Zr, Y, and La; Be was found only in the granophyre. Sr and Sc are equally abundant in the granophyre and in the basalt and pegmatitic facies. Several of the above elements were determinable only in the mineral separates. In general, the differentiation trends of the minor elements in the Michigan flows are similar to,

Sample No.		Depth (ft) [3] in flow	Cr^{3+}	Ni^{2+}	Co^{2+}	Cu^{2+}	V^{3+}	Zr^{4+}	Mn^{2+}	Ag^{2+}	Y^{3+}	Sr^{2+}	Ba^{2+}
Ionic radius[2]			0·63	0·69	0·72	0·72	0·74	0·79	0·80	0·89	0·92	1·12	1·34
Sensitivity limits (p.p.m.)			1	5	5	1	7	10	10	1	10	10	10
						Kearsage flow							
3112	amygdaloid	6	170	84	25	100	140	100		3	30	600	150
3113	basalt	18	160	84	38	200	210	200		—	40	300	200
3115	basat	30	160	180	37	60	170	100		—	30	300	1000
3117	basalt	54	140	190	41	54	140	50		—	20	300	350
3119	basalt	86	180	210	42	51	160	90		—	20	300	250
3121	basalt	118	170	180	39	80	170	100		—	20	300	200
3123	basalt	149	130	100	38	140	190	70		—	30	300	450
Total thickness		165											
						Greenstone flow							
3132	basalt	118	200	200	48	90	200	100		—	30	400	100
3134	basalt	215	160	180	42	100	190	100		3	30	400	150
3136	pegmatite	270	120	40	29	180	290	200		2	70	900	450
G-149	pegmatite	274	10	20	40	200	200	100	800	—			250
3138	basalt	315	100	71	33	83	180	100		—	30	500	300
3140	pegmatite	245	1	27	39	210	320	100		—	90	50	40
3142	basalt	387	140	76	35	130	250	100		—	30	400	450
G-253	pegmatite	378	100	30	40	200	300	100	800	—			25
G-297	pegmatite	422	200	50	50	100	500	70	2000	—			45
3144	basalt	501	210	130	40	110	210	100		—	40	400	1000
G-453	pegmatite	578	90	30	40	300	300	100	2000	—			50
3146	basalt	650	140	74	32	110	190	90		—	20	400	450
G-559	pegmatite	684	200	50	40	200	400	70	2000	—			45
3148	basalt	797	170	180	48	96	170	80		—	30	700	200
G-26	granophyre	800	1	<10	<10	60	20	400	500	—			250
3150	basalt	941	140	160	40	72	120	60		1	20	400	150
3152	basalt	1085	190	460	53	80	130	60		—	20	400	100
3154	basalt	1228	160	300	45	110	190	90		—	20	400	350
G-604	basalt	1290	100	50	40	200	300	100	2000	—			500
Total thickness		1299											
						Copper City flow							
T-1370	pegmatite	53	200	50	50	200	300	100	2000	—			25
T-1399	andesire	82	200	80	40	100	200	70	1000	—			1500
T-1413	pegmatite	96	200	40	40	200	300	100	1000	—			450
T-1501	pegmatite	184	200	50	50	200	300	100	1000	—			150
T-1522	basalt	205	300	200	50	100	200	60	1000	5			250
T-1716	basalt	400	200	200	40	200	200	60	1000	—			500
Total thickness		402											

[1] Analyses are spectrographic determinations made by K. J. Murata, U.S. Geological Survey.
Dashes indicate that element was looked for but not found.
A blank indicates that element was not looked for.
Beryllium (Be) was found only in sample No. G-26, granophyre of the Greenstone flow, which contains 2 p.p.m.

[2] Ionic radius in Ångström units at valence shown as given by Ahrens (1952).

[3] Depth given is to middle of the zone sampled.

but much less marked than, those found by Wager and Mitchell (1951, Table F) in the Skaergaard, and Nockolds and Mitchell (1948, Table 2) in Caledonian intrusives.

Minor elements in minerals of the Greenstone flow. Minor-element analyses of individual minerals in several samples of the Greenstone flow are given in Table 2. The position of these samples (sample number and depth) in Fig. 1 is given in the explanation of Table 2. Included are five samples of ophitic basalt, three from the ophitic basalt zone (3-89, plagioclase-rich zone; 3-407, olivine-rich zone; and 3-540, pyroxene-rich zone) in the lower half of the flow below the zone that contains pegmatitic layers, one from the pegmatitic zone (4-376), and one from the base of the upper chill zone (4-58) which overlies the pegmatitic zone and consists of 200 ft of fine- to medium-grained basalt. A sample representing the pegmatitic facies (4-149) and a granophyre (G-26) were also analysed.

In general, the amounts of minor elements in the minerals do not show a gradation that is clearly related to the course of crystallization. Nickel is an exception; it is markedly high in several minerals in the early fractions (samples 3-407 and 3-540) that contain concentrations of olivine and pyroxene. Several elements, as noted above, are more or less concentrated in the pegmatite (4-149) and granophyre (G-26). The most striking feature of these analyses, in addition to those already mentioned, is the marked tendency of certain elements to concentrate in certain minerals. Augite contains relatively large amounts as compared with the other minerals, of a number of minor elements including Cu, Mn, Co, Ni, Cr, V, Sc, Y, La, Ti, Zr, Sr, and Ba. Chlorite also contains a relative abundance, but generally somewhat less than augite, of most of these elements, and, in addition, some Ga.

Plagioclase, the most abundant mineral in the rocks, is the principal carrier of Ga and Ba; Sr and Ti are also relatively prominent; Cu, Mn, Co, Ni, and Cr are present in smaller amounts. The feldspar of the granophyre, predominantly oligoclase, contains these elements, except for Ga, and is in addition a major carrier of La and Y, which are concentrated in this rock.

Ilmenite and magnetite are minor constituents of the rocks, but they contain marked concentrations of Cu, Mn, Co, Ni, Y, and V, and smaller amounts of Cr and Sc. Nb is found only in these minerals, and Ti is a major constituent in ilmenite. Olivine in the unaltered form is only locally abundant in the Greenstone flow, but it contains a large amount of Ni, Mn, Ti, and Co, and smaller quantities of Cu, Cr, V, Sc, Y, Sr, and Ba.

The occurrence of each minor element is discussed below in somewhat more detail. The ionic radii and valences of the minor elements are given in Table 2, and the same data for the major constituents of the rocks are shown in Table 3. It is generally believed (Goldschmidt, 1937; Nockolds and Mitchell, 1948; Wager and Mitchell, 1951, p. 178, 201–202; Fleischer, 1955, p. 972–973) that, in oxides and silicates, minor elements occur mainly as substitutes for major elements that they resemble in ionic radius and valence. Thus Co^{2+} (radius 0·72) substitutes readily for Fe^{2+} (radius 0·74) in olivine, magnetite, ilmenite, pyroxene, and chlorite. Another example is Ga^{3+} (radius 0·62) that substitutes for Al^{3+} (radius 0·51). In this case the minor element (Ga) has a larger ionic radius than the major element it

Sample No.	Mineral separated	Depth (ft) in flow	P^{5+}	Be^{2+}	Ga^{3+}	Cr^{3+}	Ti^{4+}	Ni^{2+}	Co^{2+}	Cu^{2+}	V^{5+}	Nb^{4+}	Zr^{4+}	Mn^{2+}	Sc^{3+}	Y^{3+}	Sr^{2+}	La^{3+}	Ba^{2+}
	Ionic radius‡		0·35	0·35	0·62	0·63	0·68	0·69	0·72	0·72	0·74	0·74	0·79	0·80	0·81	0·92	1·12	1·14	1·34
	Sensitivity limits (p.p.m.)		1000	1	10	1	5	5	5	1	7	5	10	10	1	10	10	30	10
											Plagioclase								
4–58	Labradorite, altered	183	—	—	40	7	400	30	10	50	—	—	—	90	—	—	500	—	300
4–58	Labradorite, impure	183	—	—	—	4	400	20	80	60	20	—	—	70	—	—	2000	—	500
4–376	Labradorite	501	—	—	40	3	300	—	—	20	—	—	—	50	—	—	500	—	200
4–376	Labradorite	501	—	—	—	20	400	—	—	20	20	—	—	50	—	—	2000	—	800
3–89	Labradorite	774	—	—	40	4	400	7	10	20	—	—	—	70	—	—	600	—	300
3–89	Labradorite, chloritized	774	—	—	40	4	300	10	10	20	—	—	—	200	—	—	500	—	300
3–407	Labradorite	1092	—	—	40	6	400	30	20	30	—	—	30	100	—	—	600	—	500
3–540	Labradorite	1225	—	—	50	6	400	30	20	30	—	—	—	150	—	—	600	—	200
3–540	Labradorite, chloritized	1225	—	—	40	5	400	100	30	70	—	—	—	250	—	—	400	—	400
x4–149	Albite, altered	274	—	—	—	20	500	—	—	30	10	—	100	100	—	60	700	—	700
xxG–26	Quartz and oligoclase altered	800	—	7	—	4	1300	4	50	73	10	—	420	1100	20	200	400	400	1000
xxG–26	Quartz and oligoclase altered	800	—	2	—	3	760	20	20	73	7	—	260	1600	—	200	80	200	700
											Pyroxene								
4–58	Augite with 5% labradorite	183	—	—	—	1200	12000	320	96	61	690	—	20	2500	200	90	400	—	80
4–376	Augite, impure	501	—	—	—	500	5100	140	94	56	520	—	40	2800	200	100	200	—	30
3–89	Augite	774	—	—	—	270	4200	160	75	51	520	—	30	2900	100	100	60	—	—
3–407	Augite	1092	—	—	—	200	11000	380	89	61	520	—	30	2900	200	100	70	—	100
3–540	Augite, impure	1225	—	—	—	400	1300	290	93	38	310	—	—	2800	200	90	200	—	80
x4–149	Augite, impure	274	—	—	—	300	5400	93	88	320	570	—	80	2800	200	90	200	—	40
x4–149	Hedenbergite, impure	274	—	2	—	5	5100	2	83	130	40	—	180	5700	80	200	300	100	30
xxG–26	Augite, impure	800	—	10	—	10	3200	40	72	140	60	—	700	6300	200	700	200	600	800
xxG–26	Augite, impure	800	—	10	—	6	7000	60	50	300	90	—	2000	6000	200	700	400	400	400
											Ilmenite-magnetite								
4–376	Magnetite with some ilmenite	501	—	—	20	150	*	290	100	390	7000	—	—	7200	16	120	—	—	—
4–376	Ilmenite with 0·5% impurities	501	—	—	—	20	*	140	150	280	1200	80	—	9200	35	650	—	—	—
3–89	Ilmenite with 1·0% impurities	774	—	—	—	20	*	250	150	98	2300	200	—	3900	35	650	—	—	—
3–89	Magnetite	774	—	—	20	150	*	750	200	200	8000	—	—	5800	17	100	—	—	—
3–407	Ilmenite with some magnetite	1092	—	—	—	40	*	660	170	100	4500	80	—	4200	40	460	—	—	—
3–540	Magnetite with some ilmenite	1225	—	—	10	90	*	1000	200	200	7000	—	—	2000	8	200	—	—	—
3–540	Ilmenite with some magnetite	1225	—	—	—	20	*	200	200	90	2000	80	—	2000	60	200	—	—	—
x4–149	Ilmenite with some magnetite	274	—	—	—	200	*	20	100	300	700	200	—	4000	50	500	—	—	—
x4–149	Magnetite with some ilmenite	274	—	—	20	180	*	80	76	880	2200	—		7700	13	120	—	—	—
											Olivine								
3–89	Olivine	774	—	—	—	—	1200	820	230	35	20	—	—	6300	10	60	20	—	—
3–407	Olivine, impure	1092	—	—	—	9	2000	2000	230	38	40	—	—	4000	10	40	30	—	10
											Apatite								
4–376	Apatite	501	*	—	—	10	500	20	—	100	90	—	100	200	9	4000	400	2000	90
x4–149	Apatite, impure	274	*	—	—	8	200	—	—	30	70	—	300	200	9	3000	700	2000	50
											Chlorite								
4–58	Chlorite	183	—	—	—	9	630	150	180	92	90	—	—	4200	3	40	50	—	40
4–376	Brown chlorite (Fe-rich)	501	—	—	7	2	380	160	190	110	100	—	300	3500	3	100	500	—	100
4–376	Green chlorite (thuringite)	501	—	—	10	5	660	150	180	88	300	—	100	5200	9	70	500	—	100
3–89	Green and brown chlorite	774	—	—	—	2	280	720	230	52	—	—	—	3800	10	—	300	—	40
3–89	Green chlorite (thuringite)	774	—	—	—	20	230	630	160	70	20	—	—	2900	40	20	200	—	40
3–89	Green chlorite, impure	774	—	—	—	9	360	59	120	130	50	—	100	3500	2	—	500	—	200
3–89	Olive green chlorite (thuringite)	774	—	—	6	3	530	220	260	88	70	—	30	3900	10	—	400	—	20
3–407	Dark green chlorite	1092	—	—	—	5	190	1200	190	61	40	—	—	2900	7	—	60	—	60
3–407	Green chlorite with talc, impure	1092	—	—	—	20	570	920	140	110	90	—	—	2200	8	20	500	—	100
3–540	Green chlorite (thuringite)	1225	—	—	—	5	1000	200	100	50	100	—	—	4000	6	—	90	—	300
x4–149	Dark green chlorite (thuringite)	274	—	—	60	5	1700	630	140	280	100	—	200	4600	6	70	500	—	300

† All the samples except G–26 are of core from diamond drill holes Manitou 3, 4, and 5N at Delaware. G–26 is from a granophyre aplite dike, 1½ ft thick, at Lake Medora. The flow is 1300 ft thick.

All depths are measured to middle of zone sampled.

Dashes indicate that the element was looked for but not found.

A line under a cipher indicates that it is the last significant figure of that number.

Spectrographic determinations are by HARRY J. ROSE JR., U.S. Geological Survey.

An asterisk indicates that the element is a major constituent of the sample.

Plain ciphers are not significant.

The samples are identified as follows:

4–58 Ophitic basalt near base of upper chill zone, 183 ft below top of flow (equivalent to 3134 and bottom of 3132 in Fig. 1).

x4–149 Pegmatitic facies, 274 ft below top of flow (shown as G149 in Fig. 1).

4–376 Ophitic basalt, 501 ft below top of flow (equivalent to 3144 in Fig. 1).

3–89 Ophitic basalt in plagioclase-rich zone, 774 ft below top of flow (equivalent to 3148 in Fig. 1).

xxG–26 Granophyre dike, 800 ft below top of flow (shown as G26 in Fig. 1 at 280 ft below top of flow).

3–407 Ophitic basalt in olivine-rich zone, 1092 ft below top of flow (equivalent to 3152 in Fig. 1).

3–540 Ophitic basalt in pyroxene-rich-zone, 1225 ft below top of flow (equivalent to 3154 in Fig. 1).

‡ Ionic radius for six-fold co-ordination in Ångström units at valence shown as given by AHRENS (1952).

replaces, and the replacement is not made as readily as in the case of Co^{2+}, where the two elements have nearly the same size.

The respective valences of the major and minor elements also affect the ease of replacement. If the minor element has the same or higher valence than the major element it is admitted more readily as a replacement than if the valence is lower. Where the valences differ the total charge of the crystal has to be balanced by other

Table 3. Ionic radii of major elements

Element	Ionic radius*	Usual co-ordination number
Si^{4+}	0·42	4
Al^{3+}	0·51	4 and 6
Ti^{4+}	0·68	6
Fe^{3+}	0·64	6
Mg^{2+}	0·66	6
Fe^{2+}	0·74	6
Na^{1+}	0·97	7 to 10
Ca^{2+}	0·99	7 to 10
K^{1+}	1·33	8–12
P^{5+}	0·35	4

* Radius for six-fold co-ordination as given by Ahrens (1952).

substitutions. The substitution of minor elements in minerals may in certain cases be appreciably affected by other factors, such as the co-ordination number, electronegativity, and ionic potential (Pauling, 1940; Ahrens, 1952, 1953; Goldschmidt, 1954; Ringwood, 1955). Minor elements that enter the structure of major minerals of rocks easily (e.g. nickel in olivine) tend to be concentrated in the early-crystallizing mineral fractions, and those that enter minerals with difficulty (e.g. yttrium) tend to be concentrated in the late fractions.

Phosphorus does not readily enter the crystal structure of any major mineral. It remains in the magma until sufficiently concentrated to precipitate as a major constituent in apatite. Likewise, sulphur probably occurs mainly as accessory sulphides of iron, copper, and nickel. The extent to which copper substitutes for major elements (mainly Fe^{2+}) may also be questioned. Microscopic evidence, discussed in more detail below, indicates that at least part of the copper in the minerals is present as minute grains of sulphide, or as native metal.

The individual minor elements are discussed below in the order of increasing ionic radii.

Phosphorus (P^{5+}). The data in Table 2 indicate that phosphorus occurs only in accessory apatite, where it is a major constituent. Wet chemical analyses (Broderick, 1935, p. 513; Cornwall, 1951a, p. 185) show that phosphorus ranges from 0·05 to 0·21 wt.% in the Greenstone flow, and the largest amounts are found in the pegmatitic facies where apatite is most evident in microscopic examinations.

Beryllium (Be^{2+}). Minute amounts of beryllium were found in the granophyre and also in the pegmatitic facies. The beryllium is found in pyroxene and feldspar,

probably as BeO_4^{-6} tetrahedra substituting in the silicate structures (Ringwood, 1955, p. 247). Because of its small size and resultant relatively high ionic potential Be^{2+} is unique among divalent ions in its tendency to form a complex rather than remaining a free ion.

Gallium (Ga^{3+}). Most of the gallium occurs in the labradorite of the ophitic basalt. It is also found in magnetite and chlorite. In chlorite it is most abundant in the pegmatitic facies (4-149). Gallium probably replaces aluminium in the labradorite, ferric iron in the magnetite, and it may replace both of these elements in the chlorite.

Chromium (Cr^{3+}). Chromium is most abundant in pyroxene and magnetite, but small amounts are present in all the minerals. The distribution of chromium in the successive mineral fractions appears quite erratic, but it tends to be more abundant in the augite of the fractions that crystallized early (chill zones) and also of those that crystallized late (pegmatitic facies and associated basalt). The augite from the base of the upper chill zone (4-58) contains the most Cr (1200 p.p.m.). This rock is also relatively rich in Fe^{3+}. The granophyre contains very little Cr. Cr^{3+} (radius 0·63) may substitute for Fe^{3+} (radius 0·64) in the Greenstone flow.

Titanium (Ti^{4+}). This element is a major constituent in the rocks and has been determined chemically (Broderick, 1935, p. 513; Cornwall, 1951a, p. 185). It occurs mainly as a major element in ilmenite. It has been shown elsewhere (Cornwall, 1951b, Figs. 3 and 5, p. 158 and 164) that titanium is most abundant in the late differentiates of the flow, but not in the final residual granophyre. Spectrographic analyses indicate that in addition to the titanium in ilmenite there are appreciable amounts in all the other minerals, particularly in pyroxene. Titanium probably replaces aluminium and ferric iron in these minerals, and it may also replace silicon in the silica tetrahedra. The high tolerance for substitution of the pyroxene structure is indicated by the abundance in it of Ti, Mn, Cr, V, and other mineral elements.

Nickel (Ni^{2+}). Olivine contains the greatest concentration of nickel (2000 p.p.m. maximum), but nickel is also abundant in ilmenite, magnetite, augite, and chlorite. As stated above, the early-formed, olivine-rich rock (analysis 3-407) near the base of the Greenstone flow contains the most nickel, and the late-stage pegmatites and granophyre contain very little. In the olivine-rich rock (analysis 3–407) nickel is high not only in the olivine (2000 p.p.m.), but also in the chlorite (1200 and 920 p.p.m.), the ilmenite (660 p.p.m.), and the augite (380 p.p.m.). The magnetite fraction of this rock has not been analysed, but it, too, is probably rich in Ni. The magnetite in the underlying pyroxene-rich zone (analysis 3-540) contains 1000 p.p.m. of Ni. The plagioclase contains very little nickel, except for one sample (3-540) of chloritized labradorite, which contains 100 p.p.m. Ni^{2+} appears to replace Mg^{2+} very readily, particularly in olivine, but also in augite. Ringwood (1955, p. 196–198), however, believes that Ni^{2+} is prevented from substituting for Mg^{2+} by its high electronegativity (1·7) relative to that of Mg^{2+} (1·2). He thinks the Ni^{2+} in olivine and pyroxene has substituted for Fe^{2+}, which has a slightly larger ion but nearly the same electronegativity (1·65 for Fe^{2+}). That Ni^{2+} does substitute for Fe^{2+} is indicated by its abundance in magnetite and ilmenite in the Greenstone flow.

Cobalt (Co^{2+}). The precipitation of cobalt continued uniformly throughout the crystallization of the Greenstone flow. This is indicated by its uniform rate of entry into individual minerals at all stages of solidification. It entered some minerals somewhat more readily than others, however, and rocks rich in these minerals contain the most cobalt. Cobalt has entered olivine, magnetite, ilmenite, and chlorite most abundantly, and augite somewhat less so. In plagioclase it is for the most part present in very small amounts. Co^{2+} probably replaces Fe^{2+}, with which it is nearly identical in ionic size and electronegativity.

Table 4. Chemical analyses for copper and manganese in the Greenstone flow*

Sample No.	Rock type	Copper (p.p.m.)	Manganese (p.p.m.)
3132	basalt	150	1200
3134	basalt	70	1300
G–26	granophyre	70	850
G–149	pegmatite	300	1700
3138	basalt	110	1300
3140	pegmatite	290	1900
3142	basalt	110	1300
G–253	pegmatite	350	1500
G–297	pegmatite	100	1500
3144	basalt	170	1400
G–453	pegmatite	370	1600
3146	basalt	120	1300
G–559	pegmatite	380	1700
3148	basalt	130	1200
3150	basalt	100	1200
3152	basalt	100	1200
3154	basalt	80	1300
G–604	basalt	220	1300
Weighted average (whole flow)		120	1300

* Samples were analysed by the Rock Analysis Laboratory, University of Minnesota. Analyses 3132, 3134, 3138, 3140, 3142, 3144, 3146, 3148, 3150, 3152, 3154, by S. S. Goldich (Sandell and Goldich, 1943, p. 103). Analyses G–26, G–149, G–253, G–297, G–453, G–559, G–604, by L. C. Peck (Cornwall, 1951a, p. 185).

Copper (Cu^{2+}). It has been pointed out above and elsewhere (Cornwall, 1951a, p. 177, 189) that copper, along with other more volatile elements, tends to be concentrated in the pegmatitic facies of the Greenstone flow. Spectrographic analyses for copper in the rocks are given in Table 1, and chemical analyses are given in Table 4. The agreement of the two analytical methods is good. The spectrographic analyses of minerals indicate that copper is most abundant in the magnetite, but the amount in other minerals is appreciable. Thus in the copper-rich pegmatitic facies (analysis 4-149) the copper content of the minerals is: magnetite, 880 p.p.m.; ilmenite, 300 p.p.m.; augite, 320 p.p.m.; chlorite, 280 p.p.m.; hedenbergite, 130 p.p.m.; plagioclase and apatite, 30 p.p.m. each. These

are the maximum amounts found in the samples for all the minerals except plagioclase (maximum 70 p.p.m.), and apatite (maximum 100 p.p.m.).

One of the present authors (Cornwall, 1951c, p. 57–58) examined microscopically a number of polished sections of the Greenstone and other flows, and found that disseminated copper sulphides were quite common in the Greenstone flow, and native copper in the other flows. These metallic minerals occur interstitially and also within silicate, ilmenite, and magnetite crystals. The question may be raised, then, as to whether the copper found spectrographically in the separate minerals replaces major elements in crystal lattices, or is included in the metallic or sulphide

Table 5. Distribution of copper in minerals of the Greenstone flow

Sample No.	Rock type	Total copper (%)		% of total Cu in minerals
		in rock-forming minerals	in rock	
4–58	ophitic basalt	0.0066	0·010	66
4–149	pegmatite facies	0·018	0·030	60
G–26	granophyre	0·008	0·007	100
4–376	ophitic basalt	0·0047	0·017	28
3–89	ophitic basalt	0·003	0·013	23
3–407	ophitic basalt (mafic)	0·003	0·010	30
3–540	ophitic basalt (mafic)	0·0048	0·008	60

state. Cu^{2+} should replace Fe^{2+} because of their similar ionic size, and the fact that copper is most abundant in the minerals that contain Fe^{2+} suggests that Fe^{2+} has been replaced. The 100 p.p.m. in the apatite of sample no. 4–376, on the other hand, is perhaps most readily explained as an inclusion of metallic copper or copper sulphide.

Butler and Burbank (1929, p. 46), and Broderick and Hohl (1935, p. 303–304) studied the occurrence and distribution of disseminated copper in the Greenstone and other flows of the Michigan copper district, and these authors concluded that the copper occurs chiefly as copper sulphides or as the native metal.

Sandell and Goldich (1943, p. 102) found the copper in the samples from the Greenstone and Kearsarge flows to be almost completely soluble in aqua regia, and they likewise concluded that the copper is not combined in the silicates, but rather is chiefly in the form of sulphides.

In Table 5 we have estimated the per cent of total copper that was found in the rock-forming minerals which contain copper as a minor constituent. These are only estimates, based on average modal analyses for the zones sampled, and separate samples for the rock and mineral analyses, but the results should be approximately correct. Thus a fifth to two-thirds of the copper in the basalt and pegmatites is probably included in rock-forming minerals, and all the copper in the granophyre appears to be in such minerals. As stated above, however, it is doubtful that all the copper included in the rock-forming minerals has replaced major elements in the crystal lattices.

Ringwood (1955, p. 195–196) points out that the tendency of copper to precipitate late during magmatic differentiation indicates that it does not substitute readily in silicates for major elements (Na^{1+} and Fe^{2+}) with similar ionic radii. The reason for this is, he believes, that copper's high electronegativity (Cu^{1+}, 1·8; Cu^{2+}, 2·0) makes its bonds essentially covalent and thus considerably weaker than those of Na^{1+} and Fe^{2+}. In the Greenstone flow, as mentioned earlier, copper is most abundant in the minerals that contain Fe^{2+}, and this relationship supports the conclusion that Cu^{2+} has, in part at least, substituted for Fe^{2+} in the crystal structures. The concentration of copper in the late pegmatitic differentiate of the Greenstone flow and the occurrence of part of the copper as the native metal or sulphide support Ringwood's suggestion that the substitution of Cu^{2+} for Fe^{2+} in mineral structures is made with difficulty.

Vanadium ($^{3+}$). The elements that tend to form volatile compounds (P, Ti, Fe Cu, etc.) are concentrated in the late-forming pegmatitic facies, and vanadium is concentrated there too (Table 1). The pegmatitic facies averages between 300 and 400 p.p.m. of vanadium, whereas the ophitic basalt runs somewhat under 200 p.p.m. The residual granophyre contains only about 20 p.p.m. Vanadium is most abundant in magnetite (maximum 8000 p.p.m.) and somewhat less so in ilmenite. It is also prominent in augite, and locally in chlorite. The remaining minerals contain only small amounts, and it is practically absent in plagioclase.

Vanadium probably replaces Fe^{3+} (ionic radius, 0·64), but with some difficulty, because V^{3+} has a larger ionic radius (0·74). Thus the minerals in which Fe^{3+} occurs contain vanadium, and it is most abundant in magnetite, where Fe^{3+} is a major element. Vanadium is also abundant in ilmenite, where, as V^{4+}, it may replace Ti^{4+}. The radii of the two ions are similar: 0·63 for V^{4+} and 0·68 for Ti^{4+}. The relative abundance of vanadium in the late-crystallizing pegmatitic facies is probably due mainly to the concentration of magnetite and ilmenite in these rocks. The fact that V^{3+} has a larger ionic radius than Fe^{3+} may also inhibit its substitution for Fe^{3+} in the early stages of crystallization, and thus cause it to be concentrated in the residual pegmatitic fraction.

Niobium (Nb^{4+}). All of the ilmenite samples contain niobium in amounts ranging from 80 to 200 p.p.m., and it was not found in any other minerals. Nb^{4+} with an ionic radius of 0·74 probably substitutes for Ti^{4+} (radius 0·68).

Zirconium (Zr^{4+}). The rock analyses show that the basalt and pegmatitic facies contain approximately 100 p.p.m. of zirconium and the granophyre contains 400 p.p.m. In the analysed minerals, zirconium is abundant in the apatites (up to 300 p.p.m.) and pyroxenes (up to 2000 p.p.m.) of the granophyre and pegmatitic facies, and locally in the chlorites (maximum 300 p.p.m.). The remaining augites contain 20 to 40 p.p.m. Zirconium is absent from most of the plagioclases, but it is abundant in that of the granophyre (260 to 420 p.p.m.). In most of the samples the amount of zirconium in the major minerals is not nearly enough to account for the total in the rocks. Thus it is probable that zirconium is present, in part at least, as the accessory mineral zircon ($ZrSiO_4$). The erratic distribution of Zr in the chlorites is probably due to the inclusion of zircon in some of those fractions, and zircon is undoubtedly present also in the granophyre fractions (feldspar and quartz, and augite) and possibly also in the apatites. Zr^{4+} may also enter feldspar,

augite, and apatite as a replacement of Ca^{2+}, and chlorite and augite as a replacement of Fe^{2+}.

Manganese (Mn^{2+}). Manganese is very abundant (2000 to 9000 p.p.m.) in the magnetites, ilmenites, pyroxenes, olivines, and chlorites. The plagioclases contain 50 to 250 p.p.m., except the plagioclase in the granophyre, which has 1100 to 1600 p.p.m. The apatites contain about 200 p.p.m. The chemical analyses (Table 4) indicate that Mn is most abundant in the pegmatitic facies (1500 to 1900 p.p.m.), and somewhat less abundant in the basalt (1200 to 1400 p.p.m.); the granophyre contains still less (850 p.p.m.). Mn^{2+} probably replaces Fe^{2+} and Ca^{2+} in the minerals, and it is believed that this is how it occurs, rather than as a discrete manganese mineral.

Scandium (Sc^{3+}). Scandium is concentrated mainly in augite, where its distribution in the rock differentiates is remarkably uniform. Small amounts are also found in all the other minerals except plagioclase, which contains none, except for 20 p.p.m. in one fraction of granophyre. The Sc^{3+} probably substitutes for Fe^{2+} in the minerals. The valence difference necessitates other modifications in the minerals to accommodate the scandium.

Lanthanum (La^{3+}) *and yttrium* (Y^{3+}). These two elements are concentrated in the granophyre and pegmatitic facies, and are most abundant in the apatites. Yttrium is also abundant in the ilmenites, magnetites, and pyroxenes; smaller amounts occur in the chlorites and olivines. Neither element occurs in plagioclase except in the granophyre (both Y and La) and pegmatitic facies (Y only). The elements probably substitute for Ca^{2+} in the apatites, pyroxenes, and sodic feldspars. They may also replace K^{1+} in the feldspar, and yttrium probably replaces Fe^{2+} in magnetite, ilmenite, olivine, and chlorite. The concentration of these elements in late-crystallizing fractions and minerals indicates that they enter the mineral lattices with difficulty and thus remain in the magma to be concentrated in the last fraction to crystallize.

Strontium (Sr^{2+}). Strontium is moderately abundant throughout the differentiation series in plagioclases, pyroxenes, chlorites, and apatites, and a small amount found in the olivines. The maximum amounts are found in the plagioclases (2000 p.p.m.), but pyroxenes, apatites, and chlorites contain up to 700 p.p.m. Sr^{2+} undoubtedly replaces Ca^{2+} most commonly, but it must also replace other elements, possibly Fe^{2+} or Mg^{2+}, where it occurs in chlorites and olivine. Sr may also substitute for K^{1+} in some minerals.

Barium (Ba^{2+}). As in the case of strontium, barium is most abundant in the feldspars. It is also quite abundant in the pyroxenes and chlorites and is sparingly present in the apatites. Barium is most abundant in the granophyre, according to the mineral analyses. Barium probably replaces Ca^{2+} and K^{1+} in the minerals.

Minor elements in lodes. Barren and copper-bearing amygdaloidal flowtops and conglomerates, including the leading copper producers in the Michigan copper district have been analysed spectrographically for minor elements. The results are given in Table 6. Each of the producing lodes was sampled in both barren and mineralized zones. Samples of commercial copper ore are marked with an asterisk.

No clear-cut association of any minor elements with copper-rich rock is evident in these analyses except possibly boron, which is most abundant in copper-bearing

amygdaloids. Silver (Ag) is present only in the samples that actually contain metallic copper, and it is probable that the silver is contained in the copper. Arsenic is also probably concentrated in the copper. In general, the amounts of minor elements in the amydgaloids are comparable to the amounts found within flows (compare Table 6 with Tables 1 and 2). Nickel appears high in two flows (Baltic and Iroquois) and low in two (Kearsarge and Pewabic). Zirconium and beryllium are relatively high in the conglomerates, and in the Kearsarge and Pewabic flows, and low elsewhere. Niobium ranges from 10 to 20 p.p.m. in the conglomerates and is below sensitivity in the amygdaloids. Chromium, nickel,

Table 6. Minor elements in Keweenawan amygdaloids and conglomerates*
(parts per million)

Ionic radius†	B^{3+}	Be^{2+}	Cr^{3+}	Ni^{2+}	Co^{2+}	Cu^{2+}	V^{3+}	Nb^{4+}	Zr^{4+}	Mn^{2+}	Ag^{2+}
	0·23	0·35	0·63	0·69	0·72	0·72	0·74	0·74	0·79	0·80	0·89
Sensitivity limits (p.p.m.)	9	1	1	5	5	1	7	10	10	10	1
Sample No.											
*A1–5	10	3	100	30	10	10000	100	10	500	<500	20
B–1	20	1	300	80	40	100	100	—	500	±2000	—
*B–2	±100	1	200	80	40	4000	200	—	200	1000	1
*B–3	±100	1	100	60	20	3000	200	—	100	500	2
*B–4	30	2	200	80	40	5000	200	—	200	500	2
B–5	20	1	300	80	40	50	300	—	200	<500	—
C–1	10	5	70	10	8	100	100	20	500	<500	—
C–2	10	7	50	10	5	50	70	10	500	<500	—
C–3	±100	2	100	40	40	<50	300	—	300	500	—
C–4	30	2	300	80	50	<50	100	—	100	500	—
C–5	50	1	300	80	50	<50	200	—	100	1000	—
*C–6	20	5	100	20	8	10000	100	20	400	<500	3
C–7	40	1	200	100	50	<50	100	—	200	500	—
C–8	50	1	100	100	40	<50	100	—	200	1000	—
*I–62	200	—	300	60	40	2000	300		200	500	1
IDC	100	1	400	60	40	70	300	—	200	700	—
*Iq–56	200	—	600	60	50	8000	500	—	200	500	1
IqAl	100	1	400	70	40	200	300	—	300	600	—
Q–1	70	3	100	30	50	400	600	—	500	±1000	—
*Q–2	70	2	80	20	30	2000	400	—	300	500	1
Q–3	70	2	200	40	40	70	400	—	400	500	—
*Q–4	50	1	100	30	20	8000	200	—	200	400	20
*NK–22	50	3	200	30	30	8000	200	—	300	500	3
*Allouez	70	4	100	20	10	6000	200	10	400	300	8
*Centennial	80	4	200	20	30	2000	400	—	600	500	—
*Iroquois	100	1	400	60	40	1000	400	—	200	600	—
*Peninsula	70	3	300	30	40	2000	400	—	500	600	—

* Analyses are spectrographic determinations of silicate fractions made by E. W. Claffy and K. J. Murata, U.S. Geological Survey.

An asterisk indicates that sample is from rock classed as commercial copper ore.

Dashes indicate that element was looked for, but not found.

Looked for but not found in any: As, Sb, Bi, Cd, Zn, In, Ge, Tl, Pt, Au, Pd, Re, Y, Mo, W, La, Ta, Pb, Sn.

† Ionic radius in Ångström units at valence shown as given by Ahrens (1952).

Table 6—*continued*

Sample No.		Sample weight of −100-mesh rock	Sample weight of +100 mesh metallic fraction (mostly native copper)
		(grams)	(grams)
*Al–5	Houghton conglomerate	106·2	47·7
B–1	Baltic (1st west) amygdaloid	115·5	—
*B–2	Baltic amygdaloid	105·3	35·1
*B–3	Baltic (1st east) amygdaloid	108·8	31·4
*B–4	Baltic (1st east) amygdaloid	109·0	8·5
B–5	Baltic amygdaloid	101·2	0·067
C–1	Houghton conglomerate	114·8	—
C–2	Calumet and Hecla conglomerate	118·1	0·128
C–3	Kearsarge amygdaloid	128·4	—
C–4	Nonproductive amygdaloid	111·2	—
C–5	Kearsarge amygdaloid	111·8	0·292
*C–6	Calumet and Hecla conglomerate	128·8	120·0
C–7	Iroquois amygdaloid	106·5	0·164
C–8	Iroquois amygdaloid	117·0	0·163
*I–62	Isle Royale amygdaloid	119·5	22·3
IDC	Isle Royale amygdaloid	123·4	—
*Iq–56	Iroquois amygdaloid	100·3	37·3
IqAl	Iroquois amygdaloid	128·2	0·049
Q–1	Pewabic amygdaloid	118·5	2·972
*Q–2	Pewabic amygdaloid	104·9	148·0
Q–3	Pewabic amygdaloid	100·8	0·094
*Q–4	Pewabic amygdaloid	116·2	59·2
*NK–22	Kearsarge amygdaloid	113·7	36·6
*Allouez jig headings, Houghton conglomerate		125·1	122·8
*Centennial jig headings, Kearsarge amygdaloid		101·1	96·9
*Iroquois jig headings, Iroquois amygdaloid		114·8	108·4
*Peninsula jig headings, Kearsarge amygdaloid		99·8	104·7

and cobalt are appreciably less in the conglomerates than in the amygdaloidal flow tops, as would be expected. Other elements seem to be erratic in their distribution, particularly barium and manganese.

References

Ahrens L. H. (1952) The use of ionization potentials—I. Ionic radii of the elements. *Geochim. et Cosmochim. Acta* **2,** 155–169.

Ahrens L. H. (1953) The use of ionization potentials—II. Anion affinity and geochemistry. *Geochim. et Cosmochim. Acta*, **3,** 1–29.

Broderick T. M. (1935) Differentiation in lavas of the Michigan Keweenawan. *Bull. Geol. Soc. Amer.* **46,** 503–558.

Broderick T. M. and Hohl C. D. (1935) Differentiation in traps and ore deposition. *Econ. Geol.* **30,** 301–312.

Butler B. S. and Burbank W. S. (1929) The copper deposits of Michigan. *U.S. Geol. Survey Prof. Paper* **144,** 238.

Cornwall H. R. (1951a) Differentiation in lavas of the Keweenawan series and the origin of the copper deposits of Michigan. *Bull. Geol. Soc. Amer.* **62,** 159–202.

Cornwall H. R. (1951b) Differentiation in magmas of the Keweenawan series. *J. Geol.* **59,** 151–172.

Cornwall H. R. (1951c) Ilmenite, magnetite, hematite, and copper in lavas of the Keweenawan series. *Econ. Geol.* **46,** 51–67.

Dieke G. H. and Crosswhite H. M. (1943) *J. Opt. Soc. Amer.* **33,** 425.

Fleischer, Michael (1955) Minor elements in some sulfide minerals. *Econ. Geol.* 50th Ann. Vol. 970–1024.

Goldschmidt V. M. (1937) The principles of distribution of chemical elements in minerals and rocks. *J. Chem. Soc.* 655–673.

Goldschmidt V. M. (1954) *Geochemistry.* Clarendon Press, Oxford, 730.

Nockolds S. R. and Mitchell R. L. (1948) The geochemistry of some Caledonian plutonic rocks: A study in the relationship between the major and trace elements in igneous rocks and their minerals. *Trans. Roy. Soc. Edinb.* **61,** II 533–575.

Pauling Linus (1940) *The Nature of the Chemical Bond and the Structures of Molecules and Crystals.* Ithaca, Cornell Univ. Press, 450.

Ringwood A. E. (1955) The principles governing trace elements distribution during magmatic crystallization. *Geochim. et Cosmochim. Acta* **7,** 189–202, 242–254.

Sandell E. B. and Goldich S. S. (1943) The rarer metallic constituents of some American igneous rocks. *J. Geol.* **51,** 99–115, 167–189.

Wager L. R. and Mitchell R. L. (1951) The distribution of trace elements during strong fractionation of basic magma—A further study of the Skaergaard intrusion, East Greenland, *Geochim. et. Cosmochim. Acta* **1,** 129–208.

Geochimica et Cosmochimica Acta, 1957, Vol. 12, pp. 225 to 237. Pergamon Press Ltd., London

Isotopic composition of common leads and continuous differentiation of the crust of the earth from the mantle

Royal R. Marshall
Enrico Fermi Institute for Nuclear Studies, University of Chicago, Chicago, Illinois, U.S.A.

(*Received* 14 *February* 1957)

Abstract U^{238}/Pb^{204} and Th^{232}/U^{238} ratios have been calculated from nonanomalous common leads. These values that would be present today in the reservoirs which produced the ores vary systematically with the "model" lead-lead age introduced by Houtermans and his co-workers. The secular trend of the first ratio appears to be due to the addition of lead, primeval in isotopic composition, from the mantle to the crust of the earth. On the basis of a linear rate of addition of lead, relative to uranium, the following conclusions are reached:

1. The rate of addition of lead is 0·09 atom Pb/atom U^{238}/B yr.
2. The U^{238}/Pb^{204} ratio in the crust today is 9·3 ± 0·2.
3. Lead ores would contain more radiogenic component if there were no addition of primeval lead. The isotopic ratios corrected for this effect are more consistent with their evolution through the decay of uranium and thorium in chemically-closed systems.
4. The Th^{232}/U^{238} ratios which would be present today in the lead-ore reservoirs increase linearly with geologic age. Apparently, uranium is being differentiated in respect to thorium at the low rate of 0·01 atom U^{238}/atom Th^{232}/B yr.
5. The Th^{232}/U^{238} ratio in the crust today is 4·1 ± 0·1.

Introduction

Houtermans (1947) pointed out that common leads might be analysed by taking the differences between the observed amounts of the lead isotopes in a lead ore and a set of initial values. He used the following equations to formulate this procedure:

$$\alpha = \alpha_w + \mu(e^{\lambda_1 w} - e^{\lambda_1 p}) \tag{1a}$$

$$\beta = \beta_w + \varepsilon\mu(e^{\lambda_2 w} - e^{\lambda_2 p}) \tag{1b}$$

$$\gamma = \gamma_w + \mu\kappa(e^{\lambda_3 w} - e^{\lambda_3 p}) \tag{1c}$$

Lead ores were presumed to have evolved throughout w years from the initial quantities of Pb^{206}, Pb^{207}, and Pb^{208}, relative to Pb^{204}, represented by α_w, β_w, and γ_w. The measured ratios for any lead ore are, correspondingly, α, β, and γ. The U^{238}/Pb^{204} ratio, μ, is that which would be present today in the reservoir within the crust of the earth which produced the lead ore p years ago. Similarly, κ is the present-day value for the Th^{232}/U^{238} ratio. The systems producing lead ores were assumed to be chemically-closed systems in respect to lead, uranium, and thorium.

The values for the initial isotopic ratios were not apparent when Houtermans (1947) first formulated this scheme for calculating lead-lead ages (p), uranium-lead ratios (μ), and thorium-uranium ratios (κ). Subsequently, Patterson, Tilton, Inghram, and Brown (1953) isolated and mass-spectrometrically examined microgram quantities of lead from iron meteorites. The lead is relatively highly concentrated in the troilite phase of the siderites, while the amounts of uranium present in either the troilite or the metallic portion are negligible. Such lead has been isolated from uranium (and thorium) since the differentiation of the material

comprising the siderites and aerolites. This event presumably occurred at an early time in the history of the solar system, certainly much earlier than the formation of any known lead ore in the crust of the earth. With lead from an iron meteorite taken as primeval, the age of the earth is about 4·5 B* yr (Patterson, 1953) and provides a value for w.

Eberhardt, Geiss, and Houtermans (1955a) analysed a large number of lead ores representing a broad span of geologic time. They were then able to show, through the preceding equations and the isotopic composition of the troilite lead as the set of initial values, the important fact that the relative amounts of lead, uranium, and thorium in the crust of the earth have remained essentially unchanged except for radioactive decay over approximately 3 B yr. That is, to a first approximation μ and κ are constants as determined from lead ores representing several billions of years of earth history. These investigators did notice a secular trend in the values of κ from their data. This ratio increases slightly with increasing age of the lead, but they could offer no explanation for this variation.

In the present paper the change of μ with time is emphasized and it and the similar variation of κ are discussed as a consequence of the continuing differentiation of the crust from the mantle of the earth.

Secular Trend of Uranium-lead and Thorium-uranium Ratios

More than two hundred analyses of common leads have been published. The first isotopic compositions were reported by Nier, and other data have been contributed by Vinogradov, Zadorozhnyi, and Zykov; Collins, Russell, and Farquhar; Allan, Farquhar, and Russell; Ehrenberg; Geiss; Kulp, Owen, Eckelman, and Bate; Patterson, Goldberg, and Inghram (1953); Patterson (1953); and Russell, Farquhar, Cumming, and Wilson. These data and other previously unpublished values are conveniently available in a carefully documented compilation by Faul (1954).

Most of the isotopic compositions for common leads listed in Faul's book have been used to calculate p, μ, and κ from equation (1). Additional lead analyses were provided by papers by Bate and Kulp (1955) and Tilton, Patterson, Brown, Inghram, Hayden, Hess, and Larsen (1955). For the calculations, the values taken for the constants in the equations are the following:

$$\alpha_w = 9{\cdot}41$$

$$\beta_w = 10{\cdot}27$$

$$\gamma_w = 29{\cdot}16$$

$$w = 4{\cdot}486 \text{ B yr}$$

$$\lambda_1 = 0{\cdot}154 \text{ (B yr)}^{-1}$$

$$\lambda_2 = 0{\cdot}98 \text{ (B yr)}^{-1}$$

$$\lambda_3 = 0{\cdot}0499 \text{ (B yr)}^{-1}$$

$$\varepsilon = 1/139$$

* B = 10^9.

These parameters are the same as used by HOUTERMANS and his co-workers in analysing their additional mass-spectrometric measurements (EBERHARDT *et al.*, 1955a,b; BESAIRIE *et al.*, 1956), so that all the calculated values of p, μ, and κ for the scatter diagrams (Figs. 1 and 2) are compatible.

Approximately 20% of the analyses have been discarded, and only for the reason that they are obviously anomalous. The criteria used in elimination were α values greater than 20·00 or p values in obvious conflict with geologic-age relations by more than 400 M* yr. The remaining 207 analyses from the preceding references are represented in Figs. 1 and 2, plots of μ versus p and of κ versus p,

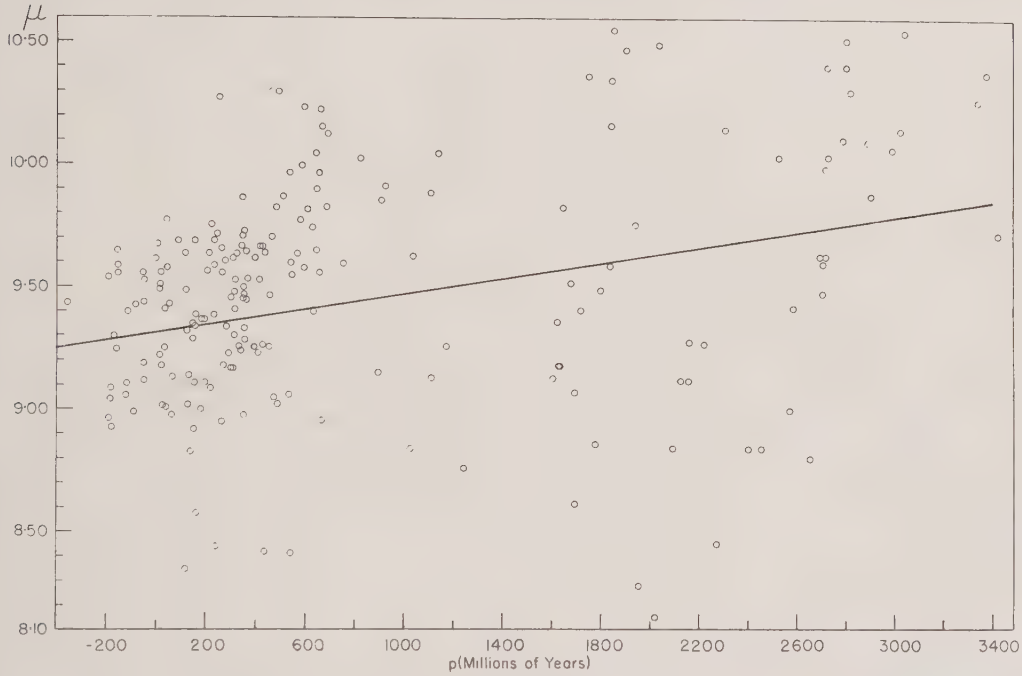

Fig. 1. U^{238}/Pb^{204} ratios (at today) in the sources of common lead as a function of their "model" lead-lead ages.

respectively. The secular trends have been fitted with a least-squares analysis assuming linear regression.†

The equations for the lines are:

$$\mu = 9{\cdot}31 + 0{\cdot}162p \tag{2a}$$

$$\kappa = 4{\cdot}10 + 0{\cdot}198p \tag{2b}$$

for p in B yr. The U^{238}/Pb^{204} ratio varies from 9·31 to 9·80 in 3 B yr and κ changes from 4·10 to 4·69 during the same period.

---

* $M = 10^6$.

† It has come to the writer's attention that Dr. EBERHARDT, Physikalisches Institut der Universität Bern, has independently made a similar analysis.

Mr. Eugene DuFresne has kindly checked the values for the slopes of the two lines (Figs. 1 and 2) as well as determining the 95% confidence limits, which are $\pm 0{\cdot}070$ for the slope of μ and $\pm 0{\cdot}004$ for that of κ. Narrow limits for the latter are obvious from Fig. 2. The trend in μ is best defined with the analyses performed at Bern (Eberhardt *et al.*, 1955a,b; Besairie *et al.*, 1956). The 95% confidence limits represent a range of only 26% in respect to the slope for this group of ninety three samples covering a wide span of geologic ages. The limits for a smaller group of analyses made at Toronto enclose those of the preceding group, but indicate considerably more scatter in the uranium to lead ratios (Table 1). The remaining analyses also display a positive bias.

Table 1. Statistical analysis of scatter diagrams (Figs. 1 and 2)

Groups of data	Number of analyses	Change in μ per B yr		Change in κ per B yr	
		Slope	95% confidence limits[1]	Slope	95% confidence limits[1]
Bern analyses	93	0·231	0·067	0·210	0·004
Toronto analyses	23	0·174	0·376	0·336	0·698
All analyses	207	0·161	0·070	0·198	0·004

[1] These are symmetrical limits ($\pm$) and include 95% probability.

The significance in the change of the uranium-to-lead ratio is difficult to appreciate from the scattered plot of Fig. 1. Fortunately, additional evidence discussed below tends to confirm the reality of this variation. In any case, the geochemical dissimilarity of lead and uranium compared to the similarity for uranium and thorium allow one to predict precisely what is observed, large variation in μ values, while κ values are closely grouped.

The Significance of Trends in Uranium-to-lead and Thorium-to-uranium ratios

In view of the approximately constant values for μ and κ throughout the greater portion of the history of the earth, it is surprising that any systematic variation in these ratios should occur at all. The thorium-uranium ratio, in particular, might be expected to have remained constant since an early date. Although the trends might have a trivial origin, it is interesting to attempt to decide, through the calculations implicit in equation (1), upon the actual values of these geochemically important ratios. One might assume that they are actually constant, and try to show this by varying the parameters in equation (1).

The values for α_w, β_w, and γ_w are especially suspect, since they are merely assumed to be those present at an early stage of the crust of the earth and subsequently modified only through the decay of uranium and thorium. The selection of other values for γ_w and w does correct most of the variation in μ and κ.

The decay-constant for U^{235}, λ_2, is possibly one of the most uncertain of the remaining parameters. Values are reported in the literature for this constant, differing by as much as 10%. Changing λ_2 shifts calculated values but does not eliminate the trends. Variation of the other parameters is unrewarding.

For example, two common leads have been selected which lie close to the best lines in Figs. 1 and 2. The Italian sample represents recent lead with the isotopic ratios 18·90, 15·71, and 38·94

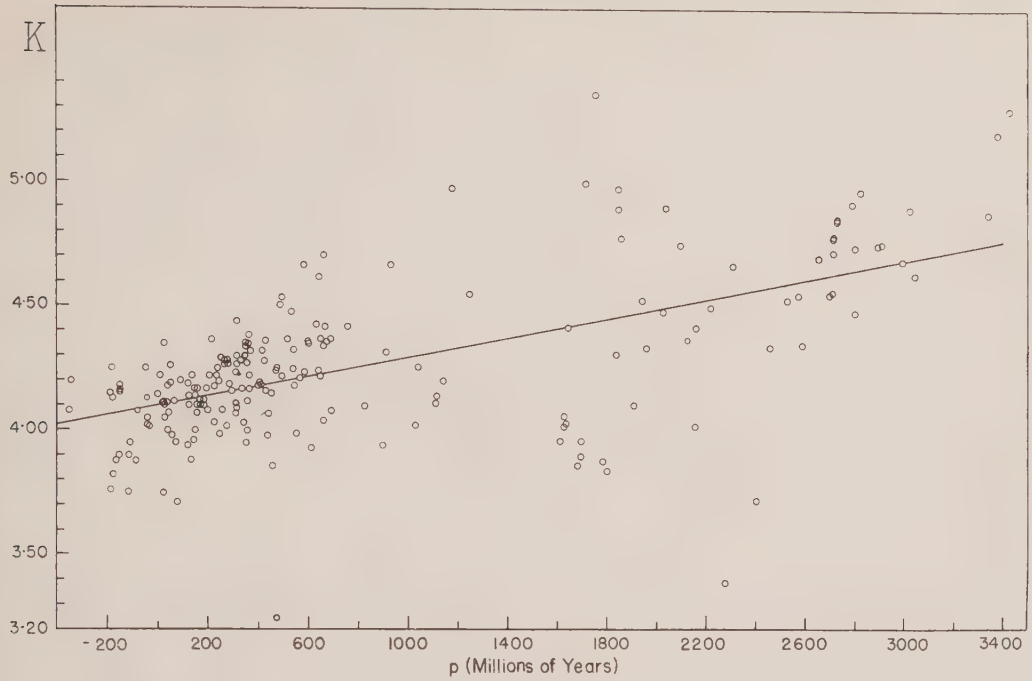

Fig. 2. Th^{232}/U^{238} ratios (at today) in the sources of common lead as a function of their "model" lead-lead ages.

(Enerhardt *et al.*, 1955a). The other is an ancient African ore, approximately 3 B yr old, with the composition 13·56, 14·80, and 33·42 (Eberhardt *et al.*, 1955a). The ratios, μ and κ, have been calculated with various sets of parameters and are listed in Table 2. Slight modification of the values for α_w, β_w, and γ_w (columns 2 and 5) has little effect on the change of μ with time. However, the value for κ is sensitive to γ_w, and in columns 2 and 5 (Table 2), the change of κ with time is significantly different from that in the columns where only the decay-constant or the U^{235}/U^{238} ratio has been changed. The last column (7) indicates that a γ_w of slightly greater

Table 2. Effect of variation of the parameters in equation (1) in the geochemical ratios.

Sample [Eberhardt *et al.* (1955a)]	Quantity calculated	1*	2*	3*	4*	5*	6*	7*
Galena, Val d'Anzasca	μ	9·43	9·26	9·34	9·80	9·43	8·98	9·15
by Domodossola, Italy	κ	4·08	3·97	4·06	4·12	3·98	4·02	3·79
Galena, Dalakura,	μ	10·07	9·89	9·90	10·91	10·27	9·18	9·10
Sula Mt., Sierra Leone	κ	4·69	4·42	4·68	4·72	4·42	4·65	4·10

* These headings refer to calculations using the following parameters:

1. Set given in text above.
2. $\alpha_w = 9{\cdot}50$, $\beta_w = 10{\cdot}36$, $\gamma_w = 29{\cdot}49$ (these are the corrected and averaged values recently reported by Patterson (1955)); others are the same as above.
3. $\varepsilon = 1/137{\cdot}8$; others are the same as those for column 1.
4. $\lambda_2 = 0{\cdot}9721$; others are the same as those for column 1.
5. $\alpha_w = 9{\cdot}50$, $\beta_w = 10{\cdot}36$, $\gamma_w = 29{\cdot}49$, $w = 4{\cdot}498$, $\lambda_1 = 0{\cdot}1538$, $\lambda_2 = 0{\cdot}9721$, $\lambda_3 = 0{\cdot}0499$, $\varepsilon = 1/137{\cdot}8$.
6. $\lambda_2 = 0{\cdot}99$; others are the same as those for column 1.
7. $\alpha_w = 9{\cdot}72$, $\beta_w = 11{\cdot}30$, $\gamma_w = 29{\cdot}89$, $w = 4{\cdot}300$; others are the same as those for column 1.

than 30 and a β_w somewhat over 11 and an α_w nearly 10 would compensate for differences in the geochemical ratios, providing the age of the crust is around 4·3 B yr. This is the age recently obtained by extrapolation of lead ores by Russell and Allan (1955). However, lead-lead ages with these parameters are in poor agreement with independent dates.

The most interesting results are obtained when γ_w and w are varied. If w is taken as 4·55 B yr, the value most recently reported by Patterson (1956) for the age of the meteorites and the earth, the systematic variation in μ disappears. With a value for γ_w of 29·93, most of the systematic variation in κ disappears. These changes in the parameters are still within the range of small corrections. However, the change in γ_w is at the limit of the estimated error (Patterson, 1956) and appears concentrated in this one isotopic ratio. Furthermore, the lead-lead ages are appreciably in error.

Since the trends in the ratios appear not to be corrected by reasonable changes in the parameters involved in the calculations, either trend or both may be true rather than apparent. With this in mind, the change of μ with time has been considered real and due to the continuous addition of primitive lead (high in Pb^{204}) to the crust of the earth.

The Relative Rate of Addition of Lead to the Crust

The linear change of μ with time is attributed to the relative addition of Pb^{204}. The rate is easily calculated from equation (2a). If b is the fraction (relative to the original amount) of Pb^{204} atoms added to the crust of the earth, since its formation w B yr ago up to the time p B yr ago, then this quantity is given by the following equation:

$$b = \frac{0{\cdot}162(w - p)}{9{\cdot}31 + 0{\cdot}162p} \tag{3}$$

Here the implicit assumption is that the curve of Fig. 1 may be extrapolated to 4·5 B yr. The rate of addition is slightly less than 0·002 atom Pb^{204}/atom U^{238}/B yr or, on the basis of primeval lead, 0·09 atom Pb/atom U^{238}/B yr.

Uranium and thorium as well as their decay products are probably concurrently added to the crust. However, as long as the lead-to-uranium ratio is higher in the mantle than in the crust of the earth, as is generally believed (Patterson *et al.*, 1955), the lead enrichment relative to uranium may be considered simply as the addition of primeval lead to a good approximation.

Correction of Observed Isotopic Ratios

With appropriate values for b, the observed isotopic ratios can be corrected to those which would be found if there had been no addition of primeval lead. The following equations are used to calculate the corrected isotopic ratios, α', β', and γ' from α, β, and γ and the primeval isotopic composition:

$$\alpha' = \alpha + b(\alpha - \alpha_w) \tag{4a}$$

$$\beta' = \beta + b(\beta - \beta_w) \tag{4b}$$

$$\gamma' = \gamma + b(\gamma - \gamma_w) \tag{4c}$$

The corrected isotopic ratios indicate that relatively more radiogenic lead would be present in the crust of the earth in the absence of differentiation. Patterson

et al. (1955) have already stated that the modern common lead appears to be slightly deficient in radiogenic lead, but underestimate the amount. Furthermore, they suggest that this may be due to the transfer of uranium from the interior to the crust.

From equations (1) and (2) and the values of the parameters listed above, the isotopic ratios for average ores may be calculated for various stages in the evolution of crustal lead. Representative lead in the crust of the earth at 1, 2, and 3 B yr ago is characterized by its isotopic ratios, α, β, and γ, in Table 3. These ratios have been corrected, according to equation (4), to those values, α', β', and γ', which would be observed if differentiation did not occur.

Table 3. Average values for isotopic composition of lead in the crust of earth at various times with and without the addition of lead

p (B yr)	α	β	γ	α'	β'	γ'
0	18·68	15·64	38·73	19·40	16·06	39·48
1	17·26	15·62	37·28	17·73	15·94	37·76
2	15·52	15·40	34·48	15·78	15·61	35·74
3	13·41	14·66	33·27	13·51	14·77	33·37

Calculation of Lead-lead Ages

(a) *Heterogeneous evolution from a homogeneous isotopic composition.*

The good agreement between the lead-lead ages calculated by Eberhardt, Geiss, and Houtermans (1955a) and the independent geologic-age estimates is more than fortuitous. The selection of the isotopic composition of lead in siderites as that for lead in the earth at the time when lead began to evolve heterogeneously was a wise choice. Although the general trend in evolution of lead ores is evident from the early attempts to establish the age of the earth (see the review of this subject by McCrady, 1952), local variations in the earth of the ratio of lead to uranium and thorium produce the second-order effect of heterogeneous evolution. This is one reason why ores in general do not provide reliable lead-lead ages. The use of primeval lead and that of an ore eliminates the generally poor assumption that two lead sources have had the same uranium-to-lead ratio. The isotopic composition of the ore alone determines the average uranium-to-lead ratio which was in the reservoir from the time portions of the earth were sufficiently isolated from one another to allow the heterogeneous development of lead until the ore was formed.

(*b*) *Effects of the addition of lead to the ore-producing reservoirs*

In the calculation of the lead-lead age for an ore younger than 2·5 B yr with average modern ore, and assuming that the uranium-lead ratio is the same for all reservoirs, the value from equations (1a) and (1b) using the observed isotopic ratios is generally too small to give a reasonable value for μ. As the time separation becomes less, μ increases rapidly. Although $\Delta\beta$ becomes small and the experimental error in the determination of β makes a larger contribution percentagewise,

this uncertainty in no way accounts for the exponental rise in μ. Since independent absolute dates for most lead ores are not available, such lead-lead ages may easily have an unsuspected error of, say, 50%. This error is not obvious until the exponential function of p is used to calculate μ and a fantastically large value is obtained.

This second discrepancy is the result of systematically adding lead, relative to uranium, from a source with a higher lead-to-uranium ratio. An equivalent statement is that uranium may be more rapidly differentiated in the silicate phase than lead, but the relative addition of uranium to the crust is proceeding at a lower rate. The error in ages due to the secular change in the U^{238}/Pb^{204} ratio is not the same as that introduced in comparing ores from reservoirs with grossly different ratios. Not only is there the random variation in μ to consider, but the lead-isotopic ratios reflect less radiogenic lead than would be formed through radioactive decay alone.

The corrected isotopic ratios, α', β', and γ', may be used to calculate more consistent ages. This is most readily seen with the use of values calculated from the curve of Fig. 1 (Table 3). For the purpose of comparison, ages have been calculated from the following equations:

$$\frac{\beta_0' - \beta'}{(\alpha_0' - \alpha')\varepsilon} = \frac{e^{\lambda_2 p} - 1}{e^{\lambda_1 p} - 1} \tag{5}$$

$$\frac{\beta_0 - \beta}{(\alpha_0 - \alpha)\varepsilon} = \frac{e^{\lambda_2 p} - 1}{e^{\lambda_1 p} - 1} \tag{6}$$

$$\frac{\beta - \beta_w}{(\alpha - \alpha_w)\varepsilon} = \frac{e^{\lambda_2 w} - e^{\lambda_2 p}}{e^{\lambda_1 w} - e^{\lambda_1 p}} \tag{7}$$

In these equations, the subscript $_0$ is used with the isotopic ratios calculated from equations 1 and 2 for $p = 0$. Table 4 lists ages calculated from the isotopic ratios of Table 3 and equations (5) through (7). There is agreement among these values except, in each case, for the one

Table 4. Ages in B yr calculated by various combinations of the isotopic ratios in Table 3

From equation	(5)	(6)	(7)
	1·00	− 4·57	1·00
	2·00	1·11	2·00
	3·00	2·73	3·00

calculated from two pairs of uncorrected ratios (equation 6). These are obviously inconsistent, because they were calculated from differences between two (average) leads from sources containing different U^{238}/Pb^{204} ratios with the assumption that these ratios were the same.

The calculations from equation (7) with uncorrected or corrected ratios are consistent for the reason already discussed, namely, from the starting-point of homogeneous isotopic composition only one value of the U^{238}/Pb^{204} ratio is involved, and that is the average value in the reservoir which produced the ore. It makes no difference if one takes the corrected isotopic ratios or the uncorrected values and subtracts the initial isotopic composition common to both reservoirs, μ has been legitimately eliminated. The correction (equation 4) is of a form which cancels out in the ratio of isotopic differences (equation 7).

(c) Calculation of lead-lead ages from individual ores

HOLMES (1956) has recently published a table which is a compilation of a number of isotopic analyses of common leads for which the geologic ages are reasonably accurately inferred from independent evidence. These isotopic ratios and their corrected values are given in Table 5. The correction factor, b (equation 3), which has been used was calculated with the lead-lead age determined from equation (7).

Table 5. Isotopic ratios for some dated common leads and their corrected values

Lead	α	β	γ	α'	β'	γ'
1. Kantangan ores (10)*	18·17	15·84	38·36	18·76	16·21	38·97
2. Galena, Mitwaba, Belgian Congo	17·76	15·88	37·58	18·27	16·22	38·09
3. Galena, Great Bear Lake	15·93	15·30	35·30	16·25	15·54	35·60
4. Native lead, Langban, Sweden (2)	15·84	15·50	36·64	16·12	15·73	35·97
5. Galena, Fahlun, Sweden	15·89	15·61	35·86	16·17	15·84	36·15
6. Galenas, Churchill Prov., Canada (9)	15·98	15·62	36·00	16·27	15·86	36·30
7. Dhawar galena, Mysore	14·17	14·74	33·80	14·33	14·89	33·96
8. Kewatin ores, Canada (11)	14·35	15·06	34·20	14·51	15·21	34·36
9. Shamvaian galenas, S. Rhodesia (2)	14·08	14·98	34·12	14·22	15·12	34·27
10. Sula Mts. galenas, Sierra Leone (3)	13·69	14·91	33·78	13·80	15·03	33·90

* Number of isotopic analyses.

The lead-lead ages for these ores have been calculated according to equations (5) through (7). The values are given in Table 6 along with the independently derived geologic ages as listed by HOLMES (1956).

The agreement of the "model" ages from equation (7) to the independent geologic ages fully justifies the assumption that the isotopic composition of the lead initially present in the crust was essentially the same as that of lead in iron meteorites.

Equation (5) is very sensitive to errors in the isotopic ratios because $\Delta\beta$ is small. Nevertheless, the corrected isotopic ratios produce much more reasonable values for the age determined in this way than do the uncorrected ratios (equation 6, Table 6). Of course, the criticism may be made that the values of α_0 and β_0 used in these calculations are not truly representative of the modern lead ore. If this point of view is accepted, even though it appears contrary to experimental observation, the isotopic ratios $\alpha_0 = 19{\cdot}18$ and $\beta_0 = 15{\cdot}93$ are indeed found to provide lead-lead ages approximating the true ages at least as well as those from the ratios in Table 3. While 19·18 and 15·93 are not as large as α_0' and β_0', respectively (Table 3), these ratios are still too large to be typical of crustal lead. The

Table 6. Lead-lead ages in B yr calculated from the data of Table 5 and equations (5) through (7)

Lead*	(5)	(6)	(7)	Independent age
1	—	—	0·61	0·62
2	—	—	0·92	1·065
3	2·47	2·03	1·63	1·40
4	1·55	0·18	1·86	~1·90
5	0·70	−7·17	1·92	~1·90
6	0·66	−23·0	1·87	~1·90
7	3·06	2·84	2·45	2·30
8	2·58	2·17	2·57	2·56
9	2·67	2·29	2·71	2·65
10	2·70	2·32	2·96	2·93

* See Table 5 for more complete description of samples.

corrected isotopic ratios are to be preferred in calculating ages, since their selection is not arbitrary.

In equation (5) the corrected average isotopic ratios, α_0' and β_0', for modern lead have been used. This is only an approximation, since the actual values for the uranium-to-lead ratios in the reservoirs are scattered about the general trend given by equation (2a). The blank spaces in Table 6 indicate that p cannot be calculated from the average β_0'. In these cases β' is greater

Table 7. Uranium-lead ratios in the individual ore reservoirs today, but with modern leads corrected for the addition of primeval lead

Lead*	μ_0	α_0'	β_0'
1	9·66	19·83	16·28
2	9·76	19·91	16·34
3	8·91	18·97	15·81
4	9·40	19·49	16·11
5	9·64	19·76	16·26
6	9·63	19·74	16·25
7	8·46	18·49	15·53
8	9·27	19·36	16·03
9	9·35	19·44	16·08
10	9·77	19·89	16·33

* See Table 5 for more complete description of samples.

than β_0'. The modern lead which should be compared to particular ore would be that present in that reservoir today. To determine this particular modern ore it is necessary to use the lead-lead age calculated from the primeval lead (equation 7), and determine μ. With p and μ, the extrapolated value μ_0 (at $p = 0$) may be found according to equation (2a). This is the U^{238}/Pb^{204} ratio which would be present today in the reservoir due to the mixing in of more primeval lead, this process presumed continuous and the same for all reservoirs. Then the isotopic composition of the corresponding modern lead may be calculated and corrected to

the final values, which are independent of the addition of lead. The latter are given by the following overall equations:

$$\alpha_0' = \alpha_w + \left(\frac{\alpha - \alpha_w}{e^{\lambda_1 w} - e^{\lambda_1 p}} - 0{\cdot}162p\right)(e^{\lambda_1 w} - 1)(1 + b) \tag{8a}$$

$$\beta_0' = \beta_w + \varepsilon\left(\frac{\alpha - \alpha_w}{e^{\lambda_1 w} - e^{\lambda_1 p}} - 0{\cdot}162p\right)(e^{\lambda_2 w} - 1)(1 + b) \tag{8b}$$

The value of b (from equation 3) is that for $p = 0$. Briefly, this signifies that for each reservoir there is an individual line of evolution parallel to the best line in Fig. 1.

Table 7 lists μ_0 ($p = 0$) values for the leads in Tables 5 and 6, and their appropriate sets of corrected modern lead isotopic ratios.

Addition of Uranium and Thorium to the Crust

Evidently uranium is being somewhat concentrated relative to thorium in the crust of the earth (Fig. 2). The rate of increase is about 0·01 atom U^{238}/atom Th^{232}/B yr. This rate is small compared to the fractionation of lead in respect to uranium, whose rate is 0·09 atom Pb/atom U^{238}/B yr, even though the effects of differentiation are most obvious in the case of the κ values.

The minimum rates of enrichment of uranium and lead are 0·05 U atom/U atom in the crust/B yr and 0·011 Pb atom/Pb atom in the crust/B yr, respectively. These figures indicate that uranium is being differentiated at a much greater rate than lead. Such a deduction is consistent with the geochemical observations that most of the uranium and thorium are concentrated in the crust and the lead, in the interior (Patterson *et al.*, 1955).

The addition of uranium and thorium further complicates the simple model represented by equation (1). However, if the process is approximately linear with Q_1 atoms U^{238} added per B yr and Q_3 atoms Th^{232} added per B yr, the solution of the differential equations is still simple. In this case the values calculated for μ and κ are

$$\frac{U^{238} - Q_1/\lambda_1 + Q_1(w - p)/(e^{\lambda_1 w} - e^{\lambda_1 p})}{Pb^{204}} \tag{9a}$$

and

$$\frac{Th^{232} - Q_3/\lambda_3 + Q_3(w - p)/(e^{\lambda_2 w} - e^{\lambda_3 p})}{U^{238} - Q_1/\lambda_1 + Q_1(w - p)/e^{\lambda_1 w} - e^{\lambda_1 p})} \tag{9b}$$

respectively.

These relationships indicate that the U^{238}/Pb^{204} ratio in the crust today is greater than the value 9·3 ± 0·2 (Fig. 1) and that the Th^{232}/U^{238} ratio today is different from 4·1 ± 0·1 (Fig. 2). Since the best estimates from experimental data place the latter ratio at somewhat less than 4, κ probably is slightly less than 4·1 and Q_1 and Q_3 small.

Summary

The secular variation of uranium-lead and thorium-uranium ratios in the crust of the earth, as revealed by lead ores formed at various times throughout approximately 3 B yr, is apparently the result of the continual development of the crust from the mantle. Lead has been added at an approximately linear rate, relative to uranium, to the crust from a source with a higher lead-to-uranium ratio.

Since uranium and lead are not geochemically similar elements, their ratio varies considerably in the rocks which are the source of lead ores. This random

variation limits the accuracy with which the trend in this ratio displayed by the crust as a whole can be determined. A large number of additional analyses of common leads, in particular those of Pre-Cambrian age, should permit a more precise estimation for this secular change. Nevertheless, on the basis of the approximate change in the U^{238}/Pb^{204} ratio, outside of radioactive decay, considered as the addition of primeval lead to the crust of the earth, observed isotopic ratios for lead-ores and average modern ore can be corrected to values from which improved lead-lead ages may be calculated to a first approximation, overlooking local variations in the uranium-to-lead ratio. The error in the calculation of a lead-lead age from the observed isotopic ratios of the ores is most apparent when values are calculated for the U^{238}/Pb^{204} and the Th^{232}/U^{238} ratios with this age. Except in the case of the most widely separated isotopic compositions, absurdly large values for the former ratio are obtained and, consequently, too low values for the latter.

The secular trend in the Th^{232}/U^{238} ratio appears to be due to the slight addition of 0·01 of an atom of U^{238} for every one of Th^{232} in the crust in a billion years.

Although the planets were probably substantially differentiated into silicate and metal phases at an early period in the history of the solar system, the crust of the earth appears to have been in continuous formation. Vertical mixing rather than horizontal mixing prevails, which is reasonable considering the epidermal nature of the crust. Wilson (1952) and others consider, from independent evidence, that the continents are continuously evolving. This conception is especially compatible with the preceding conclusion. Since the change in the composition of the crust is evinced only by ratios, no definite conclusions regarding the integrated effects of these large-scale processes may be drawn. A crustal layer with a U^{238}/Pb^{204} ratio of 10·04 (as calculated for today) may have formed in a very short time at an early stage in the history of the earth and have only slightly, but continuously, modified its composition through extensive mixing of a small amount of mantle material during intracrustal differentiation since then. In contrast, the crust may have developed at nearly constant rate over 4·5 B yr, concurrent with the expansion of the continents.

Of the two alternatives proposed by Patterson *et al.* (1955) to explain the radiogenic lead imbalance observed between granites and basalts, the proposal which considers the two phases to be chemically nonrepresentative of the source material appears the more reasonable. Lead ores would appear to be produced from the source material and simultaneously with the differentiation into basalt and granite. Combining these ideas relative to the crust of the earth is tantamount to equating period of mineralization to period of differentiation to period of orogenesis. It will be interesting to see if other experimental evidence can confirm these hypotheses and bring about a unified picture of the lithosphere based on the various, interesting, large-scale, geologic phenomena observed all over the world.

Acknowledgements—The writer wishes to express his gratitude to Dr. Johannes Geiss for many helpful discussions. The interest and encouragement of Professor H. C. Urey is greatly appreciated. Mr. S. K. Yun has kindly assisted in the

calculations. This study was sponsored by A.E.C. Contract No. AT(11–1)–101 and a National Research Council Grant.

References

Bate G. L. and Kulp J. L. (1955) Isotopic composition of common lead from Southern Africa. *Science* **122**, 970–971.

Besairie H., Eberhardt P., Houtermans F. G., and Signer P. (1956) Mesures d'age de quelques galènes de Madagascar. *C.R.* **242**, 317–319.

Eberhardt P., Geiss J., and Houtermans F. G. (1955a) Isotopenverhältnisse von gewöhnlichem Blei und ihre Deutung. *Z. Physik.* **141**, 91–102.

Eberhardt P., Geiss J., and Houtermans F. G. (1955b) Uber Blei und Schwefelisotopenverhältnisse in Bleiglanzen. *Helv. Phys. Acta* **28**, 339–340.

Faul H. (editor) *Nuclear Geology* (1954) New York, John Wiley and Sons, 414 pp.

Holmes A. (1956) How old is the earth? *Trans. Edinb. Geol. Soc.* **16**, 313–333.

Houtermans F. G. (1947) Das Alter des Urans. *Z. Naturf.* **2a**, 322–328.

McCrady E. (1952) The use of lead isotope ratios in estimating the age of the earth. *Trans. Amer. Geophys. Union* **33**, 156–170.

Patterson C. (1953) Nuclear Processes in Geologic Settings, Conference at Williams Bay, Wisconsin.

Patterson C. C. (1955) The Pb^{207}/Pb^{206} ages of some stone meteorites. *Geochim. et Cosmochim. Acta* **7**, 151–153.

Patterson C. (1956) Age of meteorites and the earth. *Geochim. et Cosmochim. Acta* **10**, 230–237.

Patterson C., Brown H., Tilton G., and Inghram M. (1953) Concentration of uranium and lead and the isotopic composition of lead in meteoritic material. *Phys. Rev.* **92**, 1234–1235.

Patterson C. C., Goldberg E. D., and Inghram M. G. (1953) Isotopic compositions of quaternary leads from the Pacific Ocean. *Bull. Geol. Soc. Amer.* **64**, 1387–1388.

Patterson C., Tilton G., and Inghram M. (1955) Age of the earth. *Science* **121**, 69–75.

Russell R. D. and Allan D. W. (1955) The age of the earth from lead isotope abundances. *Mon. Not. R. Astr. Soc., Geophys. Suppl.* **7**, 80–101.

Tilton G. R., Patterson C., Brown H., Inghram M., Hayden R., Hess R., and Larsen jr. E. (1955) Isotopic composition and distribution of lead, uranium, and thorium in a Pre-Cambrian granite. *Bull. Geol. Soc. Amer.* **66**, 1131–1148.

Wilson J. T. (1952) Orogenesis as the fundamental geological process. *Trans. Amer. Geophys. Union* **33**, 444–449.

Geochimica et Cosmochimica Acta, 1957, Vol. 12, pp. 238 to 252. Pergamon Press Ltd., London

Differentiation in the iron-nickel core of a parent meteorite body

John F. Lovering
Department of Geophysics, Australian National University, Canberra, A.C.T. Australia

Abstract—The observed range in nickel content of iron meteorites may be explained by their having differentiated during the crystallization of an originally homogeneous iron melt containing 11% nickel which formed the core of a typical parent meteorite body.

Quantitative estimates of the relative abundances of the various types of iron meteorites which can differentiate from nickel-iron melts of varying compositions are calculated. Again assuming an original melt of 11% nickel, the agreement between the calculated relative abundances and new estimates of the observed relative abundances of iron meteorites is very striking. It is significant that the metal phase of stony-iron meteorites, which may be expected to be a sample of the undifferentiated melt, has a mean nickel content of 11%.

The well-known metallurgical phenomenon of "coring" (under conditions approximating complete mixing in the liquid), which causes segregation of solute in the solid phase during the crystallization of alloys, is probably the best analogy to the differentiation process suggested.

1. Introduction

In this paper it will be assumed that meteorites have originated within either a single parent body or else within several bodies all of similar compositions and with similar evolutionary histories. One of these bodies, or else the single body itself, will be called the typical parent meteorite body. It is also assumed that at some stage the typical parent meteorite body was, broadly speaking, a homogeneous melt. The processes by which such a homogeneous melt became a solid body with a heterogeneous internal structure, from which the various types of meteorites have originated, have usually been described as being one or other of the various kinds of *differentiation* phenomena.

Differentiation (as conceived by magmatic petrologists) or segregation (as conceived by metallurgists) may be defined as including all processes by which a broadly homogeneous melt breaks up into contrasted fractions which ultimately form materials of different compositions. In the evolution of some magmatic rocks, differentiation mechanisms involving immiscible liquid fractions and crystal fractionation (i.e. separation of successive crystal fractionations from residual liquid fractions) have both been proposed, although crystal fractionation mechanisms seem generally to be preferred.

In the course of the cooling and crystallization of the parent meteorite body melt, both immiscible liquid and crystal fractionation differentiation mechanisms have apparently been operating. The cooling of an assumed homogeneous melt with a composition approaching that of a mixture of both stony and iron meteorites would require that at some stage two immiscible melts (one silicate and one metal) would separate. It is usually suggested that the denser metal melt would sink to form a core in the parent body while the essentially metal-free silicate melt would form a mantle around the core.

The subsequent crystallization of this silicate mantle to form the stony meteorites has been described by some authors as showing evidence of differentiation by crystal fractionation. Lord Rayleigh (1944) suggested that the features of certain

stony-iron meteorites (i.e. the pallasites) indicated that the silicate phase had apparently crystallized close to the base of the silicate mantle and then fallen through the associated melt to concentrate at the core boundary where the silicate crystals became enmeshed in the still molten metal phase of the outer core. Such a scheme is a case of crystal fractionation by gravitational sinking of early-formed phases and requires that crystallization began at the base of the silicate mantle while the outer regions (at least) of the metal core were still molten. In this regard most modern theories concerned with the crystallization of the earth require that the base of the earth's mantle began to crystallize before the outer zones of the core (Jacobs, 1956). Confirmatory evidence lies in the observation that the silicate phase of pallasites is apparently significantly older than the metal phase (Thomson and Mayne, 1955), although the age difference between both phases may not be as large as indicated by this work if the lower estimates of the uranium content of the metal phase of meteorites reported by Reed and Turkevich (1955) prove to be generally applicable.

Crystal fractionation by gravitational sinking has also apparently been operating during later stages in the crystallization of the upper mantle of the parent meteorite body. Hess and Henderson (1949) studied the fabric of the Moore County eucrite and found a planar layering of the crystals, concluding that such a fabric is characteristic of crystal accumulates formed by settling of crystals to the floor of a magma chamber.

As far as the iron meteorites are concerned, accurate nickel contents for about 20% of all known finds and falls are now available (Goldberg, Uchiyama, and Brown, 1951; Lovering, Nichiporuk, Chodos, and Brown, 1957), and from these data the following conclusions may be drawn:

(1) Hexahedrites and nickel-poor ataxites have nickel contents between 5·5 and 6·0%.
(2) Coarse octahedrites have nickel contents between 6·0 and 7·2%.
(3) Medium octahedrites (7·2 to 10·5% nickel) and fine octahedrites (7·7 to about 13% nickel) have overlapping compositions.
(4) Most nickel-rich ataxites have nickel contents ranging from approximately 13 to 23%, but there is evidence that occasional nickel-rich ataxites (e.g. the Oktibbeha) have nickel contents as high as 62%.

If iron meteorites have originated in the core of a parent meteorite body, how could a presumably homogeneous iron-nickel melt crystallize to form alloys with the range in nickel content shown by iron meteorites? Is it possible that some form of differentiation could have been operating during the crystallization of the core? The object of the present paper is to demonstrate that some form of differentiation does explain the compositional range in iron meteorites as well as providing a means of calculating the relative abundances of the various iron-nickel alloys within the core of the parent body.

2. Differentiation and the Range in Nickel Content of Iron Meteorites

Given (a) the iron-nickel phase diagram at the pressures estimated to be operating within the core and (*b*) the composition of the original undifferentiated

melt, it would be possible to derive quantitative data for any differentiation process affecting the crystallization of the core.

The iron-nickel phase diagram is known at 1 atm (Fig. 1), but quantitative data are unavailable to predict the effect of pressure on the system using the Clapeyron equation (after DALY, 1943):

$$\frac{dT}{dp} = \frac{0{\cdot}024 \times T_0(V - v)}{L} \tag{1}$$

where T_0 = absolute melting-point at zero pressure,

V = specific volume of liquid,

v = specific volume of solid,

L = latent heat,

$\frac{dT}{dp}$ = rate of change of melting-point per bar.

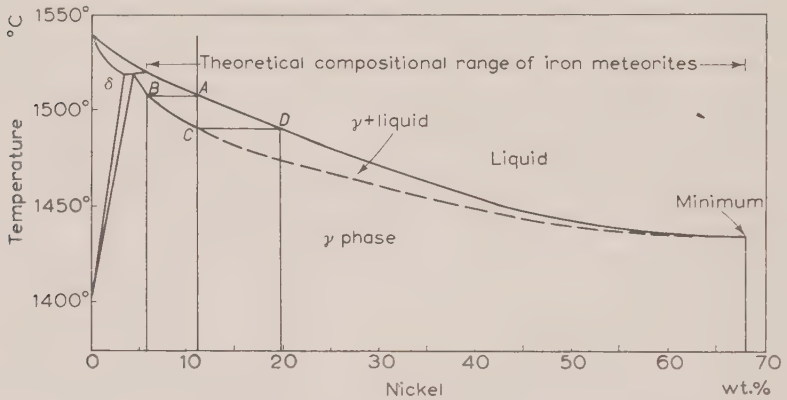

Fig. 1. Portion of phase diagram for iron-nickel alloys at 1 atmosphere (after SACHS, 1948).

The rate of change of the melting-point of pure iron with pressure has been most recently calculated by SIMON (1953) as 0·003°K/atm. However, this refers to the transition from liquid to the body-centred cubic delta phase of pure iron. The portion of the iron-nickel phase of interest to this discussion refers to the transformation from liquid to the solid face-centred cubic gamma phase of nickel-iron alloy. The volume change in this transformation is most likely less than the corresponding volume change for iron and the temperature of transformation is also less, so that dT/dp for iron-nickel alloys is most likely less than that for pure iron, assuming similar values for the latent heat in both cases.

Qualitatively it would seem likely that increased pressure moves the iron-nickel phase diagram up the temperature axis, but quantitative predictions are further complicated by changing nickel contents and changing pressures within the core of the parent body. In the light of these complications, the quantitative discussion of the differentiation process will be based on the iron-nickel phase diagram at 1 atm (Fig. 1). It is not expected that any serious error will be introduced by this approximation.

With regard to the problem of the nickel composition of the original undifferentiated melt, it would appear from the above discussion that the metal phase of stony-iron meteorites has been trapped by the silicate fragments and so would not be able to take part in the differentiation process within the core. Accordingly, the metal phase of the stony-iron meteorites (approximately 11% nickel—Lovering, Nichiporuk, Chodos, and Brown, 1957) is taken as a representative sample of the original metal melt of the core before differentiation.

Now, assuming the iron-nickel phase diagram to be as shown in Fig. 1, and also a melt of 11% nickel, the first solid γ-phase to crystallize out at point A will have a nickel content of 5·5% (B).

With equilibrium conditions of crystallization, the crystallized solid phase gradually increases in quantity and also in nickel content, while the melt decreases in volume but rapidly increases in nickel content. At point C the last drop of liquid (D) of composition approximately 20% nickel crystallizes to form the completely solidified phase with homogeneous nickel content equal to that of the original melt (i.e. 11% nickel).

However, for the purpose of calculation, it is possible to describe a cooling environment in which nonequilibrium conditions of crystallization operate such that as the first solid phase crystallizes at B with a nickel content of 5·5% it is immediately withdrawn from the system and rendered incapable of further reacting with the melt which remains. In this case a small quantity of solid phase (composition approximately 5·5% nickel) is removed and a melt with slightly greater than the original 11% nickel remains. The nonequilibrium crystallization process could then continue so that as successive crystals form, they are removed from the melt by a differentiation process, some possible mechanisms for which will be discussed later.

This differentiation process could continue in this manner until the minimum on the solidus-liquidus curve is reached, when the last drop of liquid is consumed and crystallizes as solid phase with 68% nickel. The nickel content of the crystallized phase removed during the differentiation process will vary from 5·5% to approximately 68%. It is significant that the observed range in nickel content of iron meteorites is from 5·5 to approximately 62% (see above).

3. Differentiation and the Relative Abundances of Iron Meteorites

Calculated abundances

Assuming that the differentiation process as described above operates during the crystallization of the metal core of a meteorite body, it is possible to derive from Fig. 1 a relationship between the volume per cent of the original melt crystallized and the nickel content of the solid phase crystallized at any stage in the crystallization process. That is to say, given an originally homogeneous melt of certain nickel composition, it is possible to calculate the relative volume frequency abundances of iron meteorites with certain ranges of nickel content and then to compare these calculated abundances with observed abundances.

For the purposes of making these calculations from Fig. 1, a step-by-step procedure is used in which it is assumed that the total amount of solid phase which

crystallizes while the nickel content of the melt has increased by a fixed, small but finite amount, is then removed. The smaller the increment chosen, the closer the results will be to the ideal differentiation process in which there is a continuous removal of solid phase as it forms. Calculations have been made assuming steps involving removal of all solid phase crystallizing within both 2% and 5% increments in the nickel content of the melt. Essentially no change in the final analysis results in considering 2% increments rather than 5% increments. To simplify presentation here, the following discussion refers to 5% increments.

The weight per cent (d_n) of melt which crystallizes during the progress of any particular step, n, may be calculated as follows:

For each step, n, it may be read off from Fig. 1 that if a_n is the initial nickel content (per cent) of the melt before crystallization begins, then b_n is the final nickel content (per cent) of the melt after the removal of solid phase crystallized during step n, so that $a_n = b_{n-1}$.

Also that if

f_n is the nickel content (per cent) of the solid phase crystallizing at the beginning of step n, and if

g_n is the nickel content (per cent) of the solid phase crystallizing at the end step n, then

c_n, the mean nickel content (per cent) of the solid phase crystallized during step n is given by

$$c_n = \tfrac{1}{2}(f_n + g_n) \tag{2}$$

Now, 100 mass units of melt at the beginning of step n contain a_n mass units of nickel. If a certain mass d_n of that melt crystallizes during step n with mean nickel content c_n per cent, then the weight of nickel in the crystallized material is $c_n d_n/100$ mass units. The amount of melt remaining at the end of step n is $(100 - d_n)$ mass units with nickel content b_n per cent, so that the weight of nickel in this remaining melt is $(100 - d_n)b_n/100$ mass units.

It follows that

$$a_n = c_n d_n/100 + (100 - d_n)b_n/100$$

from which,

$$d_n = \frac{100(b_n - a_n)}{(b_n - c_n)} \tag{3}$$

Table 1 lists the successive d_n values given for 5% increment steps starting with a melt of 11% nickel and deriving the various a_n, b_n, c_n, values from Fig. 1.

From these data, and assuming essentially constant densities for iron-nickel alloys with nickel contents ranging from 5·5 to 62%, the volume per cent of the original melt which has been crystallized at the end of successive steps may be calculated in the following way:

At the beginning of step 1 there are 100 volumes of melt from which a certain volume will have crystallized by the end of step 1. The volume per cent of the original melt crystallized during step 1 (w_1) will be given by the value d_1 in Table 1. The volume of melt remaining at the end of step 1 is therefore $(100 - d_1)$ volumes.

Table 1. The volume per cent (w_n) of the original melt (11% nickel) crystallized during any step n, assuming 5% nickel increments (see text).

n	a_n	b_n	f_n	g_n	e_n	d_n	w_n
1	11	16	5·50	8.25	6·9	54·9	54·9
2	16	21	8·25	12.25	10.25	46·5	75·8
3	21	26	12·25	17·00	14·6	43·8	86·4
4	26	31	17·0	23·25	20·1	46·0	92·65
5	31	36	23·25	29·25	26·25	51·3	96·4
6	36	41	29·25	36·0	32·6	59·5	98·55
7	41	46	36·0	42·0	39·0	71·4	99·6
8	46	51	42·0	47·5	44·8	82·0	99.9
9	51	56	47·5	53·5	50·5	91·0	99·99
10	56	61	53·5	59	56	100	100

The percentage of this melt which crystallizes during step 2 is given by the value d_2, so that the volume crystallizing is given by $(100 - d_1)d_2/100$ and the percentage volume (w_2) of the original melt which has crystallized at the end of step 2 is given by $w_1 + (100 - d_1)d_2/100$.

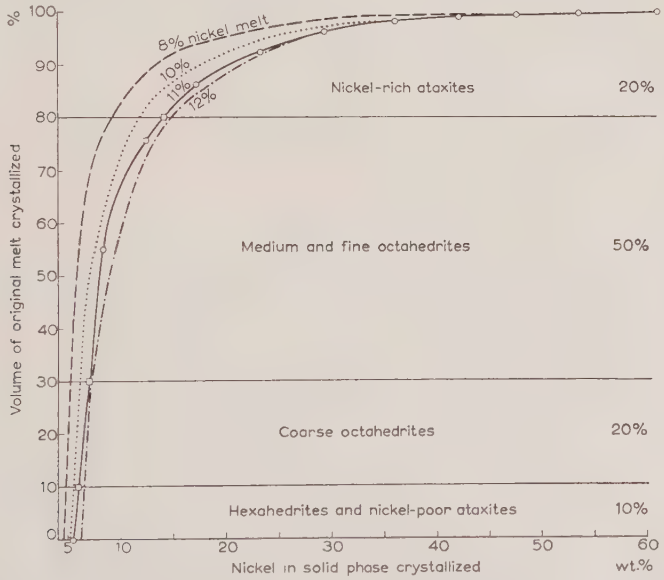

Fig. 2. Change in nickel composition of crystallized material with increasing solidification of a differentiating iron-nickel melt.

The general equation, giving the volume per cent (w_n) of the original melt which has crystallized at the end of a particular step n, is as follows:

$$w_n = w_{n-1} + (100 - w_{n-1})d_n/100 \qquad (4)$$

Fig. 2 illustrates graphically the change in composition of crystallized material with increasing solidification of differentiating iron-nickel melts with original

nickel contents of 8, 10, 11, and 12%. The data for 8, 10, and 12% nickel melts were calculated on 2% increments, while the 11% nickel melt was calculated using both 2 and 5% increments, when it was shown that the curves for both increments were essentially coincident. The 11% nickel melt curve shown in Fig. 2 is actually based on the 5% increments calculated in Table 1 and was chosen as such to reduce complication of the graph.

From Fig. 2 the following points may be made:

(i) that within certain limits the size of the increment used in calculating the quantitative progress of differentiation has little effect on the final analysis.

(ii) that a relatively small change in the nickel content of the original melt has a marked effect on the amount of material crystallizing within given ranges of nickel content.

It has been shown above that some ranges may be given for the nickel contents of the various structure types of iron meteorites. For example, hexahedrites and nickel-poor ataxites range from 5·5 to 6·0% nickel, coarse octahedrites range from 6·0 to 7·2% nickel, while nickel-rich ataxites have nickel contents greater than 13%. From 7·7 to 13% nickel an iron meteorite may be either a medium or a fine octahedrite, so that these structure types must be considered together.

Using these ranges in nickel content, the volume per cent of an original mass which crystallized to form alloys with nickel contents corresponding to the compositional ranges of the various iron meteorites can be read off Fig. 2.

Then assuming that these volume per cent values may be taken as a theoretical measure of the volume frequency of abundance of the various iron meteorites, a comparison can be made with the observed volume frequency of abundance of iron meteorites.

Observed abundances

Watson (1941) has given number frequencies for the abundance of the various iron meteorites (Table 2), and they agree in general with similar calculations made from the Prior and Hey (1953) catalogue and also given in Table 2. Watson's data for the nickel-rich ataxites would seem to be a little high.

A more significant measure of abundances, as far as this work is concerned, would seem to be given by weight frequencies.

The question which immediately presents itself is simply, can the weight-frequency data for the various finds and falls of iron meteorites be used as a measure of their abundance within the core of a parent meteorite body? If the answer to this is to be yes, then the following assumptions must be made:

(1) That the weights of the various structure types of iron meteorites which have fallen on the earth are in direct relationship to their absolute cosmic weight abundances.

(2) That there are no factors operating which would tend to make any particular structure type of iron meteorite more likely to be found or seen to fall than any other structure type.

(3) That the same proportion of material is lost from all iron meteorites during their passage through the earth's atmosphere.

Given these assumptions, and ignoring the minor density variations with

different nickel contents in the iron meteorites, observed weight abundances may be compared directly with the calculated volume abundances arising from the previous discussion. Data for the weights of individual meteorites were obtained from the Prior and Hey (1953) catalogue, and the weight abundances of the various structure types are given in Table 2.

Table 2. Number and weight-frequency abundances of iron meteorites

Structure type	Watson (1941)	This work					
	Number frequency	Number	Number frequency	Weight ($kg \times 10^3$)	Weight frequency	Mean weight (kg)	
Hexahedrites (H)	15%	39	8·5%	2·522	0·7%	64·6	
			14·0%		6·6%		365
Nickel-poor ataxites (D_2)		25	5·5%	20·874	5·9%	837	
Octahedrites: Coarsest (Ogg)	—	25	5·5%	3·360	0·9%	134	
			23·5%		15·4%		504
Coarse (Og)	—	83	18·0%	51·046	14·5%	615	
Medium (Om)	—	171	38·0%	138·04	39·0%	807	
Fine (Of)	—	56	12·5%	40·832	11·5%	730	
			18·0%		19·5%		863
Finest (Off)	—	24	5·5%	28·185	8·0%	1,170	
Total	75%	359	79·5%	261·46	73·9%		
Nickel-rich ataxites (D_1)	10%	29	6·5%	69·197	19·5%	2,400	
Total		452		354·05			

In comparing the number and weight-frequency abundances, it is apparent that not all structure types have constant mean weights. The medium and fine octahedrites are, on the average, one and a half times the weight of the average coarse octahedrite and twice the weight of the average meteorite of the hexahedrite group. On the other hand, the average nickel-rich ataxite is almost three times the weight of the average medium or fine octahedrite. The tendency is for the average size of iron meteorites to increase with a corresponding decrease in the broadness of structure of the meteorite. This trend is probably a reflection of the greater cleavability of iron meteorites with coarse structures during the process of disruption of the meteorite body and in subsequent collisions. It follows, then, that the disruption of the parent meteorite body or bodies formed a larger number of iron meteorites with coarser structures than those with finer structures, with the corollary that the iron meteorites of finer structure are, in general, larger than those of coarser structure. As regards the number frequency of iron meteorites striking the earth, the sample will be biased in one way towards the coarser irons (from the

above reasons) but probably also to a much smaller degree towards the finer irons (because they are generally larger and thus more easily recognized). On the other hand, with regard to weight frequencies, the sample will tend to be biased towards the finer irons since (i) they are more easily recognized because of their larger size, and (ii) the coarser irons, being smaller, lose more mass in proportion to their size during their passage through the atmosphere.

Table 3. Calculated and observed abundances of iron meteorites

Structure type		Observed mean weight frequency abundances	Calculated volume-frequency abundances (from Fig. 2)			
			8% nickel melt	10% nickel melt	11% nickel melt	12% nickel melt
Hexahedrites and nickel-poor ataxites (5·5–6·0% Ni)		10·5%	56%	23%	10%	—
Octahedrites	Coarse (6·0–7·2% Ni)	19·5%	15%	27%	20%	27%
	Medium and fine (7·2–13·0% Ni)	57%	20%	35%	50%	57%
	Total	76·5%	35%	62%	70%	78%
Nickel-rich ataxites (>13·0% Ni)		13%	9%	15%	20%	22%

Thus with number frequencies the abundances are biased towards the coarser irons and with weight frequencies the abundances are biased towards the finer irons. It is suggested that a better approximation to the absolute weight abundances of the various iron meteorites in the core of a typical parent meteorite body is given by the mean of the number and weight frequencies. This mean is called the mean weight abundance, and values are tabulated in Table 3.

Relation of calculated and observed abundances

In Table 3 the observed mean weight-frequency abundances for the various structure types are compared with calculated volume-frequency abundances determined from Fig. 2 for original melts with nickel contents of 8, 10, 11, and 12%. *The calculated abundances derived from the 11% nickel melt are essentially identical with the observed abundances.*

4. Possible Differentiation Mechanisms

By analogy with current theories for the crystallization of the earth's core (Jacobs, 1956), it is likely that the core of the meteorite body began to crystallize at the centre and continued to grow towards the mantle-core boundary, at least in the early stages of solidification. Given these conditions, what kind of mechanism has operated to produce the differentiation process required by the above discussion?

Metallurgists have long recognized that various mechanisms for segregation (i.e. differentiation) operate during the crystallization of cast alloys (Brick, 1945). Gravity segregation (i.e. gravitational crystal settling) by the rising of light, or the falling of heavy, early formed high-temperature alloy crystals has been observed to operate in the crystallization of certain alloys. However, a more common form of segregation, known as *coring*, is frequently found within individual crystals or dendrites, which show a difference in composition between the centre of a crystal or dendrite and its periphery.

Gravity segregation

If the core crystallized from the centre outwards, then segregation by the gravitational settling of the heavy, early formed, low-nickel-content alloy crystals would not appear to be likely a mechanism for the proposed differentiation. However, if crystallization did commence at some point within the core such that gravity settling was possible, then gravity segregation must be considered as a possible mechanism.

Segregation by coring

For coring to be applicable as a mechanism for the proposed differentiation, then solidification must have proceeded from the centre in such a way as to approximate the crystallization of a single crystal situated at the centre of the core of the meteorite body. This may mean that growth actually began and continued from a single nucleus to form an immense single crystal or else that a compact core was formed at an early stage in the solidification. In either case it is significant that Perry (1944) has previously observed that iron meteorites are apparently fragments of single crystals.

The phenomenon of coring is generally recognized as being a result of the redistribution of solute which occurs as a crystal solidifies from a melt of impure metal or alloy. For the case in which a single-phase solid is formed, the equilibrium concentration of solute in the solid at the interface between solid and liquid is different from the equilibrium concentration of solute in the liquid adjacent to it. The ratio of the former to the latter is k, the distribution coefficient, the magnitude of which may be determined from the phase diagram for the particular alloy to be studied. Tiller, Jackson, Rutter, and Chalmers (1953) have studied the redistribution of solute atoms during the normal freezing of alloys, and most of the following discussion is based on their work.

It is assumed that:

1. Diffusion in the solid is negligible.
2. The distribution coefficient, k, is constant.

The validity of the assumption that diffusion in the solid is negligible even in the times involved in the crystallization of the core of the parent meteorite body (i.e. probably of the order of 10^9 years) follows if one considers the case of the non-steady-state diffusion of nickel through a semi-infinite medium of γ-phase iron-nickel alloy. Under these conditions any point in the medium reaches a nickel concentration midway between the initial and ultimate concentrations when

$$t \simeq \frac{x^2}{D} \tag{5}$$

where t = time elapsed,
x = distance over which diffusion has taken place,
D = diffusion coefficient in solid.

Thus the distance x, away from any point in the solid γ-phase iron-nickel alloy to which appreciable diffusion of nickel can take place at a temperature about 1000°C and in time $t = 10^9$ years is given by

$$x \simeq \sqrt{tD} \tag{6}$$

where the diffusion coefficient of nickel in γ-phase iron-nickel alloy is of the order of 10^{-12} cm^2/sec (UHLIG, 1954). From equation (6) it can be calculated that appreciable diffusion of nickel can only take place within a distance of about 1 m in the solid phase forming the crystallized portion of the core of the meteorite body. If the radius of the whole core is of the order of 10^6 m (DALY, 1943), then such diffusion must play a negligible part in ironing out compositional differences within the solid core.

Since the solidus and liquidus lines on the iron-nickel phase diagram are slightly curved (Fig. 1), then assumption (2) is not strictly valid, as k will vary. However, an average value for k can be calculated for the concentration range considered. Attention will be directed to the case where $k < 1$ (i.e. as in the iron-nickel phase diagram). This is the case where the solubility of the solute (i.e. nickel) in the solid is less than in the liquid, which corresponds to "rejection" of solute atoms by the solid as it forms, and therefore to a progressively increasing concentration of solute in the remaining liquid.

To complete the discussion, the following alternative assumptions will be made:

(3a) Convection in the liquid is negligible, while diffusion in the liquid is finite and restricted,

or,

(3b) Mixing of the liquid is always complete because convection and/or diffusion in the liquid is complete.

It should be noted that assumption (3a) approaches the condition in which both convection and diffusion in the liquid are negligible (i.e. the extreme case to that of 3b). However, under these conditions the actual volume of alloy which crystallizes with a composition either greater than or less than that of the original melt is reduced to zero, and thus no coring is apparent. Assumption (3a) approaches this condition as the value of D (the diffusion coefficient in the liquid) reduces to zero. In the following discussion it will be shown how the choice of either assumptions, (3a) or (3b), has a marked effect on the shape of the curve describing the change in composition of the solute with distance in the solid (i.e. the fraction solidified).

Tiller *et al.* (1953) have shown that, in the freezing of alloys, the effects of convection are reduced to a minimum in situations where growth of the solid is vertical and also where cooling conditions are such that low-temperature gradients are operating. It is not unlikely that both these conditions can apply to the case of crystallization of the core of the meteorite body, so that convection may well play a negligible part in keeping the liquid mixed. On the other hand most current theories concerned with the origin of the earth's magnetic field require certain convective-like motions in the earth's liquid outer core.

The effectiveness of diffusion in the liquid metal is open to some discussion. Tiller *et al.* (1943) have stated that the rate of diffusion of solute in liquid metals is not large enough for even approximate levelling of concentration differences of solute in liquid, at least under ordinary conditions of alloy freezing. However, times of the order of 10^9 years are involved in the freezing of the core of the meteorite body. Assuming a diffusion coefficient of about 10 cms^2/sec for nickel in liquid iron-nickel (Tiller *et al.*, 1953), then from equation (6) it may be calculated that appreciable diffusion of nickel within the liquid may take place over distances of about 20 km in the time available. This is a considerable distance in terms of the size of the core of the meteorite body, so that at least an approach to complete diffusion in the liquid is possible. However, the solute-in-solid distributions arising from both cases (3a) and (3b) will now be discussed.

For the case of assumption (3a), the conditions are such that variations in the solute concentration of the liquid are preserved, since solute diffusion in the liquid is not complete and since convection is negligible. Let the solute concentration in the liquid be C_0 (i.e. 11% nickel in this case); then the initial layer of the solid to freeze will have a solute concentration of kC_0. From the iron-nickel-phase diagram (Fig. 1), $k \simeq \frac{1}{2}$, so that the initial solid to crystallize contains about 5·5% nickel. As the crystal grows, the liquid concentration will rise because of the solute rejected from the interface; this will cause the solid concentration to rise also. This increase of concentration will continue until a steady-state condition is attained. At this point the solid concentration adjacent to the interface will have reached a steady value approaching C_0 (i.e. 11% nickel) and the distribution of solute in the liquid near the interface will be constant also and approaching C_0/k (i.e. 22% nickel).

The form of the curve describing the distribution of solute in solid up to the steady-state condition is given by:

$$C_s = C_0 \left\{ (1 - k) \left[1 - \exp\left(-k \frac{R}{D} x \right) \right] + k \right\} \tag{7}$$

where C_s = concentration of solute in solid,
C_0 = initial solute concentration of melt,
k = distribution coefficient,
R = rate of freezing as measured by the advance of the solid-liquid interface in cm/sec.
D = diffusion coefficient of solute in liquid in cm^2/sec,
x = distance measured from the beginning of the crystal.

For complete coverage of the solute distribution in the solid, the last part of the specimen to crystallize must also be considered. The analysis of this region is complicated by the fact that a finite liquid region, in which the concentration changes at all points, must be considered. Thus the quantitative distribution of solute in this region is complicated but the qualitative distribution has been

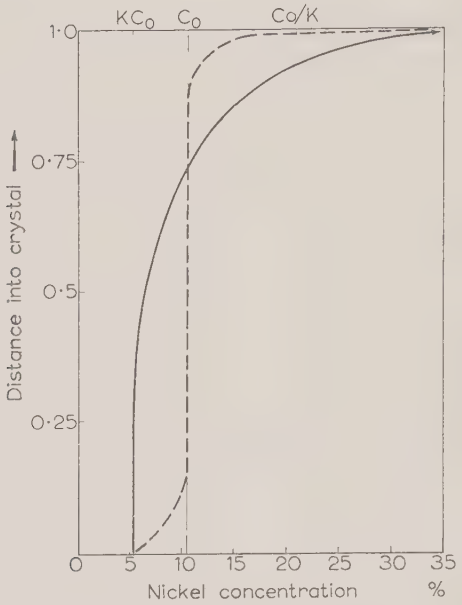

Fig. 3. Coring developed in a single crystal solidifying from an iron melt containing 11% nickel, as shown by the solute (i.e. nickel) distribution as a function of distance into the crystal in the direction of crystal growth.
Full curve: assumes complete mixing in the liquid,
Broken curve: assumes restricted diffusion and negligible convection in the liquid.

derived. The approximate form of the solute (i.e. nickel) distribution in the entirely solid specimen formed by freezing an iron melt containing 11% nickel is given by the broken line in Fig. 3.

Now, for the case given by assumption (3b), the conditions are such that solute concentration variations in the liquid are not preserved since diffusion of solute in the liquid is assumed to be complete or else convection is operating. Under these conditions it can be shown (TILLER *et al.*, 1953) that the concentration of solute in the solid (C_s) as a function of g, the fraction solidified, follows the relation:

$$C_s = kC_0(1 - g)^{k-1} \tag{8}$$

where C_0 = initial concentration of solute in the melt,
k = distribution coefficient.

The general form of the curve describing the distribution of solute (i.e. nickel) in the solid specimen formed by freezing an iron melt containing 11% nickel (for which $k \simeq \frac{1}{2}$) is shown as the full-line curve in Fig. 3.

This curve approximates the previously derived curve (Fig. 2) describing the

distribution of nickel in the differentiated core of the meteorite body, while the broken curve (based on assumption 3a) is significantly different. It is thus suggested that the most satisfactory mechanism for a differentiation process operating during the formation of iron meteorites in the crystallizing core of the meteorite body involves some form of segregation by a "coring" process involving essentially complete mixing of nickel in the liquid but no diffusion in the solid.

5. Summary

Assuming that the core of a typical parent meteorite body was an iron-nickel melt with 11% nickel, then a differentiation process by which solid phase is continuously removed from the system can explain the formation of alloys with nickel contents from 5·5 to about 68%. Such alloys are the parents of the iron meteorites (5·5 to about 62% nickel).

A quantitative elaboration of this differentiation process also explains the observed relative abundances of the various types of iron meteorites in terms of the total volume of alloy which crystallizes with nickel contents equal to those of the various types of iron meteorties as a result of this differentiation.

It is suggested that the metal phase trapped with silicate phase in the zone of transition from mantle to core (from which the stony-iron meteorites have originated) did not enter into the differentiation process and so represents the composition of the molten core before solidification and differentiation. It is significant that the mean nickel content of the metal phase of the stony-iron meteorites is 11% and agrees with the composition previously assumed for the original melt before differentiation.

The mechanism for the differentiation is suggested to be similar to that which is generally described by metallurgists as being the cause of "coring" in solidifying alloys. That is that such a differentiation or coring follows on the solidification of a single crystal if mixing in the liquid is complete at all times, but that diffusion in the solid phase is negligible.

Acknowledgements—Helpful discussions with Harrison Brown and L. T. Silver (California Institute of Technology), H. H. Uhlig (Massachusetts Institute of Technology), and J. C. Jaeger and M. S. Paterson (Australian National University) are gratefully acknowledged.

References

Brick R. M. (1945) Fundamental principles involved in segregation in alloy castings. *Trans. Amer. Inst. Min. Met. Eng.* **161,** 65–74.

Daly R. A. (1943) Meteorites and an Earth-model. *Bull. Geol. Soc. Amer.* **54,** 401–455.

Goldberg E., Uchiyama A., and Brown H. (1951) The distribution of nickel, cobalt, gallium, palladium, and gold in iron meteorites. *Geochim. et Cosmochim. Acta* **2,** 1–25.

Hess H. H. and Henderson E. P. (1949) The Moore Co. Meteorite: A further study with comment on its primordial environment. *Amer. Miner.* **34,** 494–507.

Jacobs J. A. (1956) The Earth's interior. *Encyclopaedia of Physics* (*Geophysics I*), Vol. 47. pp. 364–406. Springer-Verlag, Berlin.

Lovering J. F., Nichiporuk W. N., Chodos A. and Brown H. (1957) The distribution of gallium, germanium, cobalt, chromium, and copper in iron and stony-iron meteorites in relation to nickel content and structure. *Geochim. et Cosmochim. Acta* **11,** 263–278.

PERRY S. H. (1944) The metallography of meteoric iron. *U.S. Nat. Mus. Bull.* **184,** 206 pp.
PRIOR G. T. and HEY M. H. (1953) Catalogue of meteorites. British Museum (*Nat. Hist.*), London, 432 pp.
Lord RAYLEIGH (1944) Meteorites and some of the problems which they present. *Endeavour* **3,** 127–134.
REED G. W. and TURKEVICH A. (1955) Uranium content of two iron meteorites. *Nature* **176,** 794–795.
SACHS G. (1948) In *Metals Handbook* (*Amer. Soc. Metals*), pp. 1211–1212.
SIMON F. E. (1953) The melting point of iron at high pressures. *Nature* (*Lond.*) **172,** 746–747.
THOMSON S. J. and MAYNE K. I. (1955) The ages of three stony meteorites and a granite. *Geochim. et Cosmochim. Acta* **7,** 169–176.
TILLER W. A., JACKSON K. A., RUTTER J. W., and CHALMERS B. (1953) The redistribution of solute atoms during the solidification of metals. *Acta Met.* **1,** 428–437.
WATSON F. G. (1941) *Between the Planets,* Blakiston, Philadelphia, 222 pp.

Geochimica et Cosmochimica Acta, 1957, Vol. 12, pp. 253 to 261. Pergamon Press Ltd., London

Pressures and temperatures within a typical parent meteorite body

John F. Lovering
Department of Geophysics, The Australian National University, Canberra, A.C.T. Australia.

Abstract—Revised estimates have been made of the metal/silicate and metal/sulphide fractionations for nickel in the stony-iron and iron meteorites, respectively. Assuming equilibrium fractionations at temperatures of about 2000°K, pressures of between 10^4 and 10^5 atm must have been operating within the typical parent meteorite body.

Revised estimates of the rate of depression of the $\gamma \rightarrow \alpha$ transformation temperatures of nickel-iron alloys with pressure (Uhlig, 1954) suggest iron meteorites have transformed under pressures of approximately 7×10^4 atm. Furthermore, if about 10^8 years were available from the time of crystallization of octahedrites, through cooling into transformation regions and to the disruption of the body, the core of the parent body must have cooled to a minimum temperature of 700°K.

If graphite was transforming to diamond in the Canyon Diablo octahedrite at 700°K in the core of the parent body, pressures of between 2×10^4 and 3×10^4 atm must have been operating in the core.

This evidence indicates that pressures seem to have a maximum value of between 2×10^4 and 10^5 atm while temperatures of approximately 200°K are assumed to have been operating at the time when the mantle of the parent body was crystallized or crystallizing and when the outer metal core at least was still molten. There are indications that the crystallized core had cooled to about 700°K before it was disrupted. The volume of the typical parent meteorite body is likely to have approached that of the moon.

Introduction

Estimates of the temperatures and pressures operating within a typical parent meteorite body are of importance in determining the size of the body, and lead to a better understanding of its origin. Daly (1943), Brown, and Patterson (1948) and Uhlig (1954) have all suggested interior pressures of the order of 10^5 atm, but it is necessary to re-examine their conclusions in the light of new data concerning the meteorites.

Distribution Coefficients of Elements between Silicate, Metal, and Sulphide Phases in Meteorites

A knowledge of the distribution coefficients of elements between silicate, metal, and sulphide phases of meteorites provides the basis for estimating temperatures and pressures at which the observed distributions would represent equilibrium distributions. In this way estimates of temperatures and pressures within a typical parent meteorite body have been made.

Brown and Patterson (1948) assumed that the mean compositions of the silicate and metal phases of the chondritic stony meteorites available at the time represented equilibrium distributions of the elements at temperatures of the order of those existing within the silicate mantle of the earth (i.e. ~2000–3000°K). They then calculated that pressures of between 10^5–10^6 atm were operating in order that the observed silicate/metal distribution for nickel (Table 1), determined by laboratory experiments at 1 atm, could be raised to that calculated from the abundance of nickel in silicate and metal phases of these meteorites. Similar calculations on the distribution of nickel between the metal and sulphide phases of iron meteorites show a considerable discrepancy with observations made in the laboratory at a temperature of 1200°K and a pressure of 1 atm. The observed discrepancy

Table 1. Observed and calculated distributions of nickel between metal-silicate and metal-sulphide phase of meteorites

	Observed ZUR STRASSEN (1930, 1931)	Meteorites	
		BROWN and PATTERSON[a] (1948)	This work
	C	C	C
$Ni + FeSiO_3$ ⇌ $NiSiO_3 + Fe$	$6{\cdot}5 \times 10^{-3}$ (1750°K) $7{\cdot}25 \times 10^{-3}$ (1840°K)	240×10^{-3}	$21{\cdot}6 \times 10^{-3}$[b]
$Ni + FeS$ ⇌ $NiS + Fe$	1 (1200°K)	~0·02	0·03[b] 0·06[c]

[a] Stony meteorites
[b] Stony-iron meteorites.
[c] Iron meteorites.

cannot be explained simply by calling upon an increase in temperature, and pressures of the order of 10^5 atm must be assumed. However, there is ample evidence that the chondritic stony meteorites are not primary crystallization products from a basic magma, but rather that they are secondary accumulations of pre-existing fragments of silicate, metal, and sulphide phases from other primary meteorites (i.e. nonpolymict brecciated achondrites, stony-iron and iron meteorites). As such, there is little likelihood that the distributions of elements between these phases in chondrites represent equilibrium distributions.

If the current theory for the origin of the pallasites is correct, then these meteorites formed in the transition zone between the silicate mantle and the metal core of the typical parent meteorite body. Sulphide phase would also have been prominent in this region. The olivine appears to have crystallized at the base of the silicate mantle and become enmeshed in the molten metal (with minor molten sulphide) just within the outer boundary of the core. After some $3{\cdot}7 \times 10^9$ years had passed (calculated from the data on the relative ages of the metal and silicate phases of the Brenham pallasite, reported by THOMSON and MAYNE, 1955),* first the metal phase, and then the troilite and other minor phases, crystallized. Considering the very long time involved during which the three phases were in an essentially closed system at elevated temperatures, it is reasonable to assume that the observed abundances of the elements in the silicate, metal, and sulphide phases represented equilibrium distributions. Temperatures of the order of 2000°K may be assumed to have been operating at the time when solid silicate was in equilibrium

* Recently REED and TURKEVICH (1955) have reported that previous estimates of the uranium content of certain iron meteorites were too high. If their estimates also apply to the metal phase of stony-iron meteorites, then the age of the metal phase will be greater than reported in this discussion and so approach more closely the age of the silicate phase.

with molten iron-nickel metal in the region of the formation of the stony-iron meteorites.

The effect of the presence of:

(1) sulphide, on the distribution between silicate and metal phases, and
(2) silicate phase, on the distribution of elements between metal and sulphide phases

must be considered.

With regard to (1), Zur Strassen (1931) found that sulphur slightly displaces the equilibrium, but Brown and Patterson (1948) found that the average sulphur content of stony meteorites (1·79% by weight) is too small to produce any appreciable effect upon the equilibrium. As the average sulphur content of the stony-iron meteorites is, at the most, similar to that of the average stony meteorite (Daly, 1943), it would appear that the observed troilite content of the pallasites would have little effect on distributions of elements between the metal and silicate phases.

No previous estimate has been made of the effect of the presence of silicate phase on the distribution of elements between the metal and sulphide phases of stony-iron meteorites. The amount of silicate phase present in the system is very large compared to that of the sulphide phase, so that the silicate phase can be expected to have a considerable effect on the metal/sulphide distribution. Thus the calculated distributions for the metal/sulphide phases in stony-iron meteorites may be considered to be minimum values only.

Let us now consider the new data available on the distribution of elements between the silicate-metal and metal-sulphide phases of stony-iron meteorites, using the methods of Brown and Patterson (1948).

Silicate-metal phase fractionation

The reaction

$$\mathrm{Ni} + \mathrm{FeSiO_3} \rightleftharpoons \mathrm{Fe} + \mathrm{NiSiO_3}$$

has been studied by Zur Strassen (1930), who determined the mass-action constant, C, at various temperatures (Table 1).

$$C = \frac{(\mathrm{Fe})_m(\mathrm{Ni})_{si}}{(\mathrm{Ni})_m(\mathrm{Fe})_{si}}$$

The distribution of nickel and certain trace elements in the metal phase of the pallasites has been determined by Lovering *et al.* (1956), but few data have previously been available concerning the distribution of trace-elements in the olivine from pallasites. Samples of olivine from the Admire, Albin, Brenham, and Springwater pallasites were analysed, using a spectrographic method devised by A. A. Chodos of the Division of Geological Sciences in the California Institute of Technology. The results (Table 2) indicate the remarkable constancy of composition amongst pallasitic olivines, a fact which Edwards (1955) has also observed in conjunction with his study of the distribution of sodium and potassium in pallasitic olivines.

Table 2. Trace-element distribution in olivine from pallasites *
(p.p.m.)

	Ba	Co	Cr	Cu	Ga	Ge	Mn	Ni	Sn	Ti	V	Zr
Admire	<1	15	250	~1	<2	<20	2000	150	<10	20	15	<4
Albin	2	15	150	2	<2	<20	2000	150	~10	60	15	~10
Brenham	<1	80	100	5	<2	<20	1500	350	<10	10	17	<4
Springwater	<1	30	100	8	<2	<20	2000	350	<10	10	10	<4
Mean	<1	35	150	4	<2	<20	1900	250	<10	25	15	<4

* Mean of two analyses for each olivine.
The following elements occur in concentrations less than the sensitivities reported in Table 3: Ag, As, Au, Be, Bi, Cd, In, La, Mo, Nb, Pb, Pt, Sb, Sr, Ta, Th, Tl, U, W, Y, Yb, Zn.

Table 3. Approximate sensitivities of elements in the spectrographic analytic techniques described

Element	Sensitivity (p.p.m.)	Element	Sensitivity (p.p.m.)	Element	Sensitivity (p.p.m.)
Ag	0·5	La	100	Ta	200
As	200	Li	30	Th	200
Au	20	Mo	2	Ti	1
Be	0·8	Nb	20	Tl	50
Bi	10	Pb	10	U	500
Ca	1	Pt	50	W	100
Cd	20	Sb	200	Y	10
Ga	1	Sc	5	Yb	1
In	10	Sr	1	Zn	100
				Zr	2

The mean nickel content of the metal phase of pallasites is 11%, of the olivine phase it is 0·025%, from which $C = 21{\cdot}6 \times 10^{-3}$.

This calculated value of C is about three times the highest observed value of C, which was measured by ZUR STRASSEN at 1840°K. Then, assuming equilibrium temperature around 2000°K (see above), pressure must be considered to be the main factor operating to increase the observed value of C to the value calculated for stony-iron meteorites.

The change in free-energy with increasing pressure at constant temperature is given by:

$$\Delta F = RT \ln \left(\frac{K_{\text{obs}}}{K_{p=0}} \right)$$

where K_{obs} = observed equilibrium constant for stony-iron meteorites,
$K_{p=0}$ = equilibrium constant at zero pressure,
and also where

$$K \approx C.$$

Thus, $\Delta F \approx RT \ln 3$ and for a temperature of 2000°K, this corresponds to a free-energy change of 4·4 kcal/mole.

Now, $$\Delta F = \int \Delta V \, dP$$

and BROWN and PATTERSON (1948) have determined $\Delta V \approx 2$ c.c./mole

so that $$P \approx 9 \times 10^4 \text{ atm.}$$

In general terms, this pressure is about an order of magnitude less than that calculated by BROWN and PATTERSON (1948).

Metal-sulphide phase fractionation

The reaction

$$\text{Ni} + \text{FeS} \rightleftharpoons \text{NiS} + \text{Fe}$$

has been studied by ZUR STRASSEN (1931), and at about 1200°K he found that the constant C, where

$$C = \frac{(\text{Fe})_m(\text{Ni})_s}{(\text{Ni})_m(\text{Fe})_s},$$

has a value very close to unity.

Table 4. Trace-element distributions in troilite from iron and stony-iron meteorites

Meteorite	Type	Nickel content (metal phase)	Co (p.p.m.)	Cr (p.p.m.)	Cu (p.p.m.)	Ge (p.p.m.)	Mn (p.p.m.)	Ni (per cent)	V (p.p.m.)
Rio Loa	Hexahedrite	5·7%	150	>1%	1500	10	400	0·28	320
Henbury	Medium octahedrite	7·6	12	>1%	690	7	590	0·06	130
Toluca	Medium octahedrite	8·3	2800	>1%	730	6	480	0·6	10
Brenham	Pallasite	10·88	130	1400	960	10	320	~1	8
Spring-water	Pallasite	13·16	180	900	500	6	320	0·3	9

Mg ~ 3 p.p.m., Ti ~ 2 p.p.m., Pb ~ 10 p.p.m.
The following elements occur in concentrations less than sensitivities reported in Table 3:
Ag, As, Au, Be, Ca, Cd, Ga, In, La, Li, Mo, Nb, Pt, Sb, Sc, U, Y, Zr.

The distribution of trace-elements in the troilite phase of stony-iron meteorites has not been adequately investigated. For this study, troilite samples were taken from the Brenham and Springwater pallasites and analysed, using a spectrographic method described by BURNHAM (1955) in his study of trace-element distributions in terrestrial sphalerites and chalcopyrites. At the same time, troilite samples from the Rio Loa, Henbury, and Toluca iron meteorites were also analysed (Table 4).

From these data, the value of C for the reaction $\text{Ni} + \text{FeS} \rightleftharpoons \text{NiS} + \text{Fe}$ in pallasites is 0·07. This value is more than three times larger than the value of 0·02

obtained by BROWN and PATTERSON in 1948 (Table 1), who had estimated that a pressure of the order of 10^5 atm is sufficient to decrease ZUR STRASSEN's measured value to the value observed by them in meteorites. On the new determination of the value of C in pallasites, it follows that assuming temperatures of the order of 2000°K. equilibrium was established under pressures less than 10^5 atm and probably of the order of 10^4 atm.

From the mean nickel content of the metal phase (7·2%) and the troilite phase (0·3%) of three iron meteorites analysed (Table 4), a value of 0·06 is calculated for C. This is close to that calculated above for the pallasites, so that the pressures operating were essentially the same.

THE $\gamma \rightarrow \alpha$-PHASE TRANSFORMATION IN IRON METEORITES

UHLIG (1954) has made some interesting calculations as to the pressures which must have been operating in the core of the meteorite body. He found that if 13% nickel-iron alloys had existed in the γ-phase at a temperature of approximately 460°C (i.e. $\Delta T = 200$ centigrade degrees) in the meteorite body, pressures of about $2{\cdot}5 \times 10^5$ atm must have been operating. This calculation was based on an estimated rate of depression of the transformation temperature with pressure of about 0·0008°C/atm. In Table 5 are measured, calculated, and estimated rates of

Table 5. dT/dP for the $\gamma \rightarrow \alpha$ transformation in iron and 10% nickel-iron alloy

Reference	dT/dP ($-$°C/atm)	
	Iron	10% nickel-iron alloy
BIRCH (1940)	0·0088 (measured)	—
VOGEL and HEUMANN (1946)	—	0·006 (estimated)
UHLIG (1954)	0·0081 (calculated)	0·0008 (estimated)

depression of the $\gamma \rightarrow \alpha$-transformation temperatures in iron and 10% nickel-iron alloys. It would appear that the final value of dT/dP chosen by UHLIG is considerably smaller than that estimated by VOGEL and HEUMANN (1946) and also that estimated from the measured and calculated values for iron. It is puzzling that UHLIG (1954) also stated that for iron-nickel alloys the value of dT/dP is expected to be the same order of magnitude as that for iron, since although the volume change for iron-nickel alloys is larger, this effect is offset by a lower transformation temperature, and a higher ΔH value, but then concluded that "it is well within reason, considering all factors, to associate pressures of 10^4 to 10^5 atm with a depression of the Ni-Fe transformation temperatures in the order of two or three hundred degrees."

If it is legitimate to associate a temperature depression of about 300°C with pressures of 10^5 atm, then dT/dP should be about $-0{\cdot}003$°C/atm, a figure more

in keeping with the other estimates given in Table 5. Using this figure for dT/dP, then the pressure required to depress the $\gamma \rightarrow \alpha$ transformation of 13% nickel-iron alloys the required 200°C is about 7×10^4 atm. Such pressures would have been operating in the outer core of the parent meteorite body.

Uhlig (1954) has presented further evidence, based on the time required for the formation of the Widmanstätten pattern, that "if up to 10^9 years were available, equilibrium in octahedrites was established at 300 to 400°C and definitely not below 300°C."

These calculations of minimum temperatures are based directly on estimates of the time available for the Widmanstätten pattern to form. Perhaps a better estimate of the time available can be made in the following way. Crystallization of the meteorite body began about $4{\cdot}55 \times 10^9$ years ago, a figure based on the age of the stony meteorites given by Patterson (1956). The temperature at which crystallization began has been estimated above as being close to 2000°K. Now, the minimum temperature in the core immediately prior to its disruption has been estimated at about 600°K (as reported above by Uhlig, 1954) while the time of this disruption has been suggested as 10^8 years ago by Mayne (1956). Thus some $4{\cdot}45 \times 10^9$ years are required for the core to cool from 2000° to 600°K, a uniform cooling rate of about 3×10^{-7} °K per year. It will now be of interest to calculate the time available for the $\gamma \rightarrow \alpha$ transformation to take place before the core was disrupted. In a work in preparation it will be shown that the $\gamma \rightarrow \alpha$ transformation would begin in the core at about 800°K. If the core cooled to a minimum temperature of 600°K as Uhlig has suggested, then the cooling rate calculated above would indicate that the time available for the $\gamma \rightarrow \alpha$ transformation in the core was of the order of 10^8 years. Then, from the data presented by Uhlig (1954), if only 10^8 years are available for the formation of the Widmanstätten pattern in octahedrites, the minimum temperature to which these octahedrites have cooled must be closer to 700°K.

The Diamond-graphite Phase Diagram

A further estimate of pressures operating within the typical parent meteorite body can be derived from the graphite-diamond phase diagram recently published by Bundy, Hall, Strong, and Wentorff (1955).

Perry (1944) has reported that while graphite is reasonably common in coarse octahedrites and hexahedrites, diamond and graphite together have been reported from one coarse octahedrite (i.e. Canyon Diablo).

When the elemental carbon separated from the cooling metal phase in the core, graphite (the high temperature form of carbon) would most likely form as the first stable phase. As cooling proceeded there would come a time when the temperature had dropped sufficiently for diamond to become the stable phase at the pressures operating within the core and so diamond crystals would form within the graphite. This is apparently what has occurred in the Canyon Diablo meteorite in which small diamond crystals up to 0·9 mm long have been observed embedded in graphite nodules. If the minimum temperature to which the Canyon Diablo meteorite cooled was about 700°K, then this is the temperature at which the graphite → diamond transformation was taking place, indicating that pressures

of between 2×10^4 and 3×10^4 atm must have been operating within the core (see phase diagram in BUNDY *et al.*, 1955). On the other hand if diamond had been the stable phase within the core before disruption, then the graphite found in iron meteorites may have formed by the transformation of the diamond at the low pressures operating after the disruption of the core. Under these circumstances the pressures within the core estimated above would be *minimum* values.

At the relatively low temperatures operating close to the Earth's surface the diamond → graphite transformation is obviously extremely sluggish, since diamonds are known to have remained untransformed in surface rocks for considerable periods of time. However if the previous calculations are correct then the iron meteorites were probably at temperatures close to 700°K when the core was disrupted and at this temperature the transformation would be more rapid. The possibility of a large-scale transformation of diamond to graphite in an iron meteorite after disruption of the core will depend on the length of time at which the meteorite was at an elevated temperature prior to its cooling to sub-zero (centigrade) temperatures. This time is obviously dependent on the rate of heat loss from an iron meteorite which would be expected to be considerable, thus large scale transformation would not be expected. Indeed the occurrence of diamonds as fairly well-developed crystals within graphite nodules would suggest that such a transformation had not taken place to any extent. However, small-scale transformations (i.e. within single diamond crystals) might well be expected

Table 6

Region within parent meteorite body	Evidence	Temp. (°K)	Pressure (atm)
Mantle-core boundary	Silicate/metal nickel fractionation in stony-iron meteorites	~2000 (at equilibrium)	$\sim 10^4$–10^5
	Metal/sulphide nickel fractionation in stony-iron meteorites	~2000 (at equilibrium)	$\sim 10^4$–10^5
Within metal core	Metal/sulphide nickel fractionation in iron meteorites	~2000	$\sim 10^4$
	Depression of $\gamma \rightarrow \alpha$ transformation temperatures in iron meteorites.	—	$\sim 7 \times 10^4$
	Time to form Widmanstatten pattern	~700 (minimum temp. of core)	—
	Graphite-diamond phase transformation in iron meteorites	~700 (at equilibrium)	$\sim 2 \times 10^4$

after disruption of the core and such a situation has been observed in the Magura coarse octahedrite where graphite nodules containing diamond crystals and also graphite pseudomorphs after diamond crystals have been reported by UREY (1956).

It is concluded, then, that at the time of disruption of the core graphite was in the process of transforming to diamond at temperatures of about 700°K and thus pressures of from 2×10^4 to 3×10^4 atm.

SUMMARY

In Table 6 a summary is made of the estimated temperature and pressures operating within the meteorite body. Pressures between 10^4 and 10^5 atm and temperatures of approximately 2000°K are assumed to have been operating at the time when the mantle of the parent body was crystallized or crystallizing and when the outer metal core at least was still molten. There are indications that the crystallized core had cooled to about 700°K before it was disrupted.

ALLEN and JACOBS (1956) have estimated that the central pressure inside the moon is about 5×10^4 atm, so that the typical parent meteorite body must have had a volume to closer that of the moon than to Mars.

REFERENCES

ALLEN D. W. and JACOBS J. A. (1956) The melting of asteroids and the origin of meteorites. *Geochim et Cosmochim. Acta* **9,** 256.

BIRCH F. (1940) The alpha-gamma transformation of iron at high pressure and the problem of the earth's magnetism. *Amer. J. Sci.* **238,** 192.

BROWN H. and PATTERSON C. (1948) The composition of meteoritic matter—III. Phase equilibria, genetic relationships and planet structure. *J. Geol.* **56,** 85.

BUNDY F. P., HALL H. T., STRONG H. M., and WENTORF R. H. (1955) Man-made diamonds. *Nature* **176,** 51.

BURNHAM W. C. (1955) Ph.D. dissertation. California Institute of Technology, Pasadena (unpublished).

DALY R. A. (1943) Meteorites and an earth-model. *Bull. Geol. Soc. Amer.* **54,** 401.

EDWARDS G. (1955) Sodium and potassium in meteorites. *Geochim. et Cosmochim. Acta* **8,** 285.

LOVERING J. F., NICHIPORUK W., CHODOS A., and BROWN H. (1957) The distribution of gallium, germanium, cobalt, chromium and copper in iron and stony-iron meteorites in relation to nickel content and structure. *Geochim. et Cosmochim. Acta* **11,** 263.

MAYNE K. I. (1956) Terrestrial helium. *Geochim. et Cosmochim. Acta* **9,** 174.

PERRY S. H. (1944) The metallography of meteoric iron. *U. S. Nat. Mus. Bull.* **184,** 206 pp.

REED G. W. and TURKEVICH A. (1955) Uranium content of two iron meteorites. *Nature (Lond.),* **176,** 794.

THOMSON S. J. and MAYNE K. I. (1955) The ages of three stony meteorites and a granite. *Geochim. et Cosmochim. Acta* **7,** 169.

UHLIG H. H. (1954) Contribution of metallurgy to the origin of meteorites. Part I—Structure of metallic meteorites, their composition and the effect of pressure. *Geochim. et Cosmochim. Acta* **6,** 282.

UREY H. C. (1956) Diamonds, meteorites, and the origin of the solar system. *Astrophys. J.* **124,** 623.

VOGEL R. and HEUMANN T. (1946) Über die Bildungsmöglichkeiten der Widmannstättenschen Struktur des meteorischen Eisens unter hohem Druck. *Nach. Akad. Wissen. Göttingen, Math. Phys. Klasse* **2,** 123.

ZUR STRASSEN H. (1930) Das Gleichgewicht Zwischen Eisen, Nickel und ihren Silikaten im Schmelzfluss. *Zeitschr. anorg. Chemie* **191,** 209.

ZUR STRASSEN H. (1931) Die Wirkung von Schwefel aus das schmelzflüssige Gleichgewicht. *Zeitschr. anorg. Chemie* **200,** 46.

Geochimica et Cosmochimica Acta, 1957, Vol. 12, pp. 262 to 270. Pergamon Press Ltd., London

Meteoritic and terrestrial abundance of tin

Hiroshi Onishi* and E. B. Sandell
University of Minnesota, Minneapolis, Minn.

(*Received* 10 *November* 1956)

Abstract—The following averages for tin have been obtained: chondrites 1 p.p.m., metal phase of chondrites 5 p.p.m., iron meteorites roughly 2 p.p.m. (range from <0·5 to ~10 p.p.m.), ultramafic rocks ~0·5 p.p.m., mafic rocks ~1·5 p.p.m., and granitic rocks ~3 p.p.m. Sn. The tin content of the upper lithosphere may be taken as 2 ± 1 p.p.m., granitic and mafic rocks being weighted equally.

Introduction

This note presents abundance data for tin in igneous and sedimentary rocks and in meteorites, based mostly on analyses of composite samples, except for iron meteorites, which were analysed individually.

Because the present values differ considerably from many of the earlier ones, it seems desirable to list for comparison most of the earlier data for meteorites, igneous rocks, and sedimentary rocks (Table 1). Literature values are also available for metamorphic rocks, pegmatite minerals, sulphides, etc., but these are not considered here.

Analytical Method

Tin was determined colorimetrically or photometrically with dithiol (Onishi and Sandell, 1956). Silicate rocks were decomposed with sulphuric-nitric-hydrofluoric acid and tin was separated by distillation with hydrobromic and hydrochloric acids. Since the photometric method has a sensitivity of only 3 p.p.m. Sn with 1 g of sample, the visual comparison method was used for most samples. This method has a sensitivity of 0·5 p.p.m. with a 1-g sample. Samples of 1 g were usually taken. The error is not likely to exceed ±0·5 p.p.m. Sn in the range of a few p.p.m. Sn.

Shales and deep-sea deposits were first treated with sulphuric, nitric, and hydrofluoric acids. The residue from this treatment was fused with sodium hydroxide, the melt was taken up in hydrochloric acid, and the combined solutions were distilled after addition of hydrobromic acid.

Iron meteorites (0·5 g) were dissolved in nitric-sulphuric acid, and the tin distillation was carried out after evaporating the excess acid. The error is not likely to exceed ±1 p.p.m. Sn. Total tin in chondrites was determined by treating the sample with nitric-sulphuric acid, evaporating to strong fumes, bringing the residue into solution with sulphuric-hydrofluoric acid in a platinum dish, and then distilling. Tin was determined in the metal phase of chondrites after magnetic separation. A correction was applied for silicate in the magnetic fraction.

Discussion

Igneous and sedimentary rocks. From the data for tin in igneous rocks (Table 2), the following averages for different rock types are obtained:

	Sn (p.p.m.)
Granitic rocks (80 samples)	3
Basaltic rocks (36)†	~1·5
Ultramafic rocks (13)	~0·5

* Present address, Government Industrial Research Institute, Nagoya, Japan.
† Greenstone and Kearsarge flows of Michigan counted as one sample each.

The granitic average is based on a fair number of samples, and if these are representative of the granitic rocks of the earth, the true average may be expected to lie in the range 2–4 p.p.m. The basaltic and ultramafic averages are more uncertain, partly because of the small number of samples and partly because of the greater effect of the analytical error at the lower tin contents. However, it seems safe to say that, as a general trend, tin in igneous rocks increases with silica. The variability among both granitic and mafic rocks appears to be comparatively great, so that it is not unusual for a diabase to have a higher tin content than a granite.

At present it is uncertain to what extent a possible regional factor in the distribution of tin may affect estimates of its abundance in granitic rocks. Such rocks in areas of tin mineralization may contain appreciable amounts of tin. For example, Westerveld (1936) records 0·09% SnO_2 in a "tin granite." Transitional rocks of this kind, ranging from tin-rich greisen to "normal" granitic rocks of the district, are to be expected from the concentration of tin by pneumatolytic and related processes. Ottemann (Table 1) found 90 and 67 p.p.m. Sn in two granites of the Erzgebirge, a tin province, 50 p.p.m. in a granite from a locality adjacent to the Erzgebirge, and 25 p.p.m. in a granite from the Harz mountains, a non-tin area. Butler (1953) determined tin in five granitic rocks of the Lizard, Cornwall, and found 45, 20, and 15 p.p.m. Sn in three and no detectable tin in two (Table 1). The sample containing 45 p.p.m. Sn is reported to show signs of pneumatolytic alteration. From the quantitative standpoint the increased tin content of igneous rocks in areas of tin deposits may be of much smaller importance than lesser variations on a large regional scale. The limited data on tin in granitic composites (Table 2) show that some variation among similar granitic rocks is to be expected, and the more extensive data of Okada (1955) on individual samples furnish more concrete evidence on this point. However, the values in Table 2 do not indicate that the average tin contents of granitic rocks of Minnesota, central Texas, California, and Japan are greatly different. The variations among the averages are comparable to those found with such elements as beryllium, molybdenum, tungsten, arsenic, and chlorine.

The average tin content of the lithosphere is very likely less than 5 p.p.m. Nockolds and Allen (1953, 1954) found tin to lie below the limit of detectability (5 p.p.m.) in rocks of the calc-alkali and alkali series of wide geographical distribution. A rough value for tin in the upper lithosphere may be obtained by weighting mafic and granitic rocks equally: $1/2(1{\cdot}5 + 3) = 2$ p.p.m. A lithospheric value below 5 p.p.m. is consistent with the few tin determinations that have been made on sedimentary rocks and deep-sea deposits, which represent igneous rocks with additions of tin from hydrothermal solutions and the like (tin in the ocean can be neglected).

In sedimentary rocks, tin is no doubt chiefly found in the shales. Too few shales were analysed in the present work to furnish a reliable average. The weighted average of thirty-six European Paleozoic shales and twenty-four Japanese Paleozoic and Mesozoic shales is 4 p.p.m. (Table 3). It may be noted that Goldschmidt and Peters found 40 p.p.m. Sn in the composite of thirty-six European Paleozoic shales, a value eight times greater than our result on the same sample.

Meteorites. On the basis of the values in Table 4, the tin content of chondrites

Table 1. Literature data on the abundance of tin

	Sn (p.p.m.)	Author
	Meteorites	
Silicate meteorites, average	4	Noddacks (1930)
Troilites, average	1610	Noddacks (1930)
Irons, average	102	Noddacks (1930)
Silicate meteorite, Imilac, Chile	0	Noddacks (1931)
Silicate meteorite, Vigamo, Italy	8	Noddacks (1931)
Silicate meteorite, Tennasilm, Esthonia	2	Noddacks (1931)
Troilite of Toluca iron, Mexico	400	Noddacks (1931)
Troilite of Canyon Diablo iron	>1000	Noddacks (1931)
Troilite, Tennasilm	15	Noddacks (1931)
Iron, Canyon Diablo	50	Noddacks (1931)
Iron, Mukerop, S.W. Africa	120	Noddacks (1931)
Iron, Toluca, Mexico	60	Noddacks (1931)
Troilite of iron, Coahuila, Mexico	10	Goldschmidt and Peters (1933)
Iron (hexahedrite), Coahuila, Mexico	100	Goldschmidt and Peters (1933)
Troilite of iron, Canyon Diablo	20	Goldschmidt and Peters (1933)
Iron (octahedrite), Canyon Diablo	100	Goldschmidt and Peters (1933)
Troilite of iron, Toluca, Mexico	20	Goldschmidt and Peters (1933)
Iron (octahedrite), Toluca, Mexico	50–100	Goldschmidt and Peters (1933)
Troilite of iron, Corrizatillo, Chile	10–20	Goldschmidt and Peters (1933)
Iron (octahedrite), Corrizatillo, Chile	100	Goldschmidt and Peters (1933)
Troilite of iron, Russell Gulch, Colo.	20	Goldschmidt and Peters (1933)
Iron (octahedrite), Russell Gulch, Colo.	50	Goldschmidt and Peters (1933)
Chondrite, Aztec (Holbrook), Ariz.	10	Goldschmidt and Peters (1933)
Silicate phase of Aztec chondrite	.4	Goldschmidt and Peters (1933)
Metal phase of Aztec chondrite	50–100	Goldschmidt and Peters (1933)
Iron, Morradal, Norway	50	Goldschmidt and Peters (1933)
Iron, Krasnojarsk, Siberia	100	Goldschmidt and Peters (1933)
Troilites, average	15	Goldschmidt and Peters (1933)
Irons, average	100	Goldschmidt and Peters (1933)
Chondrites, average	40	Noddacks (1934)
Tektite	2·4	Heide (1936)
	Igneous rocks	
Basalt, Kaiserstuhl; lava, Vesuvius	6, 5	Noddacks (1931)
Granite, southern Norway	1	Noddacks (1931)
14 German granites, average	80	Goldschmidt and Peters (1933)
24 nepheline syenites, average	4–8	Goldschmidt and Peters (1933)
Plateau basalt, Asotin, Wash.	4	Goldschmidt and Peters (1933)
11 German gabbros, average	8	Goldschmidt and Peters (1933)
Dunite, Nordfjord, Norway	- -	Goldschmidt and Peters (1933)
36 Greisen rocks, average	800–8000	Goldschmidt and Peters (1933)
2 granites, Eibenstock and Schellerhau, Erzgebirge;	90, 67;	Ottemann (1940)
1 granite, Epprechtstein, Saxony	50	
1 granite, Brocken, Harz, Mtns.	25	Ottemann (1940)
9 silicic volcanic rocks (perlite, obsidian, felsite), Juniper Ridge, Oregon	0–50, avg. 16	Harrison and Allen (1942)

Table 1—*continued*

	Sn (p.p.m.)	Author
	Igneous rocks (continued)	
4 monzonites; 1 granite; 1 syenite, New Hamp., U.S.	~10, ~10, <10, <10; <10; <10	Billings and Rabbitt (1947)
3 granite gneisses, Västergötland, Sweden; granite, Mount Buklja, Serbia	10, 41, 28;69	Miholić (1949)
Lava, Nyamuragira eruption (1938–40)	80	Verhoogen (1948)
Basalts and dolerites, S. Africa	~200–400	Walker and Poldervaart (1949)
Tertiary lavas (basalts, trachytes, rhyolites), N.E. Ireland	<5	Patterson (1952)
Basalts, dolerites, etc., Scotland	<5	Higazy (1952)
Adamellite; 4 granites; 1 gabbro, Cornwall, Eng.	45; 20, 15, <15, <15; <15	Butler (1953)
Calc-alkali igneous rocks, southern Calif., Lassen Peak, Crater Lake, etc.	<5	Nockolds and Allen (1953)
Alkalic igneous rocks, Scotland, Hawaii, Polynesia, etc.	<5	Nockolds and Allen (1954)
26 potassic lavas, Uganda and Belgian Congo	<5	Higazy (1954)
3 potassic lavas, Uganda and Belgian Congo	5, 10?, 35	Higazy (1954)
67 granitic rocks, Japan	<20	Okada (1955)
13 granitic rocks, Japan	"trace"	Okada (1955)
6 granitic rocks, Japan	20, 20, 46, 46, 200, 440	Okada (1955)
Syenite, monzonite, olivine basalt, Norway	<10 or 15	Butler (1955)
Basalts (tholeiitic), Ireland	<5	Patterson and Swain (1955)
	Sedimentary rocks	
36 European shales (Paleozoic), composite	40	Goldschmidt and Peters (1933)
Bauxites, various localities, avg.	80	Goldschmidt and Peters (1933)
2 limestones, S. Africa and Sweden	0, 10	Higazy (1954)
Limestones, Germany, composites of 93	~3 to 5	Wedepohl (1955)
Bituminous sediments and rocks	<10 to 50	Goldschmidt, Krejci-Graf, and Witte (1948)

is taken to be $1 \pm 0{\cdot}5$ p.p.m. This is much lower than the average (40 p.p.m.) reported by the Noddacks (1934) and also lower than the few values given by Goldschmidt and Peters (1933).

It is of interest to see how the new value for the abundance of tin compares with the abundances of elements adjacent to tin in the periodic table. Fig. 1 shows the meteoritic (or approximate cosmic) atomic abundances of these elements, as far as known at the present time, compared to Si as 10^6. We follow Urey in taking chondrites as probably representing the closest approach to material giving cosmic abundances of nonvolatile elements. The available abundance data are of

Table 2. Tin in igneous rocks

	Sn (p.p.m.)
Granites, composite of 8, U.S.A. and Canada; avg. SiO_2 = 77·0%	2·5
Granites, etc., composite of 9, California; avg. SiO_2 = 74·1%	2
Granitic rocks, composite of 18 Antarctica 3, Rhodesia 1, Canada 4, Newfoundland 1, New Hampshire 1, Rhode Island 1, New York 2, Missouri 2, central Texas 1, California 1, unknown locality 1	4
Granitic rocks, composite of 11, Minnesota Granite porphyry 2, Benton Co. and Sauk Rapids; granite 2, Benton Co.: hornblende granite, Stearns Co.; quartz monzonite 2, Kanabec Co. and near Pierz, Morrison Co.; granodiorite 2, Benton Co.; granite-gneiss 2, Aitkin Co. and Morton	3, 2·5*
Granites, composite of 6, Llano region, Texas	4
Granitic rocks, composite of 12, Japan and China Fukushima Prefecture 2, Gifu Pref. 3, Gumma Pref. 1, Ibaraki Pref. 1, Nagano Pref. 1, Okayama Pref. 1, Yamanashi Pref. 1, Prefecture unknown 1; China 1	3·5
Granite-gneiss, composite of 14, Canada, U.S.A., and elsewhere	2·5
Quartz monzonite, Warman, Minn.	1, 1·5
Granite, Westerly, R.I., standard G-I	2, 2·5
Andesites, composite of 6, Japan Gifu Prefecture 1, Kumamoto Pref. 1, Nagano Pref. 4	1
Basalts and diabases, composite of 11, mostly North America Basalts: Alaska 1, Newfoundland 1, Connecticut 2, Idaho 1, India 1; diabases: New York 1, Virginia 2, Antarctica 2	2
Basalts and diabases, composite of 6, mostly U.S.A. New Jersey 2, Colorado 2, Washington 1, Sicily 1	1·5
Basalt, weighted composite of Greenstone flow, Michigan	1
Basalt, weighted composite of Kearsarge flow, Michigan	1
Basaltic rocks, composite of 8, Keweenawan of Michigan	1.5
Olivine basalt, composite of 7, Oregon	0, 0·5
Diabase, Fairfax Co., Virginia, Standard W-1	2·5, 3
Gabbro, Duluth, Minnesota	2
Ultramafic rocks, composite of 13, U.S.A. and Canada Peridotite 4, dunite 3, bronzitite 1, harzburgite 2, pyroxenite 1, unspecified ultramafic 2	0·5

* Residue from hydrofluoric and sulphuric acid treatment fused with sodium hydroxide.

unequal reliability. The values for Cu,* Ga, Ge,† As, Sn, and Sb were obtained by us by colorimetric analysis of the same group of chondrites, the Si content of which is taken as 18%. Chondritic data are largely lacking for the other elements considered, at least data which can reasonably be relied upon to lie in the range one-half to two times the reported value. For these elements, values have been selected as follows. Zinc in meteorites is taken as 150 p.p.m. by rounding off the Goldschmidt average of 138 p.p.m. Little confidence can be placed in this

* Data of Jean'ne Shreeve, University of Minnesota, 1955.
† Data of H. Onishi (1956).

Table 3. Tin in shales and oceanic red clays

	Sn (p.p.m.)
Shales, composite of 7, North America Alaska 4, Arkansas 1, North Dakota 1, Maine 1	11*
Shales, composite of 24, Japan, Paleozoic and Mesozoic (Minami, 1935)	2·5
Shales, composite of 36, Europe, Paleozoic (Noll, 1934)	5
Red clays, composite of 8, Pacific Ocean (Onishi and Sandell, 1955)	1·5, 1·5†

* Without sodium hydroxide fusion of residue from hydrofluoric-sulphuric acid decomposition only 3 p.p.m. Sn found.

† The same value was found with and without sodium hydroxide fusion.

Table 4. Tin in chondrites

	Sn (p.p.m.)
Composite I (Arriba, Beenham, Cope, Cotesfield, Morland, Plainview, Roy)	1
Composite II (Alamogordo, Estacado, Gladstone, Gruver, Kingfisher, Ladder Creek, Melrose)	1
Estacado	1
Potter	0·5
Metal phase (11%) of Composite I	5
Metal phase (13%) of Composite II	5
Metal phase of Estacado, Haven, and Plainview	6
Nonmagnetic phase of Composites I and II (5.7% FeS)	0·4 ± 0·2

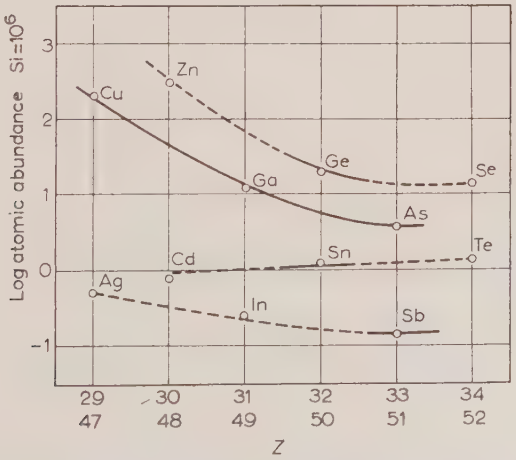

Fig. 1. Abundances of elements 29–34 and 47–52 in meteorites according to data available in 1956. Broken portions of curves represent abundances considered less reliable than others.

value, but the abundance of zinc can hardly be less than 90 p.p.m., the chondritic average for copper. For selenium the meteoritic value of 7 p.p.m. assigned by Goldschmidt (1954) has been accepted as giving a rough approximation; it receives some support from the data of Byers (1938). The abundance of cadmium is very uncertain. The Noddack figure of 1·6 p.p.m. Cd in chondrites is of questionable reliability, and some confirmation is desirable. A very rough estimate can be obtained from the Cd/Zn ratio in the earth's crust. According to Sandell and Goldich (1943), mafic rocks contain about 0·2 p.p.m. Cd and 130 p.p.m. Zn; data for ultramafic rocks, which perhaps would be more pertinent, are lacking. On the reasonable assumption that zinc is not more siderophilic and chalcophilic than cadmium, the weight ratio Cd/Zn in metal and troilite phases should be greater than 0·2/130 or greater than 0·0015. Taking the zinc content of chondrites as 150 p.p.m. (mostly in the nonsilicate phases), we then conclude that at least $150 \times 0{\cdot}0015 = 0{\cdot}25$ p.p.m. Cd is present in chondrites. We will arbitrarily take twice this value (corresponding to an atomic abundance of 0·7) as the best guess that can be made.

On the basis of Goldschmidt's values for silver in iron meteorites and troilite, one calculates an abundance of about 0·75 p.p.m. Ag in chondrites. But silver (A.N. 47) should be less abundant than palladium (A.N. 46) whose meteoritic value (on the 10 iron: 5 troilite: 85 silicate basis) is about 0·5 p.p.m. as calculated

Table 5. Tin in iron meteorites

		Sn (p.p.m.)
Ainsworth, Nebr.	Coarsest octahedrite*	1
Altonah, Duchesne Co., Utah	Fine octahedrite	1
Arispe, Mexico	Coarsest octahedrite	3
Canyon Diablo, Ariz.	Medium octahedrite	7, 10†
Coahuila, Mexico	Hexahedrite	0, 0
Costilla Peak, N. Mex.	Medium octahedrite	0
Coya Norte, Chile	Hexahedrite	0‡
Deport, Texas	Coarse octahedrite	6
Duchesne, Utah		3
Edmonton, Ky.	Finest to fine octahedrite	5
Goose Lake, Calif.	Medium to coarse octahedrite	7
Henbury, Australia	Medium octahedrite	5, 4†
Mount Joy, Pa.	Coarsest octahedrite	1
Perryville, Mo.	Finest octahedrite (?)	0
Sacramento Mountains, N. Mex.	Medium octahedrite	0
Sandia Mountains, N. Mex.	Brecciated hexahedrite	0
Spearman, Texas	Medium octahedrite	1
Wallapai, Ariz.	Fine octahedrite	1·5
Willow Creek, Wyo.	Medium octahedrite	1
		avg. 2·3

* Descriptions from Prior and Hey (1953).
† Photometric.
‡ 2γ Sn found after adding 2γ Sn to the sample and running through the procedure.

from the data of Goldberg *et al.* (1951) for iron meteorites. As a compromise we will take one-half of 0·75 p.p.m. or 0·4 p.p.m. by weight for silver in chondrites. For indium we accept an abundance of 0·2 p.p.m., rounding off the value 0·15 p.p.m. given by Goldschmidt for chondrites. An estimate of the abundance of tellurium will be made by taking the atomic ratio Se/Te as 10 (Te $\sim$ 1 p.p.m.).

The present value of 1 p.p.m. for the abundance of tin places it in consistent relationship with Ga, As, and Sb. The Goldschmidt-Peters value of 20 p.p.m. (atomic abundance = 26, log = 1·4) would place tin in an unlikely position between the Cu—Ga—As and the Zn—Ge—Se series.

The present work has not furnished the tin contents of the silicate and troilite phases. Roughly one-half the tin of chondrites is found in the metal phase. The data of Goldschmidt and Peters indicate that most of the remainder is present in the troilite phase.

The tin content of iron meteorites varies over a wide range (Table 5).* Eleven of the nineteen irons analysed contain 1 p.p.m. or less of tin. The highest content is about 10 p.p.m., and the average is about 2 p.p.m., but this has little significance. No relation between tin and nickel contents is apparent, except that the three hexahedrites (5·5, 5·6, and 6·0% Ni) contain no detectable ($<$1 p.p.m.) tin. Plots of tin against palladium and gold (not reproduced here) show an ill-defined tendency for tin to rise with these elements in iron meteorites, the more satisfactory correlation being shown with gold.

References

Billings M. P. and Rabbitt J. C. (1947) *Bull. Geol. Soc. Amer.* **58,** 573.
Butler J. R. (1953) *Geochim. et Cosmochim. Acta* **4,** 157.
Butler J. R. (1955) *Geochim. et Cosmochim. Acta* **6,** 268.
Byers H. G. (1938) *Ind. Engng. Chem.* News Ed. **16,** 459.
Goldberg E., Uchiyama A., and Brown H. (1951) *Geochim. et Cosmochim. Acta* **2,** 1.
Goldschmidt V. M. (1954) *Geochemistry* p. 533, Oxford.
Goldschmidt V. M., Krejci-Graf K., and Witte H. (1948) *Nachr. Akad. Wiss. Göttingen, Math.-Phys. Klasse No.* 2, 35.
Goldschmidt V. M. and Peters C. (1933) *Nachr. Ges. Wiss. Göttingen Math.-Phys. Klasse*, 278.
Harrison H. C. and Allen J. E. (1942) Oregon Dept. Geol. Mineral Ind. Bull. No. 23.
Heide F. (1936) *Forschungen u. Fortschr.* **12,** 232.
Higazy R. A. (1952) *Trans. Edinb. Geol. Soc.* **15,** 150.
Higazy R. A. (1954) *Bull. Geol. Soc. Amer.* **65,** 39.
Miholić S. (1949) *Bull. Soc. Chim. Belgrade* **14,** 121.
Minami E. (1935) *Nachr. Ges. Wiss. Göttingen, IV,* N.F. **1,** 143.
Nockolds S. R. and Allen R. (1953) *Geochim. et Cosmochim. Acta* **4,** 105, 138.
Nockolds S. R. and Allen R. (1954) *Geochim. et Cosmochim. Acta* **5,** 245.
Noddack I. and Noddack W. (1930) *Naturwiss.* **18,** 757.
Noddack I. and Noddack W. (1931) *Z. physik. Chem.* **A154,** 207.
Noddack I. and Noddack W. (1934) *Svensk Kem. Tidskr.* **46,** 173.
Noll W. (1934) *Chem. Erde* **8,** 537.
Okada S. (1955) *Sci. Repts. Tokyo Kyoiko Daigaku, Sect. C,* **4,** 163.
Onishi H. (1956) *Bull. Chem. Soc. Japan* **29,** 686.
Onishi H. and Sandell E. B. (1955) *Geochim. et Cosmochim. Acta* **8,** 219.
Onishi H. and Sandell E. B. (1956) *Analyt. Chim. Acta* **14,** 153.

* We are indebted to Dr. Harrison Brown and W. Nichiporuk for samples of the irons analysed.

Ottemann J. (1940) *Z. angew. Mineral.* **3,** 142.
Patterson E. M. (1952) *Geochim. et Cosmochim. Acta* **2,** 283.
Patterson E. M. and Swaine D. J. (1955) *Geochim. et Cosmochim. Acta* **8,** 173.
Prior G. T. and Hey M. H. (1953) Catalogue of Meteorites, 2nd ed., British Museum (Natural History), London.
Sandell E. B. and Goldich S. S. (1943) *J. Geol.* **51,** 171, 173.
Verhoogen J. (1948) *Inst. Parcs Nat. Congo Belge.* **1,** 1–186.
Walker F. and Poldervaart A. (1949) *Bull. Geol. Soc. Amer.* **60,** 591.
Wedepohl K. H. (1955) *Nachr. Akak. Wiss. Göttingen, Math.-Phys. Klasse* **5,** 79.
Westerveld J. (1936) *Verhandl. Akad. Wetens. Amsterdam, Sect. Sci.* **39,** 1199.

Geochimica et Cosmochimica Acta, 1957, Vol. 12, pp. 271 to 272. Pergamon Press Ltd., London

GEOCHEMICAL NOTE

Determination of yttrium, lanthanum, cerium, neodymium, and ytterbium in test samples granite G-1 and diabase W-1 by a combined chemical-spectrochemical technique*

(*Received* 17 *January* 1957)

THE use of the granite G-1 and diabase W-1 as interlaboratory standards has been discussed by AHRENS (1955) and others.

The purpose of this investigation originally was to determine the Y content of W-1 spectrochemically following a preliminary chemical concentration of Y and removal of the interfering elements Fe and Mn. The concentration procedure adopted fortunately made it possible to determine La, Ce, Nd, and Yb of G-1 and W-1 in addition to Y.

The chemical concentration of the rare-earth elements was effected through HF-H_2SO_4 decomposition of the samples, ammonia precipitation of the R_2O_3 group, ether extraction of iron, and a final ammonia precipitation and ignition of the R_2O_3 group. The ignited oxides were analysed spectrochemically by the d.c.-arc "total energy" method.

The results of these analyses and comparisons with the results of other investigators (AHRENS, 1955), are given in Table 1. The spectral lines of the elements and their sensitivities are given in Table 2. The values derived from the present work are to be considered as merely indicating the correct orders of magnitude, because the time available did not permit an extensive check on the precision and accuracy of the determinations.

Table 1. Yttrium, lanthanum, cerium, neodymium, and ytterbium content of granite, G-1, and diabase, W-1
(Values are parts per million by weight, calculated from determinations made on the chemical concentrates.)

Analyst	Method	G-1					W-1				
		Y	La	Ce	Nd	Yb	Y	La	Ce	Nd	Yb
BERMAN S. (this paper)	Optical spectrograph	20	200	600	100	1	30	30	70	50	2
ADLER I. and AXELROD J. M. (this paper)	X-ray fluorescence*	—	—	700–1400	—	—	30–50	—	—	—	—
MITCHELL R. L.	Optical spectrograph	30	430	—	—	—	n.d.	32	—	—	—
MURATA K. J.	Optical spectrograph	n.d.	190	—	—	—	—	n.d.	—	—	—
GORFINKLE L. G. and AHRENS L. H.	Optical spectrograph	24	130	—	80	—	n.d.	n.d.	—	n.d.	—
NOCKOLDS S. R.	Optical spectrograph	10	60	—	—	—	—	—	—	—	—
SHAW D. M. and WEBER G. R.	Optical spectrograph	20	—	—	—	—	35	—	—	—	—
HARVEY C. O.	Semiquantitative	<20	100	—	—	—	30	<5	—	—	—
AHRENS L. H.	Recommended values	21	160	—	(80)	—	—	(32)	—	—	—

* Yttrium value obtained directly from W-1 and cerium value obtained from the G-1 concentrate.
n.d. = not detected.
Figures in parentheses denote orders of magnitude.

* Publication authorized by the Director, U.S. Geological Survey.

Table 2. Spectral lines used

	Wavelength (Å)	Sensitivity (p.p.m.)
Yttrium-II	3327·875	50
Lanthanum-II	4333·734	50
Cerium-II	4222·599	200
Neodymium-II	4303·573	100
Ytterbium-II	3289·37	1

Acknowledgements—The author wishes to express his appreciation to his colleagues in the U.S. Geological Survey, H. Bastron and M. K. Carron, for their helpful suggestions, and to I. Adler and J. M. Axelrod for the X-ray fluorescence analysis.

Sol Berman

U.S. Geological Survey,
Washington 25, *D.C.*

Reference

Ahrens L. H. (1955) *Quantitative Spectrochemical Analysis of Silicates* pp. 20–38. Addison-Wesley Press, Cambridge, Mass.

Geochimica et Cosmochimica Acta, 1957, Vol. 12, pp. 273 to 276. Pergamon Press Ltd., London

ABSTRACTS FROM CURRENT LITERATURE

Variation in the chemical composition of carbonate rocks of Russian platform*

A. P. Vinogradov, A. B. Ronov, and V. M. Ratynskii

The present review summarizes the results of a comprehensive study of the chemical composition of carbonate rocks of Russian platform, which was undertaken by the Institute of Geochemistry and Analytical Chemistry of V. I. Vernadskii, Moscow, USSR.

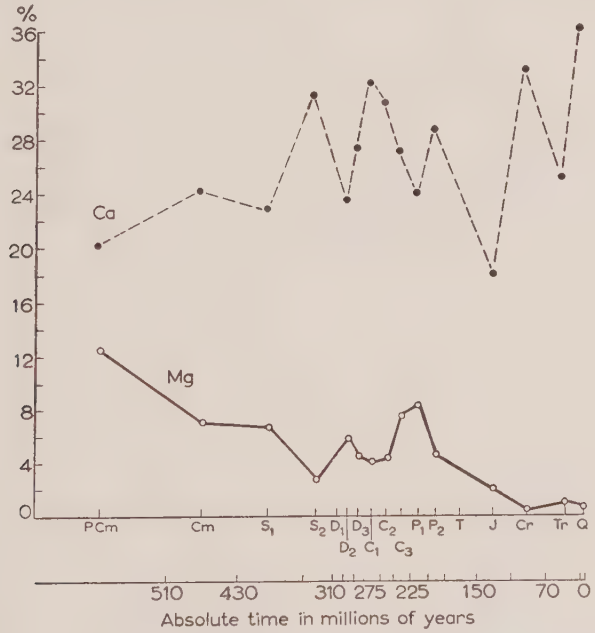

Fig. 1. Changes in average Ca and Mg contents (in %) of carbonate rocks of Russian platform with time. (All figures taken directly from original article.)

Figs. 1 and 2 show the variation of Ca and Mg contents of the carbonate rocks of Russian platform with time; and are based on (1) 97 analyses of average assays (weighted for the thickness of formations) from 3659 samples, and (2) literature review —2826 analyses for Ca and 2583 analyses for Mg. Thus, Figs. 1 and 2 are based on analyses of almost 7000 samples.

Fig. 2 shows a general increase in the average Ca/Mg ratio in going up the geologic column. These results are in close accord with those obtained by the reviewer for the Canadian and U.S. limestones and dolomites (Chilingar, 1956).

* From *Izv. Akad. Nauk SSSR, Geol. Ser.*, 1952, No. 1, pp. 33–50. Reviewed by George V. Chilingar, Assistant Professor of General and Petroleum Engineering, University of Southern California. The reviewer is greatly indebted to Dr. A. B. Ronov for sending a reprint of his article (in Russian), which was received on 1 December 1956. This reprint is available from the reviewer (see also p. 276).

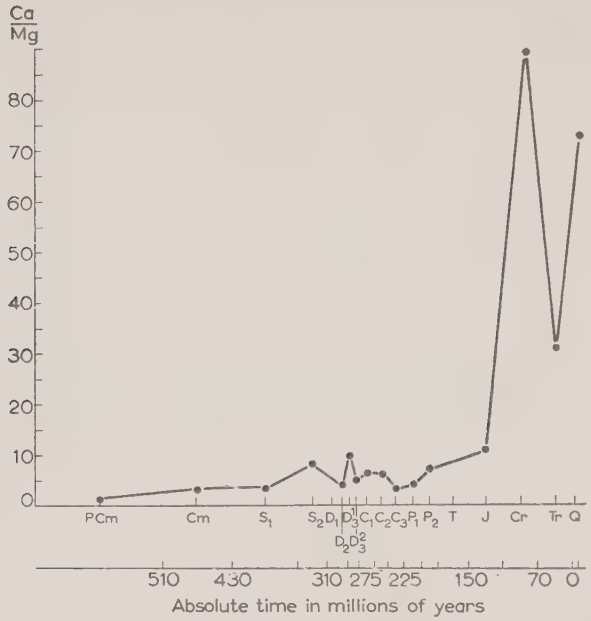

Fig. 2. Changes in average Ca/Mg ratio of carbonate rocks of Russian platform with time.

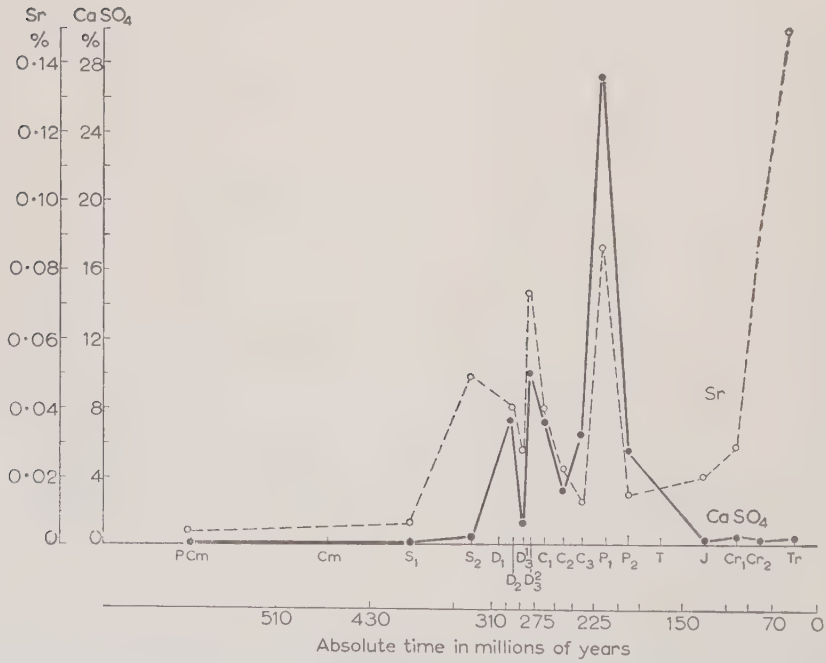

Fig. 3. Variation of $CaSO_4$ and Sr contents (in %) of carbonate rocks of Russian platform with time.

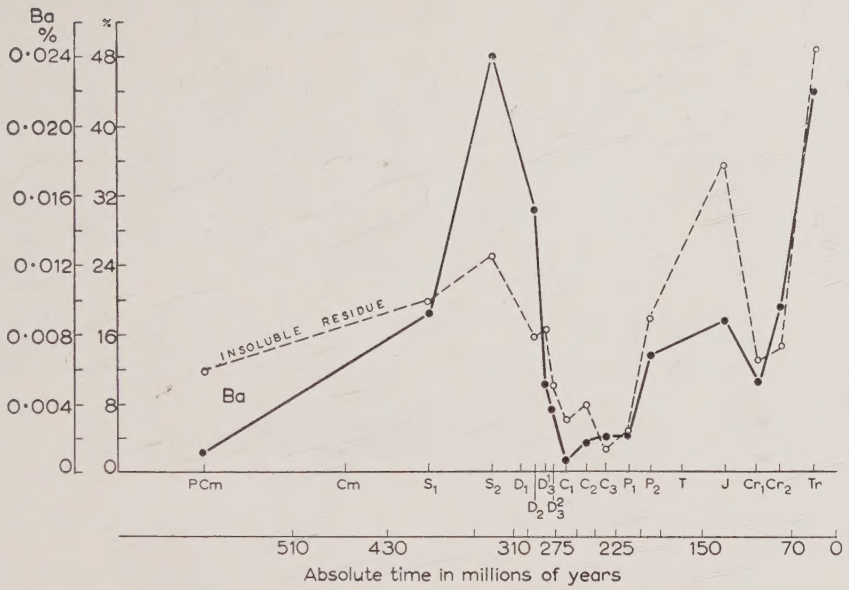

Fig. 4. Variation of Ba and insoluble residue (dashed line) contents of carbonate rocks of Russian platform with time.

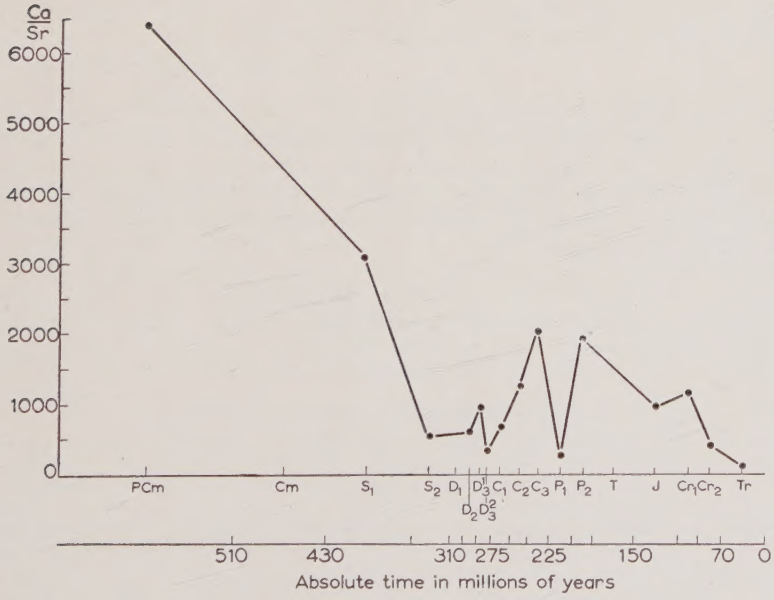

Fig. 5. Variation of Ca/Sr ratio of carbonate rocks of Russian platform with time.

Fig. 3, which is based on 97 analyses of composite samples from 3659 spot samples, shows the variation of $CaSO_4$ and Sr contents of carbonate rocks of Russian platform with time. The $CaSO_4$ and Sr contents are very small in the Pre-Cambrian and lower Paleozoic carbonate rocks. Higher contents of $CaSO_4$ and Sr are indicated for the middle and upper Paleozoic, and their curves exhibit parallelism until the Mesozoic time. From the beginning of Mesozoic time, however, the $CaSO_4$ content becomes almost nil, whereas the Sr content rapidly increases.

Fig. 4 shows the variation of Ba and insoluble residue contents of carbonate rocks with time, and is based on 90 analyses of average assays from 3530 samples. A definite parallelism exhibited by the curves for Ba and insoluble residue contents owes its origin to the pelitic portion of alumino-silicates. Vinogradov, Ronov, and Ratynskii found that the values obtained on recalculating the Ba content for insoluble residues closely approach the average content of Ba in clays.

Vinogradov, Ronov, and Ratynskii also studied the variation of Ca/Sr ratio of carbonate rocks with time (Fig. 5). Fig. 5, which is based on 94 analyses of compound samples from 3563 individual samples, shows a decrease in the Ca/Sr ratio with time. This decrease in the Ca/Sr ratio of carbonate rocks of Russian platform with time is more pronounced than the one found by Kulp, Turekian, and Boyd (1952) for U.S. carbonate rocks.

According to Vinogradov, Ronov, and Ratynskii, the periodic fluctuations in the content of some chemical elements (Mg, Ca, Sr, Ba, and Th) are closely correlatable with the tectonic history of the Russian platform.

References

Chilingar G. V. (1956) *Bull. Amer. Assoc. Petrol. Geol.* **40**, No. 9, 2256–66.
Kulp J. L., Turekian K., and Boyd D. W. (1952) *Bull. Geol. Soc. Amer.* **63**, 701–16.

A full translation of this material can be obtained from the Pergamon Institute, a non-profit-making foundation, under the co-operative cost-sharing scheme, the cost being shared, after a period of six months has elapsed, between those purchasing a copy. The maximum charge will not exceed £1. 10s. 0d. ($4.00) per thousand Russian words. Requests for translations should be addressed to:

The Administrative Secretary,
Pergamon Institute,
4 & 5 Fitzroy Square,
LONDON, W.1.

or The Administrative Secretary,
Pergamon Institute,
122 East 55th Street,
New York 22, N.Y.

INFORMATION FOR CONTRIBUTORS

I. GENERAL

1. Papers on geochemistry should be submitted to the editors for the appropriate country or language (*Papers on cosmochemistry should be sent to Prof. F. A. Paneth, F.R.S.*). Papers submitted for publication will naturally be judged from the standpoint of scientific originality and novelty. Technical details of apparatus used in scientific investigation can, however, be presented in brief notes. Critical comments or preliminary results requiring early publication should be submitted as letters to the editors. Where possible, letters should be confined to 500 words. The preparation of progress reports and review articles will be invited by the editors from time to time. The journal appears as independent and complete numbers, which are combined into volumes of about 300 pages.

2. Only papers which have not been previously published can be accepted. Authors must agree not to publish elsewhere a paper submitted to and accepted by *Geochimica et Cosmochimica Acta*.

3. Fifty reprints of each paper are provided free. Additional copies can be purchased if ordered at the time the first proofs are returned. A reprint order form will accompany first proofs.

II. SCRIPT REQUIREMENTS

1. Scripts must be written in one of the three official languages—English, French, or German

2. The script should be typed (not a carbon copy). The text must be ready for printing and should be carefully checked for errors. Authors will receive proofs for correction.

3. Illustrations should accompany the script, mounted on separate sheets. Line diagrams that require to be redrawn should include all relevant details. Half-tone illustrations should be restricted to the minimum necessary. Photographs should be enlarged sufficiently to permit their clear reproduction, and if words or numbers appear on them, two copies should be sent, one clearly printed and the other without inscription. All illustrations should be provided with descriptive legends, which should be given on a separate sheet.

4. References in the text should be given by quoting the author's name and year of publication, i.e. AHRENS (1952). **Full references should be listed at the end of each paper, in alphabetical order, in the following manner:**

AHRENS L. H. (1952) *Geochim. et Cosmochim. Acta* **2**, 168.

and should include the standard abbreviated title of the journal, year, volume number, and page number.

5. The text of articles submitted should be concise and in a readily understandable style The technical description of the methods used should only be given in detail when such methods are new. The essential contents of each paper should be briefly recapitulated in an abstract in English. Such an abstract may, however, be submitted by the author in the language of the original typescript for translation into English by the editorial staff.

6. To conserve space, authors are requested to mark less important portions of the paper (such as description of methods, record of experimental results, etc.) for printing in smaller type.

Pergamon Press are also publishers of the following Journals

JOURNAL OF NUCLEAR ENERGY (*including* THE SOVIET JOURNAL OF ATOMIC ENERGY *on behalf of the Pergamon Institute, a non-profit-making foundation*)
JOURNAL OF INORGANIC AND NUCLEAR CHEMISTRY
TETRAHEDRON (*the International Journal of Organic Chemistry*)
INTERNATIONAL JOURNAL OF APPLIED RADIATION AND ISOTOPES
*BIOPHYSICS
*JOURNAL OF MICROBIOLOGY, EPIDEMIOLOGY AND IMMUNOBIOLOGY
*PROBLEMS OF HEMATOLOGY AND BLOOD TRANSFUSION
*PROBLEMS OF VIROLOGY
*PROBLEMS OF ONCOLOGY
*PHYSIOLOGICAL JOURNAL OF THE U.S.S.R. (SECHENOV)
CHEMICAL ENGINEERING SCIENCE
JOURNAL OF ATMOSPHERIC AND TERRESTRIAL PHYSICS
SPECTROCHIMICA ACTA
JOURNAL OF THE MECHANICS AND PHYSICS OF SOLIDS
ACTA METALLURGICA (*for the Board of Governors of Acta Metallurgica*)
INTERNATIONAL JOURNAL OF THE PHYSICS AND CHEMISTRY OF SOLIDS
DEEP-SEA RESEARCH
JOURNAL OF NEUROCHEMISTRY
JOURNAL OF PSYCHOSOMATIC RESEARCH
JOURNAL OF INSECT PHYSIOLOGY
INTERNATIONAL ABSTRACTS OF BIOLOGICAL SCIENCES (*for Biological and Medical Abstracts Ltd.*)
JOURNAL OF EDUCATION

**Translations of Russian journals published on behalf of the Pergamon Institute, a non-profit-making foundation.*

IN STACKS
1 3 1958

19Feb '65F

I. R. MAXWELL & CO LTD

SECOND-HAND & OUT-OF-PRINT DEPARTMENT

Scientists and Librarians

Please check this list of periodicals against your library. We urgently require these to fill orders for university and industrial libraries at home and abroad. We shall be most grateful for any you can offer, and will pay highest market prices. Please send us a list of your holdings of learned books and periodicals that you are willing to sell. We shall also be glad to receive a list of your wants of out-of-print books and journals to check against our extensive holdings. We shall send our quotations by return.

ACTA MATHEMATICA: Vol. 85–86, 88–89.

AMERICAN GEOPHYSICAL UNION, TRANSACTIONS: Vol. 1 to date.

AMERICAN JOURNAL OF PHYSICS: Vol. 1–7.

AMERICAN METEOROLOGICAL SOCIETY, BULLETIN: Vol. 1–22, 28 to date.

ANNALEN DER HYDROGRAPHIE UND MARITIMEN METEOROLOGIE: Vol. 1 to date.

ANNALEN DER METEOROLOGIE: Vol. 1 to date.

ANNALEN DER PHYSIK: Series II: Vol. 92, 106, 111. Series III: Vol. 2. Series V: Vol. 1–43, no. 8. Series VI: Vol. 1, 2, 12.

ANNALES D'ASTROPHYSIQUE: Series IX: Vol. 1–2, 4–20. Series X: Vol. 1–12. Series XI: Vol. 17. Series XII: Vol. 1–11.

ARCHIV FÜR HYDROBIOLOGIE: Vol. 38–43.

ASTROPHYSICAL JOURNAL: Vol. 1–116.

BIOGEOGRAPHICAL SOCIETY OF JAPAN, BULLETIN: Vol. 1–14, with BIOGRAPHICA: Vol. 1–3.

GEOFISICA PURA ED APPLICADA: Vol 1 to date.

GEOLOGICAL SOCIETY OF AMERICA, BULLETIN: Vol. 1 to date.

GEOLOGISCHES ZENTRALBLATT: Vol. 1 to date.

GEOLOGISTS' ASSOCIATION, LONDON. PROCEEDINGS: Vol. 1–48.

HONKONG OBSERVATORY. Meteorological Observations: Vol. 1 to date. Monthly Meteorological Bulletin: Vol. 1 to date.

JOURNAL OF GEOPHYSICAL RESEARCH: Vol. 1 to date.

JOURNAL OF METEOROLOGY: Vol. 1 to date.

JOURNAL OF THE AERONAUTICAL SCIENCES: Vol. 1–12, 17–23.

Single issues and duplicate volumes as well as complete or part sets welcomed

Maxwell and Co. are the world's leading specialist booksellers aiding progress in science, medicine, industry and education. We offer the individual book buyer and professional librarian many up-to-date services, hitherto not available anywhere. We have the following service departments at your disposal:

New Book Department
Subscription to Periodicals and Serials Department
Out of Print and Difficult to Get Department
Micro films and micro cards Department
Technical Translating Department
Technical Writing Department
Information Department
Bookbinding Department
Library Valuation Department

For full details of services offered, please write to the address convenient for this free descriptive booklet.

I. R. MAXWELL & CO LTD ***International University and Industrial Booksellers***

LONDON
4 & 5 FITZROY SQUARE, LONDON W.1

NEW YORK
122 East 55th Street, New York 22, N.Y.

PARIS
24 Rue des Écoles, Paris V^e^